# A coupled hydrodynamic-ecological model to test management options for restoration of lakes Onoke and Wairarapa



## ERI Report No. 111

Prepared for Greater Wellington Regional Council

By Mathew Allan[1], David P. Hamilton[1,2], and Kohji Muraoka[1]

1. Environmental Research Institute
University of Waikato, Private Bag 3105
Hamilton 3240, New Zealand

2. Current address: Australian Rivers Institute
Griffith University, Brisbane Australia

Environmental Research Institute
Te Pūtahi Rangahau Taiao
THE UNIVERSITY OF WAIKATO

THE UNIVERSITY OF
WAIKATO
Te Whare Wānanga o Waikato

**Citation**
Allan, M.G, D.P. Hamilton, K. Muraoka 2017. A coupled hydrodynamic-ecological model to test management options for restoration of lakes Onoke and Wairarapa. Environmental Research Report No. **111**, University of Waikato, Hamilton, New Zealand.

**Availability**
Available on a Creative Commons Attribution 3.0 New Zealand Licence.

**Contributing authors**
Allan, M.G, D.P. Hamilton, and K. Muraoka

**Data providers**
GWRC, NIWA, Jacobs, GNS.

**Cover photo**
Landsat seven image captured 24/10/2012

**Photo on this page**
Lake Onoke on 28/11/2015 (David Hamilton)

*Reviewed by:*
*by:*

*Approved for release by:*

**Dr Moritz Lehman**

Research Fellow

Environmental Research Institute

University of Waikato

**Dr John Tyrrell**

Research Developer

Environmental Research Institute

University of Waikato

# Executive Summary

This report describes a modelling and remote sensing study of lakes Onoke and Wairarapa that seeks to determine water quality and ecological effects of specific management scenarios, and therefore inform the Ruamāhanga Whaitua Committee of potential water quality management options for lakes Onoke and Wairarapa.

The study applied both one dimensional (1-D) and three dimensional (3-D) ecologically coupled hydrodynamic models to simulate current and scenario-based water quality variables. The Baseline model (calibration) simulates "current conditions" including management practices between 1992 and 2014. Business As Usual (BAU), SILVER and GOLD scenarios were all run using representative data catchment inflow and nutrients for mitigation taking effect in 2025, 2040 and 2080. Additional hydrodynamic scenarios were modelled (which also include catchment mitigations above). They were: deepening both lakes by 1 m, Ruamāhanga diversion back into Lake Wairarapa, and Lake Onoke summer outlet closed scenarios. These scenarios were provided by the Ruamāhanga Whaitua Committee.

Within Lake Wairarapa, catchment mitigation-based scenarios showed considerable potential for the improvement of water quality. These mitigations simulated that the trophic state of the lake could change from the current supertrophic category, to the top of the eutrophic category (GOLD and SILVER mitigations). However, this still indicates poor water quality and high turbidity/low water clarity. In addition, these catchment mitigations did not move the lake from a NOF D category for total phosphorous (TP). Simulations indicated that larger reductions in TP (60%) (with SILVER2080 mitigations of other nutrients) could achieve a NOF C category for TP. Simulations that included the re-establishment of macrophytes also indicated NOF C category for TP (under SILVER2080), however only under a 1 m depth increase scenario, and under Ruamāhanga diversion scenario. These simulations indicated that the trophic status could move to the mid-eutrophic category. However, this is still indicative of poor water quality.

Catchment scenarios had a greater influence on Lake Onoke trophic status compared to Wairarapa, due to the shorter residence time and low internal load (from the sediments) relative to external load. In effect, the composition of Onoke aligns closely with that of its inflows. Water quality in Lake Onoke is susceptible to changes in water quality in Lake Wairarapa, particularly in relation to chlorophyll *a* (chl *a*) and total suspended solids (TSS). High sediment resuspension events in Lake Wairarapa transport increased levels of suspended sediment to Lake Onoke. The very low residence time in Onoke does not allow adequate time for significant phytoplankton growth within the lake. However, 3-D simulations show higher phytoplankton concentrations at times in the western lake, relating to flushing and transport effects. The outlet-closed scenario in Lake Onoke simulated increased water quality in both 1-D and 3-D models However, we note that the risk of cyanobacteria blooms was low, but marginally increased. Also 1-D models suggested that the simulated TLI under SILVER2080 was almost identical to outlet closed SILVER2080. The 3-D model simulated lower chlorophyll concentrations and higher TSS under SILVER2080 outlet closed (compared to SILVER2080 and Baseline), largely due to changes in hydrodynamics and flushing. Therefore, these results show no conclusive evidence that water quality would be significantly increased or decreased in comparison to SILVER2080 under an outlet closed scenario. However, we note that *in situ* monitoring and expert opinion has indicated that under outlet closed conditions the lake is more susceptible to eutrophication.

## Key points

- Lake Wairarapa - trophic state moves from current supertrophic category, to the top of the eutrophic category (GOLD and SILVER mitigations). However, this still indicates poor water quality and high turbidity/low water clarity.

- Lake Wairarapa - Simulations indicated that larger reductions in TP (60%) (with SILVER2080 mitigations of other nutrients) could achieve a NOF C category for TP

- Lake Wairarapa - the re-establishment of macrophytes also indicated NOF C category for TP (under SILVER2080). Macrophytes could re-establish within the lake, dramatically increasing the water quality within the lake, reducing TLI to 4.4 in Lake Wairarapa (under the 1 m depth increase scenario)

- Lake Wairarapa -  Hysteresis due to interacting ecological/ physical processes stabilising the current turbid state. Resuspension from sediments decreases available light, limiting the potential for macrophyte reestablishment

- Lake Onoke - catchment scenarios had a greater influence on Lake Onoke trophic status compared to Wairarapa, due to the shorter residence time and lower internal load (from the sediments) relative to external load, which was negligible. In effect the composition of Onoke aligns closely with that of its inflows

- Lake Onoke - water quality is susceptible to changes in water quality in Lake Wairarapa, particularly in relation to chlorophyll *a* (chl *a*) and total suspended solids (TSS)

- Lake Onoke - low residence time does not allow for significant phytoplankton growth. However, 3-D simulations show higher phytoplankton concentrations at times in the western lake, relating to flushing and transport effects

- Lake Onoke - no conclusive evidence that water quality would be significantly increased or decreased in comparison to SILVER2080 under an outlet closed scenario

- Running the 3-D models for longer time periods would increase the robustness of any derived conclusions and decrease uncertainty for in lake scenarios

- Quantification of marine intrusion flow volumes and nutrient concentrations into Lake Onoke would also decrease uncertainty in model simulations

- Climate change could enhance eutrophication in mesotrophic and eutrophic lakes due physiochemically and biologically induced higher internal loading

# Table of contents

# Table of figures

## Table of tables

## Introduction

This report describes a modelling and remote sensing study of lakes Onoke and Wairarapa that seeks to:

- Apply remote sensing and modelling to determine the spatial distribution of optically active constituents and other key water quality variables within lakes.
- Determine water quality and ecological effects of specific management scenarios.
- Inform the Ruamāhanga Whaitua Committee of potential water quality management options for lakes Onoke and Wairarapa by modelling water quality of the lakes.

Over the past three decades pastoral land use has intensified in New Zealand, along with significant increases in nutrient and sediment export from land to surface waters and groundwater, contributing to the degradation of New Zealand's freshwater ecosystems (Gluckman et al., 2017; PCE, 2012, 2013). Very rapid intensification in recent years, increasing nutrient and sediment loads to lakes have resulted in reduction in biodiversity, amenities and aesthetic values of waterbodies (Gluckman et al., 2017). New Zealand's regional regulatory authorities now have a legal obligation to manage sediment and nutrient losses to aquatic systems. The National Policy Statement for Freshwater Management (NPS–FM, 2014), and its subsequent amendments in 2017, includes the National Objectives Framework (NOF), a numeric and descriptive framework which enables regional councils to set environmental policy regarding freshwater management (MFE, 2017b, 2017a). In regard to lake water quality, the NOF has limits for phytoplankton (chlorophyll (chl) *a*), cyanobacteria (biovolume), concentrations of total nitrogen (TN), total phosphorus (TP), ammonia (toxicity) and *E. coli* (colony-forming units (CFU) per 100 mL).

Regional councils now have a mandate to set limits for water quality and quantity through a community-based process. Within the Ruamāhanga catchment (Wellington region, NZ), the Ruamāhanga Whaitua Committee was established in December 2013. The Whaitua process is a community based collaborative limit setting process. One of the first tasks of the Ruamāhanga Whaitua Committee was to determine what values Ruamāhanga communities place on their local water ways (including lakes, wetlands, groundwater, and surface water) and catchments. The Committee will present their recommendations in a Whaitua Implementation Programme (WIP), which will be integrated into the Greater Wellington Regional Council (GWRC) Natural Resources Plan (NRP). The Ruamāhanga WIP will become a Ruamāhanga chapter of the NRP.

The current study is designed to inform the Ruamāhanga Whaitua Committee of potential water quality management options for lakes Onoke and Wairarapa by modelling water quality of the lakes, and potential lake restoration scenarios. To enable effective lake restoration, an integrated approach of catchment and in-lake management is required (Hamilton et al., 2016). The restoration and management options may include, for example, river diversion, riparian buffer zones, constructed wetlands, land-use change, bio-manipulation, and best practice management techniques within agricultural land to reduce nutrient loss. However, it should be noted that the effectiveness of these techniques can vary widely. For example, riparian afforestation can significantly reduce run-off, sediment yield and nutrient loss from pastoral catchments (Menneer et al., 2004) but results can be highly variable (Parkyn et al., 2000). Water quality monitoring is critical to assess the efficacy of management practices, both before and following their implementation.

Approaches to assess water quality may be categorised into three main types; traditional in situ sampling, numerical modelling and remote sensing (Dekker et al., 1996). In situ methods using grab samples are generally suited to monitoring at low temporal resolution. By contrast autonomous water quality monitoring sensors allow for monitoring at high frequency and potentially in real time. However, neither of these methods is well suited to effectively capture horizontal heterogeneity of water quality and temperature. Remote sensing can provide synoptic monitoring of water quality and temperature, whereby water quality over the entire lake surface is captured by one satellite image (e.g., Kloiber et al. 2002, Dekker et al. 2002a). It is highly suitable for providing comprehensive spatial coverage. Three-dimensional (3-D) and one-dimensional (1-D) hydrodynamic modelling that couples ecological models can produce simulations of temperature and water quality variables. These simulations may be able to be validated with satellite and traditional monitoring data for water quality and temperature, and to extend the analysis to the vertical domain.

While remote sensing can provide cost effective synoptic monitoring, limitations of this method must also be considered. Remote sensing using visible and infrared (IR) radiation is not possible during periods of extensive cloud cover, which are frequent in New Zealand. Remote sensing does also not allow derivation of non-optically active water constituents, such as nutrient concentrations. Measurements of total radiance from satellites may comprise up to 90% atmospheric path radiance, making it difficult to quantify radiance from optically active constituents of water (Vidot & Santer, 2005). Atmospheric correction is therefore essential for the standardisation of image time series. In optically complex Case 2 waters found in lakes, bio-optics are a function of at least three optically active constituents which can vary independently (Blondeau-Patissier et al., 2009). The retrieval of water constituent concentrations from Case 2 waters is more demanding in terms of algorithm complexity and the satellite sensor spectral resolution (Matthews, 2011). This is the case when using broadband sensors such as Landsat's Enhanced Thematic Mapper (ETM), and estimations of water quality in optically complex waters can be limited to water quality variables that are constituent in nature, such as Secchi depth, light attenuation, and TSS.

## Methods

### Lake Wairarapa study site

Lake Wairarapa is a shallow (max depth 2.6 m), supertrophic (Perrie & Milne 2012; Perrie 2005) riverine lake (area 7737.4 ha) located in the Wairarapa region in the lower North Island (Fig. 1). Due to the large shallow nature of Lake Wairarapa, it is very susceptible to sediment resuspension and it is mostly isothermal and well-mixed vertically. Strong westerly winds can cause lake set-up on the eastern shore, and alter water levels by up to 1.2 m (Mitchell, 1989). The surficial lake sediments can be classified as medium to coarse silt (Trodahl, 2010). The hydraulic residence time is 69 days (calculated over the present study period with modelled inflows).

Lake Wairarapa is the largest lake in the Wellington region and the 11th largest lake in New Zealand. A national conservation order was placed on Wairarapa in 1989 in order to protect the high ecological values associated with the lake and its catchment. For example, Lake Wairarapa forms part of the largest wetland complex in the southern North Island.

## Locations for 1-D modelling

Only two locations in the lake have monitoring data for 1-D modelling. The ideal Lake Wairarapa monitoring location for comparison to 1-D models is Lake Wairarapa Middle Site, due to its central location at the deepest point (2.6 m) within the lake (Fig. 1). However, monitoring data for this site is only available from January 2014. Therefore, for 1-D model calibration and validation data from Wairarapa Site 2 was adopted, as data are available from February 1994. This is also the second deepest monitoring site (2.2 m). While the model was calibrated for Site 2, model output data is considered valid for a reporting location at Lake Wairarapa Middle Site, due to the fact that the model horizontally averages hydrodynamic and water quality variables.

## Locations for 3-D modelling

For 3-D lake modelling, cells were selected from the model that included Lake Wairarapa Site 2, Middle, Alsops and Outlet (labelled DS barrage gates, Fig. 1).
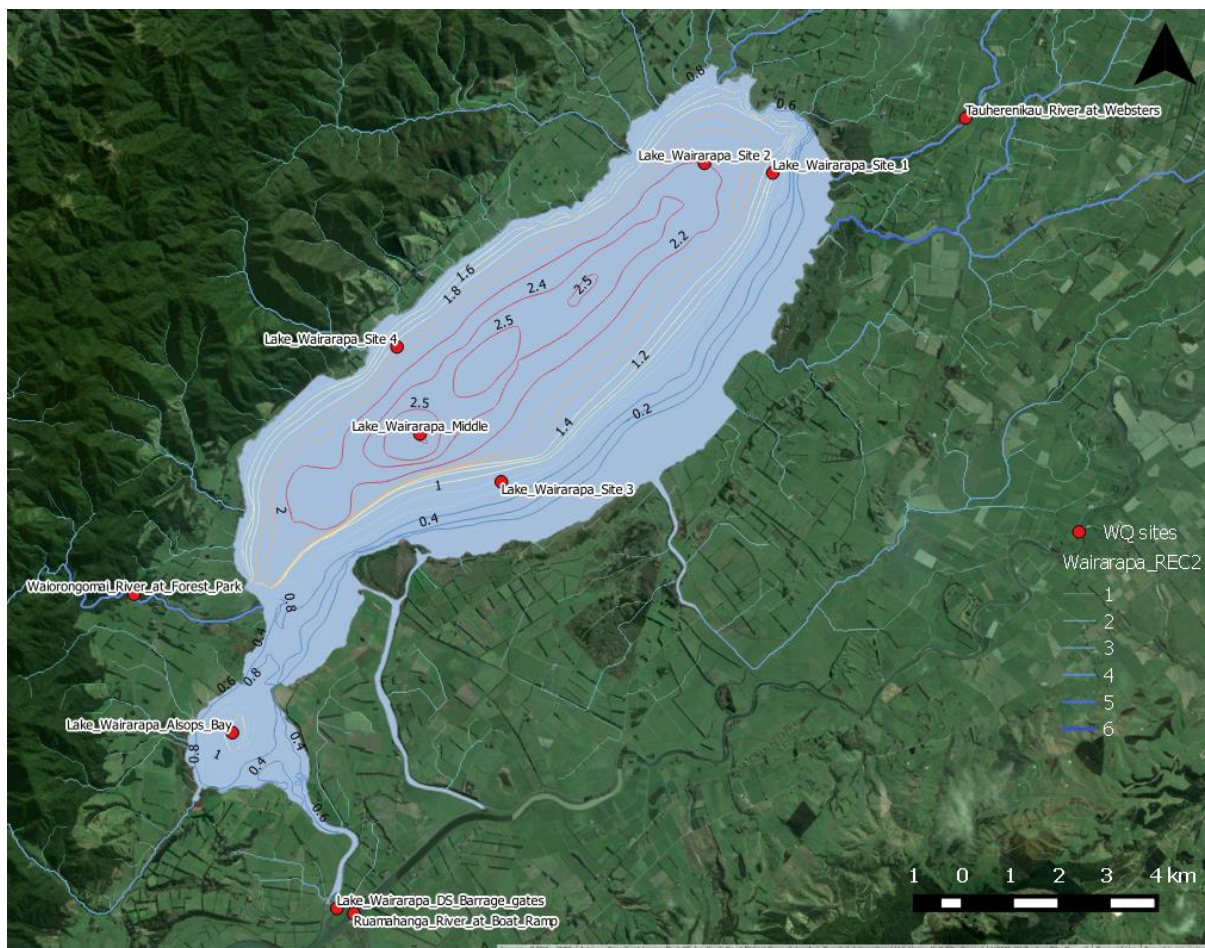


**Figure 1. Lake Wairarapa study site with water quality (WQ) monitoring locations, River Environment Classification (NIWA) stream order (shades of blue; see scale on right-hand side), and isobaths labelled by depth (m).**

## Catchment

The catchment of Lake Wairarapa (65449.6 ha) ranges from a maximum elevation of 732.1 m above mean sea level (ASL) to the average lake surface level of 0.98 m ASL (10.2 m

3

Schemes datum). The maximum lake level post-barrage gate construction is 2.89 m ASL (12.2 m Schemes datum) (Thompson & Mzila, 2015). According to the Land Cover Database (LCDB) v.4.0 (Landcare Research), catchment land cover is primary comprised of high producing exotic grassland (44.8), indigenous forest (24%), lake or pond (11%) and broadleaved indigenous hardwoods (7.8%), with the remaining land cover classes comprising of 11.8% (Fig. 2, Table 1).
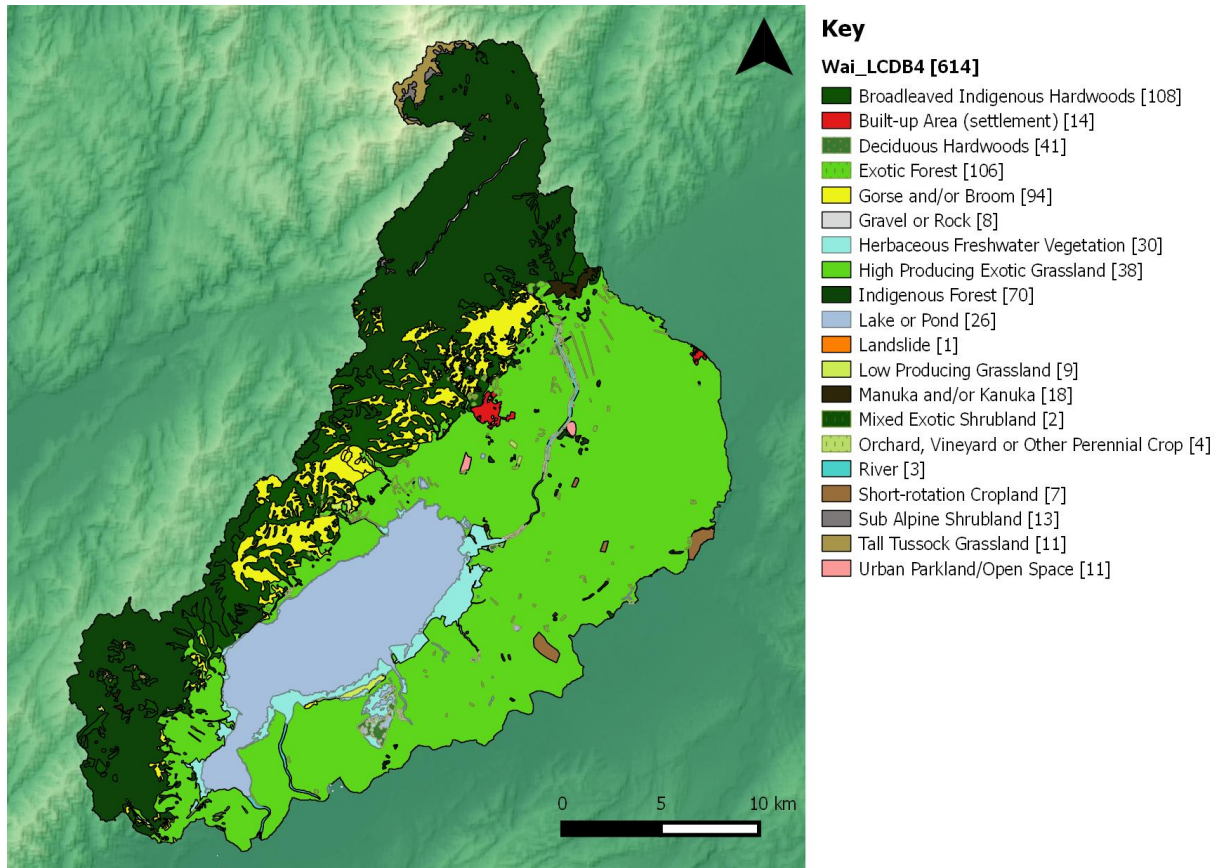


**Figure 2. Lake Wairarapa catchment Land Cover Database v.4.0, with bracketed numbers showing the sum of the number of polygons present within each class.**

**Table 1. Lake Wairarapa catchment Land Cover Database v.4.0 land cover summed areas.**

| LCDB4 2012 land cover | Area (ha) | Percent |
|---|---|---|
| High Producing Exotic Grassland | 29302.4 | 44.77 |
| Indigenous Forest | 16058.3 | 24.54 |
| Lake or Pond | 7221.6 | 11.03 |
| Broadleaved Indigenous Hardwoods | 5119.3 | 7.82 |
| Gorse and/or Broom | 3693.6 | 5.64 |
| Herbaceous Freshwater Vegetation | 1686.6 | 2.58 |
| Tall Tussock Grassland | 377.2 | 0.58 |
| Deciduous Hardwoods | 310.1 | 0.47 |
| Exotic Forest | 267.8 | 0.41 |
| Manuka and/or Kanuka | 241.4 | 0.37 |
| Short-rotation Cropland | 228.6 | 0.35 |
| River | 226.2 | 0.35 |
| Built-up Area (settlement) | 198.5 | 0.30 |
| Sub Alpine Shrubland | 146.4 | 0.22 |
| Low Producing Grassland | 133.9 | 0.21 |
| Gravel or Rock | 123.8 | 0.19 |
| Urban Parkland/Open Space | 70.6 | 0.11 |
| Mixed Exotic Shrubland | 25.4 | 0.04 |
| Orchard, Vineyard or Other Perennial Crop | 16.8 | 0.03 |
| Landslide | 1.1 | 0.002 |

*History*

There is evidence that in 6500-year BP Lake Wairarapa was part of a large shallow embayment environment extending to Palliser Bay (including Lake Onoke). At this time sea levels were slightly higher or similar to current (Leach & Anderson, 1974). More recently, the hydrology of the catchment has been altered significantly by human intervention. One of the modifications included relocating the Tauherenikau River's outlet to a more northerly location in the 1950s. The largest hydrological modification occurred during the construction of the 1964 Lower Wairarapa Valley Development Scheme (LWVDS), which was designed for flood protection in the Wairarapa Valley (Airey et al., 2000). It allows protection against a 1-in-20-year flood. The scheme covers an area extending from 2 km below the Waiohine/Ruamāhanga confluence to Lake Onoke, which includes the Tauherenikau River and tributaries of Lake Wairarapa/Ruamāhanga River. The scheme takes advantage of natural high land and includes the constructed stop banks. As part of the LWVDS, the Ruamāhanga River was diverted away from Lake Wairarapa in the early 1980s via the construction of the Ruamāhanga diversion channel which crosses the Kumenga Peninsula. The flow was diverted directly to the lower Ruamāhanga, reducing the effective catchment area of Lake Wairarapa by approximately 80% (Thompson & Mzila, 2015). The construction of Barrage gates has allowed authorities to regulate flow between Ruamāhanga River and Lake Wairarapa, and

largely independently control lake levels of both Wairarapa and Onoke (location shown in Fig. 1).

### Inflows

Lake Wairarapa is connected to the lower Wairarapa groundwater system. The groundwater system is conceptually closed, with limited exchange between the groundwater system and the sea (Gyopari & McAlister, 2010). Most of the groundwater discharging into Lake Wairarapa originates from shallow unconfined aquifers (also discharging into inflowing streams and rivers), however, near Lake Wairarapa groundwater becomes confined, with flow converging on the lake. Slow discharge may also occur from deep confined aquifers (Gyopari & McAlister, 2010). Groundwater discharge into the lake has been estimated at 0.4 $m^3$ $s^{-1}$, however it should be noted that this was derived from the residual of a model of the Wairarapa Lower Valley groundwater model (Gyopari & McAlister, 2010).

The major inflows to the lake include the Tauherenikau River (northeast), Otukura stream (northwest), Waiorongomai River (south-western), the Ruamāhanga River (during flooding via the Oporua floodway), and back-flow from the Barrage gates (southern).

### Outflows

The outflow to the lake is via the barrage gates at the south-eastern end of the lake. The barrage consists of six gates that can be operated individually. Under normal operating conditions when the mouth of Lake Onoke is open and flood conditions are not present, the barrage gates operate to maintain consented levels, as stipulated by the resource consent, which targets lake levels of between 0.68 and 0.93 m ASL (9.9 and 10.15 m Schemes datum). An automated alarm system is used to alert operators to high or low water level and the gates are adjusted in response. To allow for fish passage there are automated daily openings of two of the six gates (Thompson & Mzila, 2015). If the mouth of Lake Onoke becomes blocked the barrage gates are operated in order to raise the lake levels of Onoke to the maximum consented level. The Onoke spit is then opened (via excavator) allowing floodwaters to drain and the level of the Ruamāhanga River/Lake Onoke to return to normal. During large swells opening is not possible, and under this scenario the barrage gates are opened to allow backflow into Lake Wairarapa. During a large flood event the barrage gates are closed to maintain Lake Wairarapa water level, and flood flows ideally drain through the Onoke spit.

The flow at the barrage gates has been monitored since August 2012, using a 'side-looking' Acoustic Doppler Current Profiler (ADCP). There are also 11 consented abstractions with maximum daily abstraction of 39,635 $m^3$ $day^{-1}$ (Thompson & Mzila, 2015).

### Water quality and ecological status

Water quality monitoring of Lake Wairarapa commenced in June 1994. The monitoring was initially quarterly, with monthly monitoring data available from July 2011. A detailed analysis of the water quality of Lake Wairarapa can be found in Perrie & Milne (2012). The authors found the supertrophic classification (2006 – 2010) of Lake Wairarapa was influenced by the constituents of a hypertrophic classification of Secchi depth, while concentrations of total phosphorus (TP), while total nitrogen (TN) and chlorophyll (chl) *a* concentrations were classed as eutrophic. Nitrogen (N) was suggested as the main limiting nutrient (based on Redfield ratios), which could potentially favour the dominance of cyanobacteria (Havens et al., 2003). The cyanobacterium, *Anabaena lemmermanni,* which

6

potentially can both produce toxins and fix nitrogen, was associated with a bloom in May 2008.

When the level of Lake Onoke is high, backflow of brackish water can occur through the barrage gates. It has been demonstrated that saline intrusions into Lake Wairarapa have a statistically significant positive 'diluting' effect that reduces the Trophic Lake Index (TLI). It was also noted that there was a statistically significant increase in water clarity and reduction in dissolved reactive phosphorus (DRP) based on monitoring from 1994 to 2010 (Perrie & Milne 2012).

Small areas of submerged macrophytes have been observed in the north and the west of the lake (Mcewan, 2009), and emergent macrophytes can also be observed around the shoreline. Areas of indigenous *Ruppia sp.* have been observed in the southern basin (Perrie pers. comm.). Fish communities consist of a total of eight native and three exotic species. In a previous study shortfin eels and perch were the dominant large-bodied species found in the lake (Mcewan, 2009).


## *Lake Onoke study site*

Lake Onoke is a relatively shallow (max. depth 6.8 m) supertrophic (Perrie & Milne 2012), intermittently closed and open lake/lagoon (ICOLL) (Roy et al., 2001). It is located in the Wellington region and has an area of 622.3 ha (Fig. 3). The lake has a very high sedimentation rate, exceeding 10 mm/year (Oliver & Milne, 2012). In addition, the residence time is very low, averaging c. 2.5 days.


### *Locations for 1-D modelling*

Within Lake Onoke, data from the only routine monitoring point within the lake (Site 1, 1.4 m depth) was used for calibration and validation of the 1-D model and is used a reporting point for Site 1 (Fig 2).

### *Locations for 3-D modelling*

The Middle and Deepest sites at Lake Onoke were included as output from the 3-D model. The deepest point site is located to the south east of Lake Onoke at c. 6.8 m depth (Fig. 3).
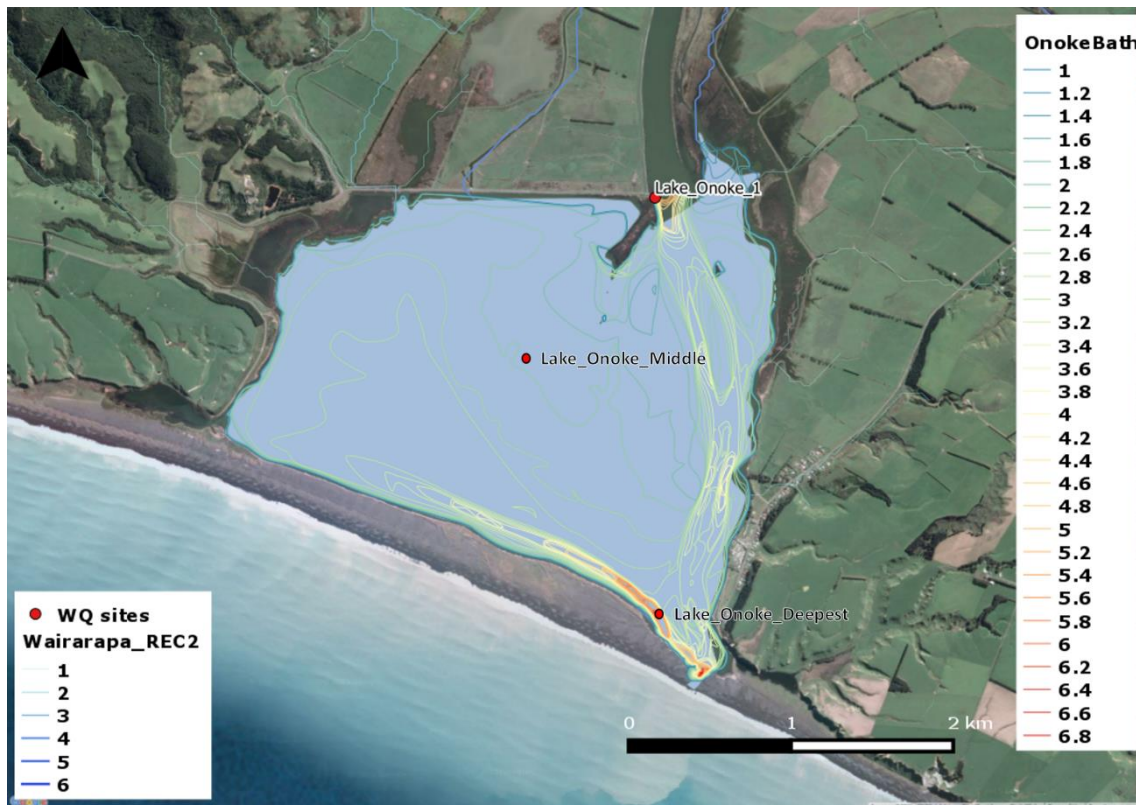
**Figure 3. Lake Onoke study site with water quality (WQ) monitoring location shown (Lake_Onoke_1), and River Environment Classification stream order (shades of blue) and bathymetric isobaths, with depth (m) displayed in the legend.**

## Catchment

The area of Lake Onoke catchment is 342,926.3 ha and the elevation ranges from the average water surface level of 10.02 m to a maximum of 1,048 m. According to the LCDB v.4.0 (Landcare Research) land cover comprises high producing exotic grassland (58.6 %), indigenous forest (17.1 %) at higher elevations, broadleaved indigenous hardwoods (4.6 percent), exotic forest (4%), and manuka/kanuka (3%), with the remainder of the catchment covering 12.5% of various land cover classes (Fig. 4, Table 2).
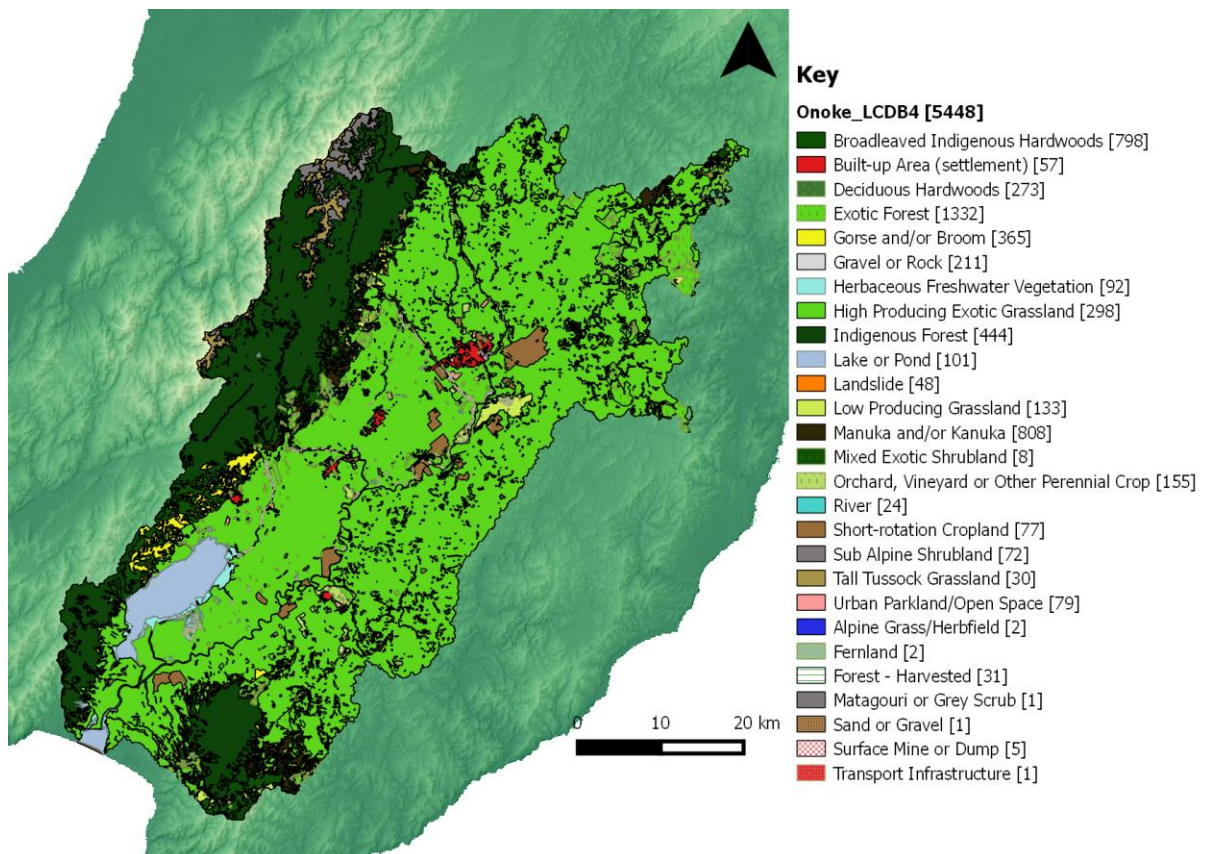
**Figure 4. Lake Onoke catchment land cover based on Land Cover Database v4.0, with bracketed numbers showing the sum of the number of polygons present within each class.**

**Table 2. Lake Onoke catchment Land Cover Database v.4.0 land use summed areas.**

| LCDB4 2012 Land Cover | Area (ha) | (Percent) |
|---|---|---|
| High Producing Exotic Grassland | 201235.7 | 58.68 |
| Indigenous Forest | 58855.1 | 17.16 |
| Broadleaved Indigenous Hardwoods | 15857.1 | 4.62 |
| Exotic Forest | 13982.0 | 4.08 |
| Manuka and/or Kanuka | 10293.1 | 3.00 |
| Lake or Pond | 8102.0 | 2.36 |
| Gorse and/or Broom | 5619.4 | 1.64 |
| Short-rotation Cropland | 5573.6 | 1.63 |
| Sub Alpine Shrubland | 4600.7 | 1.34 |
| Low Producing Grassland | 3412.3 | 1.00 |
| Tall Tussock Grassland | 3264.4 | 0.95 |
| Herbaceous Freshwater Vegetation | 2110.6 | 0.62 |
| Built-up Area (settlement) | 2002.6 | 0.58 |
| Deciduous Hardwoods | 1842.0 | 0.54 |
| Orchard, Vineyard or Perennial Crop | 1807.9 | 0.53 |
| Gravel or Rock | 1427.6 | 0.42 |
| River | 1239.8 | 0.36 |
| Forest - Harvested | 707.2 | 0.21 |
| Urban Parkland/Open Space | 639.2 | 0.19 |
| Fernland | 110.7 | 0.03 |
| Sand or Gravel | 80.6 | 0.02 |
| Landslide | 79.8 | 0.02 |
| Mixed Exotic Shrubland | 42.0 | 0.01 |
| Surface Mine or Dump | 22.2 | 0.01 |
| Alpine Grass/Herbfield | 7.3 | 0.002 |
| Matagouri or Grey Scrub | 6.0 | 0.002 |
| Transport Infrastructure | 5.5 | 0.002 |

*Inflows*

The major inflow to Lake Onoke is via the Ruamāhanga River entering in the north-east. Other inflows include the Turanganui River which enters directly to the west of the Ruamāhanga River (the two inflows are separated by narrow spit) and Pounui Stream (via Pounui Lagoon) in the north-west. In addition, when open to the sea, saline intrusions occur.

*Outflow*

Lake Onoke is separated from Palliser Bay by a narrow spit. The outflow is in the southeast of the lake through the spit, and across a shallow gravel bar. This bar gets closed approximately nine times per year. However it is opened (consented activity) to maintain a connection to the ocean and prevent water level rise. Factors that can lead to the closure of the outlet include low inflow volumes and large swells which deposit gravel. When the

outflow is blocked the lake level can increase leading to brackish backflow via the Ruamāhanga River, and through the barrage gates into Lake Wairarapa.

### Water quality and ecological status

Lake Onoke has been sampled approximately monthly for water quality variables since 2009. A detailed analysis of Lake Onoke water quality is presented in Perrie & Milne (2012). The authors found that Lake Onoke is supertrophic (Aug 2009 – July 2011), with TP and Secchi depth measurements falling within the supertrophic range and TN and chl *a* within mesotrophic/eutrophic range. Based on analysis of TN and TP ratios, and relationships between chl *a* and TP and TN, the phytoplankton are most likely to be co-limited. Phytoplankton growth is limited by factors other than nutrient concentrations, such as light availability, flushing rates, or other physical conditions. It was demonstrated that concentrations of TN and TP and non-volatile suspended solids were higher during periods of higher inflow. Chlorophyll *a* values were higher when the mouth was closed or had been recently closed. Robertson & Stevens (2007) also noted that the lake was more susceptible to eutrophication when the mouth was closed. It has been shown that ICOLL nutrient and chl *a* concentrations are significantly lower in estuaries that are permanently open to the ocean (Lill et al., 2013), as opposed to ICOLLS. Estuaries that connect to the ocean have increased flushing and scouring compared with ICOLLs. However, this finding is not generally applicable to all ICOLLs as the trophic status is also dependent on catchment inputs and biogeochemical properties (Lill et al., 2013). It was noted that the water quality at the Lake Onoke's main monitoring site (location shown in Fig. 1) may be more representative of inflows than of the lake due to its location near the inflow site.

Currently there is little or no information on the presence or absence of macrophytes. There is a diverse range of native fish present (Drake et al., 2010), and the lake is an important migratory route for all diadromous species found in the Ruamāhanga Catchment, including inanga (and spawning area) and eels.

### 1-D Water quality modelling - DYCD

DYRESM-CAEDYM (DYCD) is a 1-D water quality model that has been developed at the Centre for Water Research, University of Western Australia (Hamilton & Schladow, 1997). DYRESM simulates vertical distribution of temperature, salinity and density based using a horizontal Lagrangian (generalised coordinates) layer approach. The horizontal Lagrangian layers are free to move vertically and can contract and expand based on changes in inflows, outflows and surface mass fluxes. The layer thicknesses also adjust during model simulations in order to more effectively represent vertical density gradients than with fixed grids. DYRESM is based on an assumption of one dimensionality where variations in the vertical dimension are assumed to be greater than variations in the horizontal dimension (Imerito, 2007). The DYRESM model coupled to CAEDYM (Computational Aquatic Ecosystem Dynamics Model) enables simulation of several biological and chemical variables broadly constituting 'water quality'. CAEDYM is a general biogeochemical model that can simulate specific ecological interactions between species or groups. A detailed description of the model can be found in Hamilton and Schladow (1997).

The model includes comprehensive process representations of carbon (C), N, P (Fig. 5), and dissolved oxygen (DO) cycles, and several size classes of inorganic suspended solids. Several applications have been made of DYRESM-CAEDYM to different New Zealand lakes (e.g., Burger et al., 2008; Özkundakci et al., Trolle 2011; Trolle et al., 2011) and these publications provide detailed descriptions of the model equations.

11
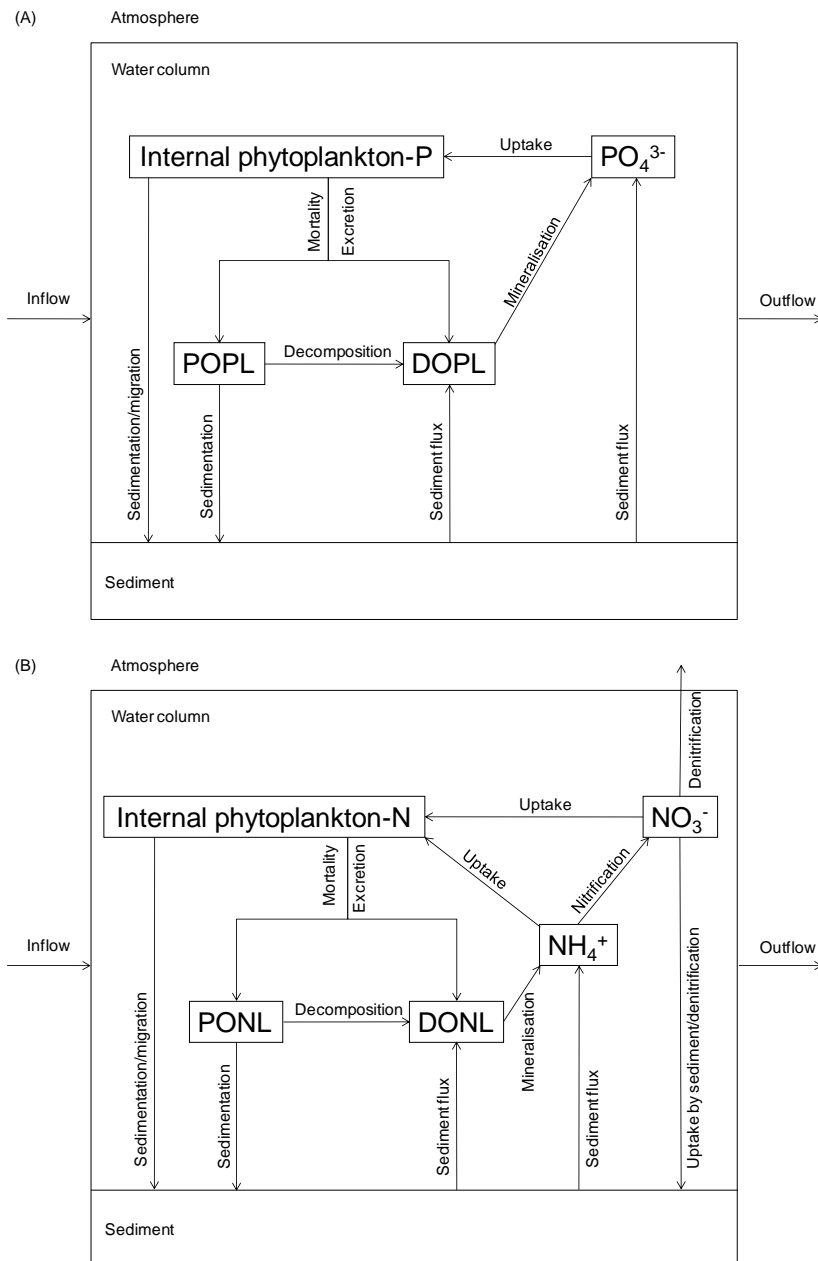
**Figure 5. Conceptual model of the (A) phosphorus and (B) nitrogen cycles represented in DYRESM-CAEDYM for the present study.  POPL, PONL, DOPL and DONL represent particulate labile organic phosphorus and nitrogen, and dissolved labile organic phosphorus and nitrogen, respectively.**

The biogeochemical variables in CAEDYM may be configured according to the goals of the model application and availability of data. In this study, two groups of phytoplankton were included in CAEDYM, representing generically diatoms and cyanobacteria. The interactions between phytoplankton growth and losses, sediment mineralisation and decomposition of particulate organic matter influence N and P cycling in the model as shown in Fig. 5. Fluxes of dissolved inorganic and organic nutrients from the bottom sediments are dependent on temperature, nitrate and DO concentrations of the water layer immediately above the sediment surface.

12

Lake morphometry is specified within the 1-D model using an ascii text file which contains lake height and area (volume is calculated by the model).

### Water quality modelling – DYCD macrophytes

Macrophytes were modelled using a specific version of DYCD (Jones et al., 2018), modified to include dynamic feedback between submerged macrophyte biomass and sediment resuspension. The results from these simulations are not directly comparable to other 1-D simulations, however the calibration results are numerically similar.

### 3-D Water quality modelling – AEM3D

The Aquatic Ecosystems Model (AEM3D) is a three-dimensional (3-D) numerical model (Hodges & Dallimore, 2016) that uses hydrodynamic and thermodynamic models in order to predict velocity, salinity and temperature in waterbodies (Fig. 6). The hydrodynamic component of this model is an updated version of the Estuary, Lake and Coastal Ocean Model (ELCOM). The hydrodynamic model solves the unsteady, viscous Navier-Stokes equations for incompressible flow using the hydrostatic assumption for pressure. A Euler-Lagrange method is used for advection of momentum with a conjugate-gradient solution for the free-surface height (Casulli & Cheng, 1992). Passive and active scalars are advected using a conservative Ultimate Quickest discretization (Leonard, 1991). AEM3D was also coupled to CAEDYM (Schladow & Hamilton, 1997) for the purpose of resolving horizontal distributions of biological and chemical variables.
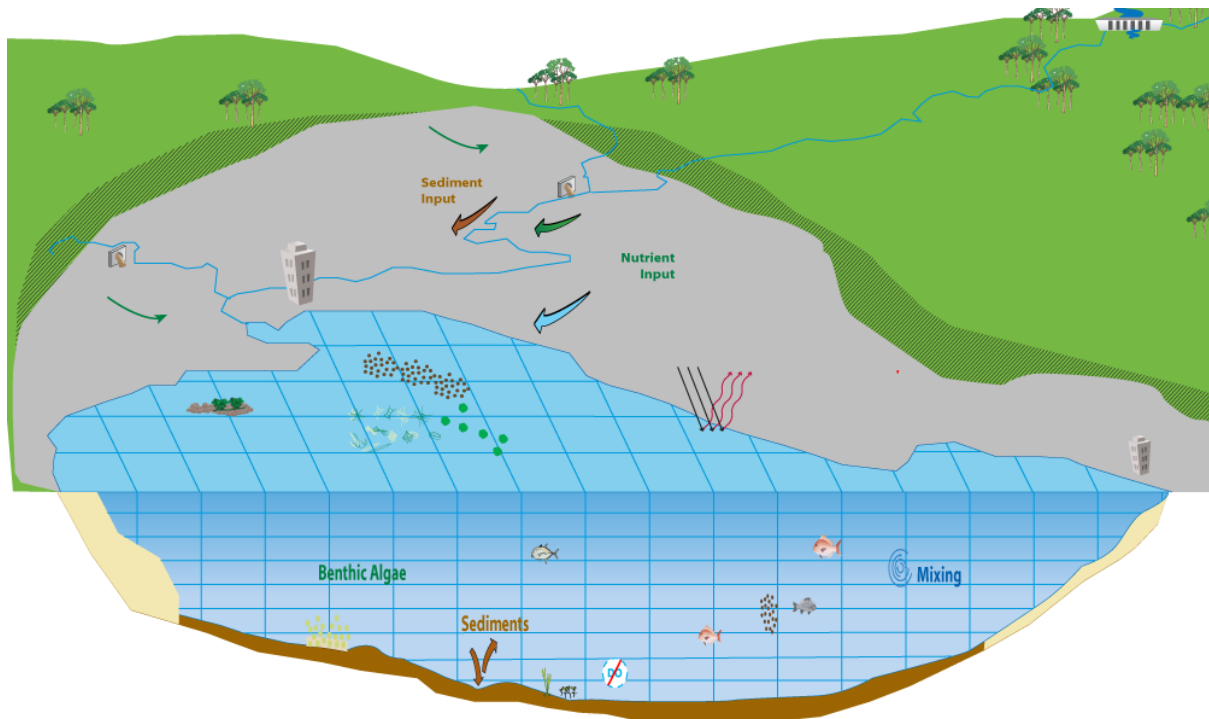


Symbols courtesy of the Integration and Application Network, University of Maryland Center for Environmental Science (ian.umces.edu/symbols/).

**Figure 6. Conceptual model of Aquatic Ecosystems Model (AEM3D), which is forced by meteorological data, inflow volume, temperature, salinity and nutrient/suspended sediment concentration. 3-D lake bathymetry is also required. Note that for this project AEM3D used CAEDYM ecological model option in AEM3D.**

## *One-dimensional modelling versus three-dimensional modelling*

DYRESM CAEDYM 1-D modelling is a simplification of reality whereby we assume the lake is horizontally homogeneous across the lake surface, and only variation over lake depth is simulated (Fig. 7). This means we have multiple cells from the lake surface to the lake bottom. This allows models to run fast, and therefore run over long time periods, and be easily calibrated.
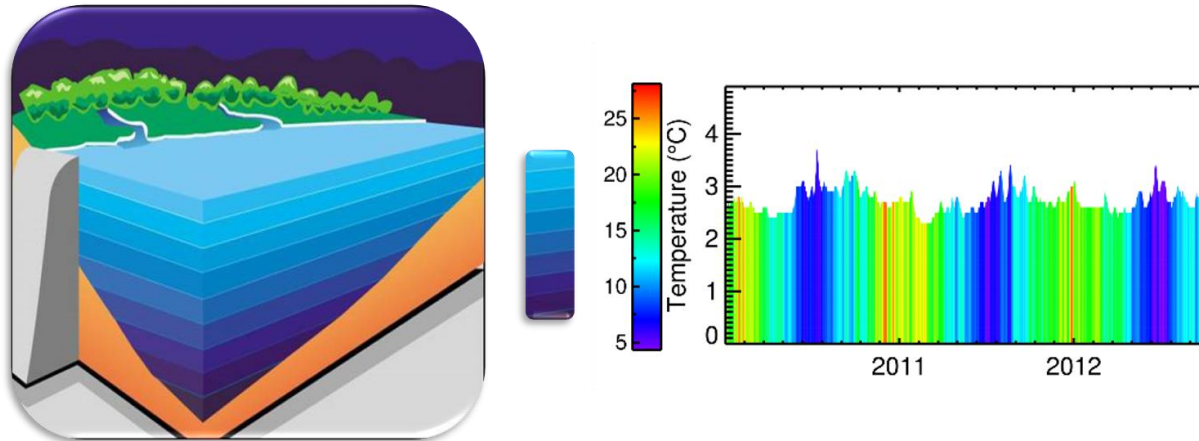


**Figure 7. Schematic of the 1-D horizontally homogenous assumption where the model grid structure is made up of vertical cells (which are able to vary in depth) of different volumes and exchanges of water and solutes are calculated between these layers.**

AED CAEDYM 3-D modelling is a close representation of reality where we can simulate and look at the lake from any spatial perspective. This method divides the lake into cells across the lake surface and from the lake surface to the lake bottom (Fig. 8). AED CAEDYM 3-D models require much more computation time, hence are much more difficult to calibrate. Considering the large spatial variation of water quality in lakes Onoke and Wairarapa, 3-D modelling would provide more robust information on any scenario that changes the spatial variation of hydrodynamics and water quality inputs, when compared to 1-D models.
AED CAEDYM 3-D was run over comparatively short time periods of three months in the summer of 2012 from January to the end of March. This time period was chosen firstly because a summer period was needed for the Onoke outlet close scenario. The 2012 summer period was chosen as it included periods of both high and low flow within inflows.

14
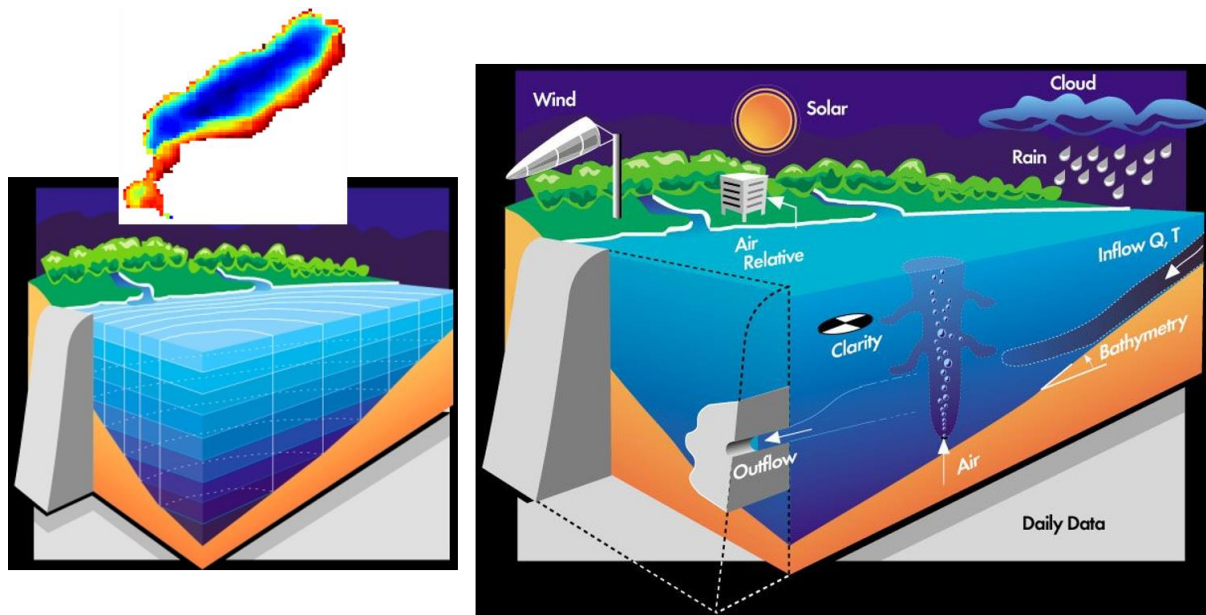
**Figure 8. Schematic of the 3-D model grid structure whereby the model accounts for both horizontal and vertical variation in simulated variables such as water temperature and water quality.**

## *Delft sediment transport of Lake Wairarapa*

Delft3D-FLOW is a 3-D hydrodynamic numerical model that simulates non-steady flow from tidal and meteorological forcing on a rectilinear or curvilinear boundary fitted grid (Deltares systems, 2014). The model has been extensively validated for hydrodynamics and sediment transport applications (Hu et al., 2009; Lesser et al., 2004; Zarzuelo et al., 2015). The model grid cell size was 200 m for the application to Wairarapa (Fig. 9).

**Table 3. Key questions and model used.**

| Key question | Method | Notes |
|---|---|---|
| **Determine spatial distribution of water quality variables** | 3-D modelling and Landsat based remote sensing for total suspended solids (TSS) | AEM3D model used for water quality and *E.coli*. Bio-optical model used for TSS |
| **Model Baseline water quality** | 1-D modelling | DYRESM CAEDYM including *E.coli* |
| **Model catchment-based scenario's water quality** | 1-D modelling | DYRESM CAEDYM including *E.coli* |
| **Model catchment and hydrodynamic (e.g. 1 m depth increase/river diversions) based scenario's water quality** | 1-D modelling and 3-D modelling | DYRESM CAEDYM (1-D) and AEM3D CAEDYM (3-D) including *E.coli* |
| **Sediment transport in Lake Wairarapa** | 3-D modelling | Delft 3-D |

15
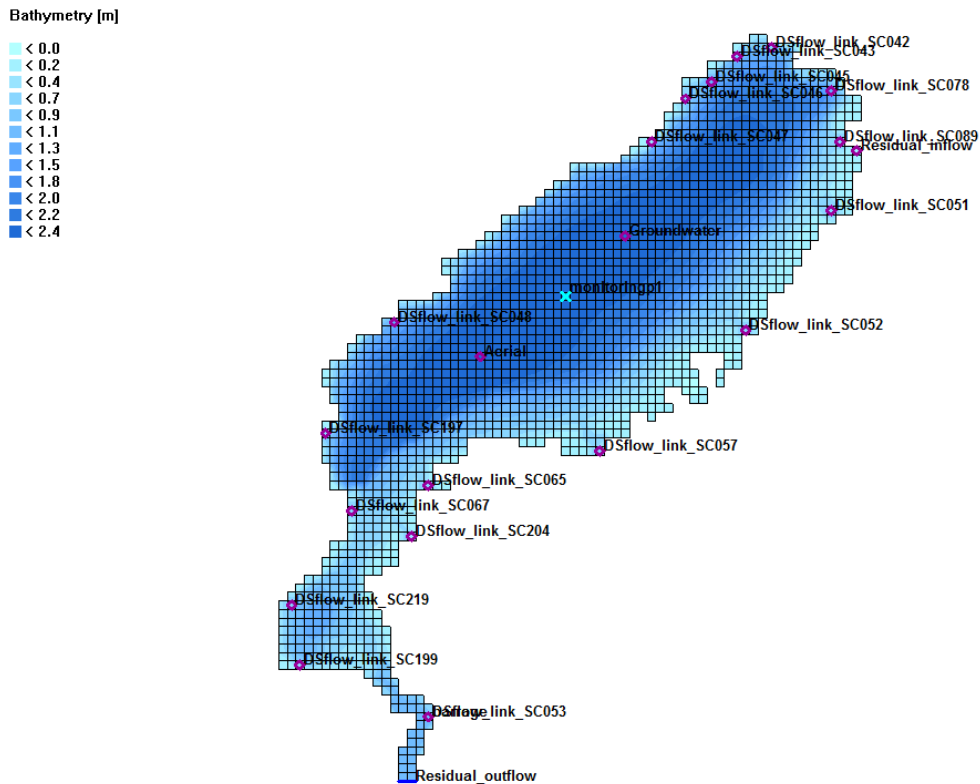
**Figure 9. Grid bathymetry and inflow locations for Lake Wairarapa sediment erosion deposition model using Delft (rectilinear grid).**

The simulation period was from 1 September 2011 until 1 September 2013, encompassing a broad range of meteorological events. In addition, 2012 was the first year that flow in and out of the Barrage Gates was measured. The model was initially set up with zero available sediment on the lake bottom, and inflows were created using an Interactive Data Language script which populated Delft-Flow input files using those generated from a MODFLOW groundwater model application for the catchment. Suspended particle concentrations in MODFLOW were partitioned equally into two sediment grain sizes and corresponding critical shear stresses and settling velocities:

1: 0.03 N/m$^2$ critical shear stress, 0.0002 mm/s settling velocity
2: 0.05 N/m$^2$ critical shear stress, 0.0002 mm/s settling velocity

The model was then run to estimate locations on the lake bottom where resuspension or erosion occurred.

### *E. coli modelling 1-D and 3-D*

Modelling for *E. coli* was completed using DYCD (1-D) and AEM3D CAEDYM. The following assumptions were used:

- Mortality was modelled using a first order decay rate and a specified settling velocity
- Bacteria were present in the water column and did not accumulate in the sediment;
- Bacteria did not grow in the lake.

16

## Forcing variables for modelling

### Modelled inflows

Lake stream/river inflow volumes and nutrient concentrations were derived from a linked combination of specialised catchment models (Fig. 10). The specific details of this modelling are not covered in this report. In summary, hill country flows are modelled with TopNet (NIWA), which is a semi-distributed hydrological model for simulating catchment water balance and flow. This flow is then assimilated by the United States Geological Survey (USGS) model MODFLOW, which is a 3-D finite difference coupled groundwater/surface water model. Groundwater contaminant flow was modelled using the Modular 3-D Multi-Species Transport Model (MT3DMS) for simulation of advection, dispersion, and chemical reactions of contaminants in groundwater systems (Moore et al., 2017). The model eSource was used to model surface water contaminant flow (Sands, 2018). The resulting flow and nutrient concentrations entering the lakes were input into the 1-D and 3-D lake models at daily time-step.
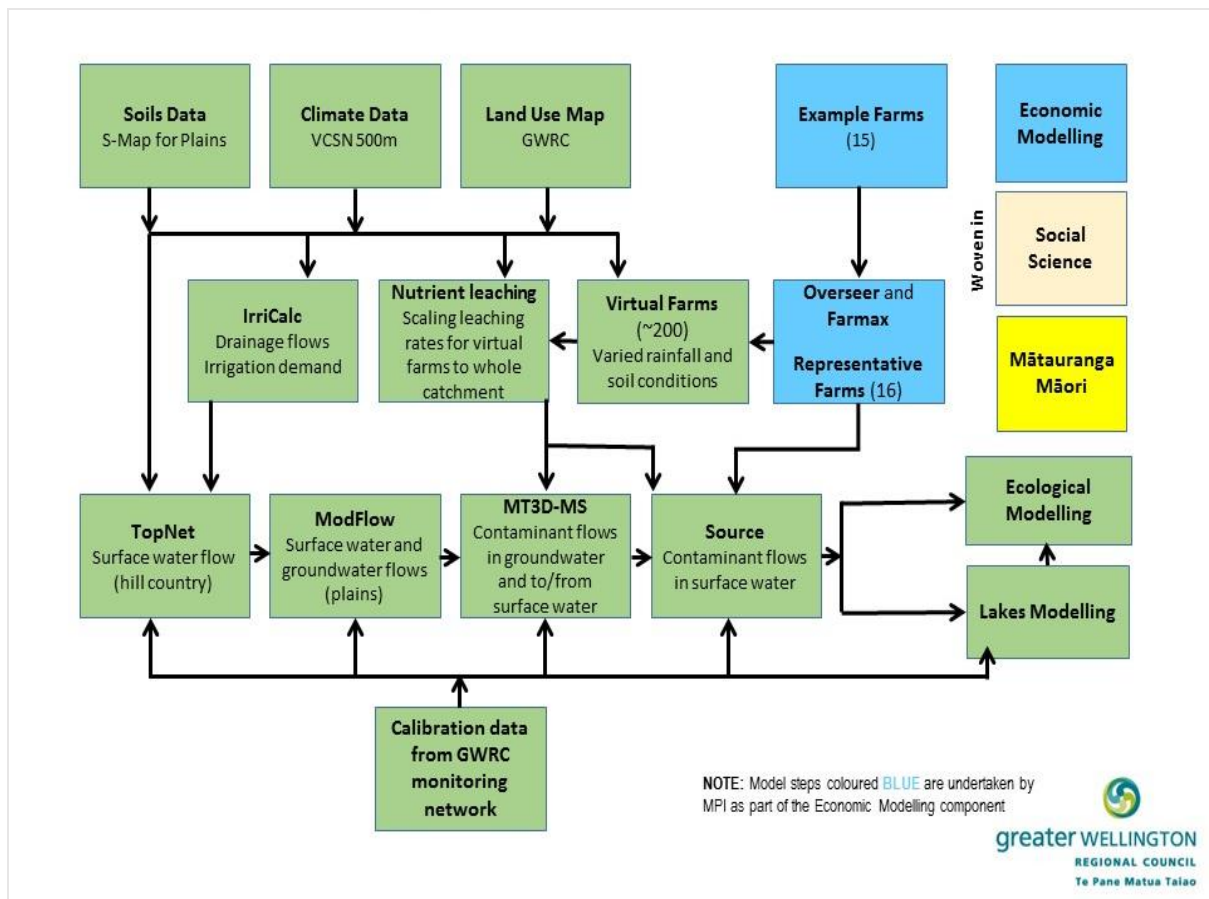


**Figure 10. Ruamāhanga Whaitua modelling architecture. Note the simulation period is 1992-2014.**

### Calibration/simulation time period

The calibration/simulation period spanned from 1 July 1992 through 30 June 2014. All 1-D scenario runs used the same time period as the calibration, and identical meteorological data (climate change was not simulated).

## Meteorological forcing

Meteorological forcing of DYRESM included daily average air temperature (ºC), shortwave radiation (W m$^{-2}$), cloud cover (fraction of whole sky), vapour pressure (hPa), wind speed (m s$^{-1}$) and rainfall (m) (Fig. 11). Meteorological forcing of ELCOM included daily average wind speed (m s$^{-1}$), wind direction (degrees), air temperature (ºC), shortwave radiation (W m$^{-2}$), atmospheric pressure (Pa), relative humidity (% fraction), rainfall (m) and cloud cover (fraction of whole sky). Note that 2025, 2040 and 2080 simulations used this meteorological data.
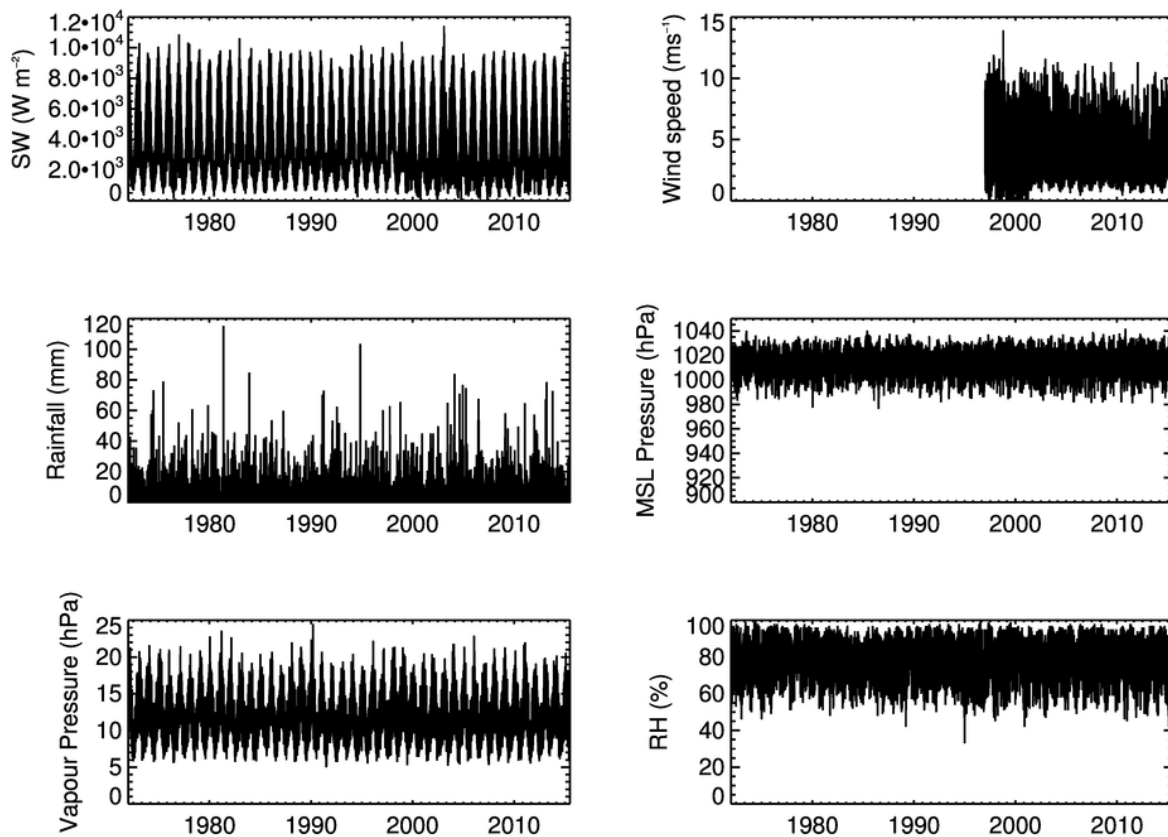


**Figure 11. Meteorological data used as input to DYRESM. SW is shortwave radiation. Data were obtained from the NIWA Virtual Climate Station data. Wind speed data was not available in the VCN until 1997.**

## Water balance

A daily water balance was determined for each lake, which included inflows, estimates of groundwater inflow, rainfall and calculated evaporation from estimates of the evaporative heat flux (Fischer, 1979) and the saturation vapour pressure, together with water-level induced changes in lake volume (Fig. 12). Where outflow measurements were unavailable (i.e. for Lake Onoke and before ADCP flow data were available for Lake Wairarapa), a residual term in the water balance was used to derive a daily outflow.

The flow at the barrage gates has been monitored since August 2012, using a side-looking Acoustic Doppler Current Profiler (ADCP) (Thompson & Mzila, 2015), however estimations for backflow into Lake Wairarapa were needed for the entire simulation period. A statistical

18

model was applied using a symbolic regression model trained over the monitored barrage flow period. This model used Onoke water levels and Lake Wairarapa outflow as inputs:

*Barrage inflow* = (324.89*Onoke water level - 3018618.30)/exp(*barrage outflow*) (10)

for simulations *barrage outflow* was determined using a water balance. Correlation Coefficient = 0.58, mean absolute error=122125.75 m3/day. Note that this method underestimated large barrage inflows (Appendix Fig. 1).

Within Lake Onoke modelled ocean inflows were allowed to occur when GWRC data indicated that the mouth was unblocked. During unblocked periods any increase in lake height was attributed to ocean inflow and calculated based on volume changes derived from the hypsographic curve (Fig. 13). Ocean inflow nutrient concentrations were adopted from coastal and estuarine water quality statistics: (http://archive.stats.govt.nz/browse_for_stats/environment/environmental-reporting-series/environmental-indicators/Home/Marine/coastal-estuarine-water-quality.aspx). Dissolved nutrients: nitrate- and nitrite-nitrogen (0.01 mg/L), ammoniacal nitrogen (0.01 mg/L), and total phosphorus (0.02 mg/L). Ocean inflow *E.coli* concentrations were adopted from Oliver & Milne (2012) at 2.8 CFU/100ml.

### *Lake bathymetry*
Lake bathymetry data was sourced from GWRC, and originated from ADCP soundings collected in 2010 (Fig. 13). However, using this method, simulated salinity levels were unrealistically low, so the estimated ocean inflow was estimated through multiplicative iteration. Therefore, the final ocean inflow was derived from the initial change in lake height estimated inflow, multiplied by a factor of eight.

Inflow water temperature for all flows within what lake Wairarapa and Lake Onoke were estimated from an empirical relationship between Tauherenikau water temperature and the average of daily VCN min and max air temperature ($r^2 = 0.32$):

$INFLOW\_TEMP = 0.52*AIR\_TEMP + 6.07$ (1)

19
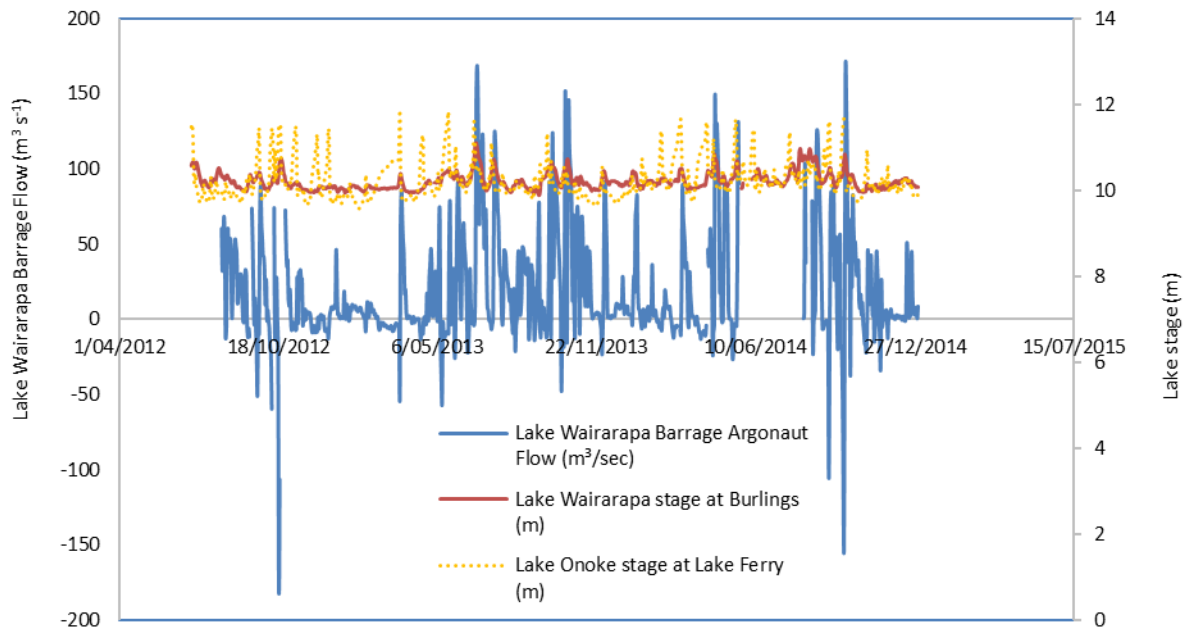
**Figure 12. The stage of Lake Wairarapa (red line, right axis) and Lake Onoke (orange dashed line, right axis), and Lake Wairarapa barrage flow (blue line, left axis).**
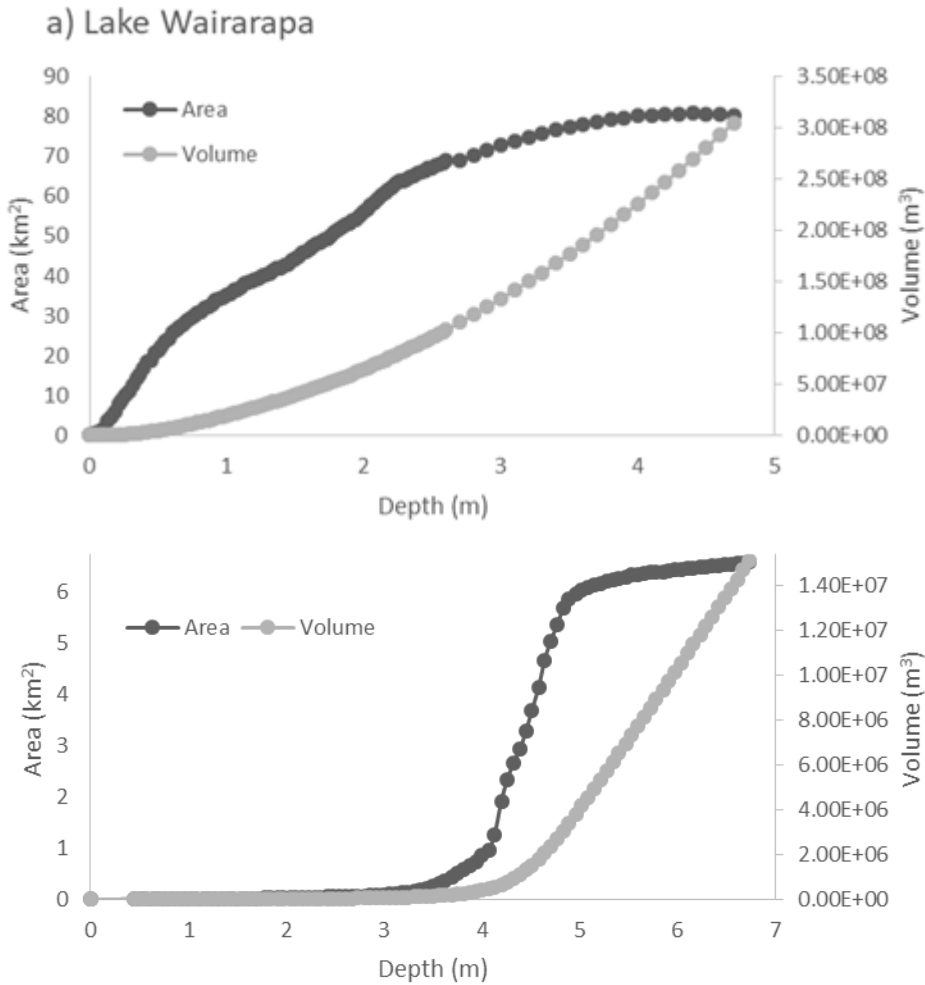
**Figure 13. Hypsographic curves of area and volume vs. depth for; a) Lake Wairarapa and b) Lake Onoke.**

*Modelled catchment and within lake scenarios*

The basis for catchment-related scenarios are given in detail within Blyth (2018) and appendix Table 16. The Baseline model (calibration) is based on "current conditions" simulating management practices between 1992 and 2014. BAU (business as usual), SILVER and GOLD scenarios were all run using representative catchment modelling data for 2025, 2040 and 2080, with time periods relating to when management options take effect (2025, 2040 and 2080 simulation periods used simulation time period and meteorological forcing data from 1 July 1992 through 30 June 2014 – climate change was not considered). Mitigation options include retirement of land, pole planting, land treatment of wastewater, minimum flow rules, and on-farm mitigations (Muirhead et al., 2016), and took effect for the simulation period. Lake specific modelling scenarios were run in addition to catchment scenarios (Table 4, Appendix Table 16).

**Table 4. Lake specific modelling scenarios and catchment scenarios**

| Modelling shorthand naming conventions | Description |
|---|---|
| ALL_RUA_SILVER2080<br>ALL_RUA GOLD2080 | All flows of the Ruamāhanga River enter Lake Wairarapa.<br>No flow by-passing via the diversion. |
| MEDIAN_RUA_SILVER2025/2040/2080 | Flows below the median go into Lake Wairarapa, and flows above median are by-passed |
| Outlet_Close_SILVER2025/2040/2080,<br>Outlet_Close_Rua_All_SILVER2025/2040/2080 | Lake Onoke outlet closed January to March each year.<br>Lake Onoke outlet closed January to March, all Ruamāhanga flows diverted into Lake Wairarapa before entering Onoke |
| 1m_Inc_SILVER2025/2040/2080 | Deepening both lakes by 1 m |

### *Significant assumptions*

Nutrient loads to lakes come from external sources (catchment surface and groundwater flows) and internal sources (derived from diffusion and resuspension from nutrients stored in lake bed sediments). These nutrients derived from the lake sediments can comprise a significant proportion of the total load to the lake and therefore any modelling of lake ecology must consider these. Therefore, any changes to nutrient concentrations derived from catchment modelling or from changes in flow regimes (Ruamāhanga diversion into Lake Wairarapa) were applied to sediment nutrient release rates based on a percentage reduction or increase applied to sediment nutrient release rates in relation to baseline conditions. This enabled simulation of the influence of different catchment loads on the release rates within the sediment. In reality, there is a lag time for sediments to reach equilibrium, usually between 10 and 15 years (Jeppesen et al., 2005), but sometimes persisting for more than 20 years for internal loading of phosphorus (Søndergaard et al., 2003).

For BAU, GOLD and SILVER lake water levels were based on historical measurements.

### *Trophic Level Index calculation*

The lake TLI value was calculated to indicate overall changes in water quality. The relevant equations for determination of the TLI are (Burns & Bryers, 2000):

$$TL_{Chla} = 2.22 + 2.54 \ \log(Chla) \tag{2}$$

$$TL_{SD} = 5.1 + 2.27 \ \log\left(\frac{1}{SD} - \frac{1}{40}\right) \tag{3}$$

$$TL_{TP} = 0.218 + 2.92\log(TP) \tag{4}$$

$$TL_{TN} = -3.61 + 3.01 \ \log(TN) \tag{5}$$

$$TLI\text{-}4 = \frac{1}{4}\sum\left(TL_{Chla}, TL_{SD}, TL_{TP}, TL_{TN}\right) \tag{6}$$

$$TLI\text{-}3 = \frac{1}{4}\sum\left(TL_{Chla}, TL_{TP}, TL_{TN}\right) \tag{7}$$

where:

$TL_{Chla}$, $TL_{SD}$, $TL_{TP}$ and $TL_{TN}$ represent the individual trophic level indices for the variables of chl $a$ (mg/m$^3$), Secchi depth (m), TP (mg/L) and TN (mg/L), respectively.

### *Secchi depth calculation*

As Secchi depth is not explicitly included in the model, this variable was derived from the model-predicted attenuation coefficient for photosynthetically active radiation as (Holmes, 1970):

$$z_{SD} = 1.44\,K_d \tag{8}$$

where:

$z_{SD}$ is the Secchi depth (m)

$K_d$ is the diffuse attenuation coefficient for PAR (m$^{-1}$).

$K_d$ is calculated as (Gallegos, 2001):

$$K_d = K_w + K_c * chl_a + K_y * DOC + K_s * TSS \tag{9}$$

where:

$K_w$ is the background extinction coefficient with a value of 0.3315 (m$^{-1}$).

$K_c$ is the specific attenuation coefficient for chl $a$ with a value of 0.0122 (m$^2$ (mg chl $a$)$^{-1}$).

$K_y$ is the specific attenuation coefficient for dissolved organic carbon with a value of 0.0507 m$^2$ (g DOC)$^{-1}$.

$K_s$ is the specific attenuation coefficient for total suspended sediment with a value of 0.2 (m$^2$ (g TSS)$^{-1}$).

### *National Objectives Framework band calculation*

Note that percentile calculation is within the present study for *E.coli* concentrations use Hazen methods. Details of the equations for all NOF variables can be found in MFE (2017a).

### Remote sensing

### Satellite imagery and software

United States Geological Survey (USGS) on demand atmospherically corrected Landsat imagery was ordered from http://espa.cr.usgs.gov/index/, including 91 images captured from 1999 - 2015. Atmospheric correction applies the radiative transfer model 6sv (Second Simulation of a Satellite Signal in the Solar Spectrum), which corrects for atmospheric scattering and absorption effects of gases, and aerosols (Kotchenova et al., 2008). All image processing routines were automated using scripts written in Interactive Data Language (IDL).

TSS was estimated from Landsat subsurface remote sensing reflectance ($r_{rs}$) using a similar semi-analytical algorithm to that found in Allan et al., (2015) and (Dekker et al., 2002a) except that only Landsat Band 3 (b3) was applied to estimate TSS. Forward bio-optical modelling was used to quantify the physical processes responsible for relationships between Landsat measured $r_{rs}$ and TSS concentrations. These relationships were used to predict TSS from inverted $r_{rs}$. The relationship between $r_{rs}(\lambda)$ and the total backscattering coefficient ($b_b$) (m$^{-1}$) and total absorption $a$ (m$^{-1}$) is (Gordon et al., 1988):

$$r_{rs}(\lambda) = g_0 u(\lambda) + g_1 [u(\lambda)]^2 \qquad (10)$$

where $u$ is defined as (Dekker et al., 1997):

$$u(\lambda) = \frac{b_b(\lambda)}{a(\lambda) + b_b(\lambda)} \qquad (11)$$

and $g_o$ and $g_1$ are empirical constants that depend on the anisotropy of the downwelling light field and scattering processes within the water. The constant $g_o$ is equivalent to $f/Q$ where $f$ represents geometrical light factors and $Q$ represents the light distribution factor, which is defined as upwelling subsurface irradiance/upwelling subsurface radiance). It has been suggested that $g_o$ and $g_1$ should be considered as variables in optically complex inland waters (Aurin & Dierssen, 2012; Li et al., 2013). Therefore we used fitted values for $g_o$ and $g_1$ of 0.103 and 0.009 respectively, which were derived previously for Lake Ellesmere (Allan, 2014).

The absorption and backscattering coefficients are comprised of individual optically active constituents:

$$b_b(\lambda) = b_{bw}(\lambda) + B_{bTSS}\, b^*_{TSS}(\lambda)\, C_{TSS} \qquad (12)$$
$$a(\lambda) = a_w(\lambda) + C_\phi\, a^*_\phi(\lambda) + a_{CDOMD}(\lambda) \qquad (13)$$
$$a_{CDOMD}(\lambda) = a_{CDOMD}(\lambda_{440})\, \exp[-S\,(\lambda - \lambda_{440})] \qquad (14)$$

where:

$b_{bw}(\lambda)$ = backscattering coefficient of water
$B_{pTSS}$ = backscattering ratio from TSS
$b^*_{TSS}(\lambda)$ = specific scattering coefficient of TSS
$C_{TSS}$ = concentration of TSS
$b^*_\phi(\lambda)$ = specific scattering coefficient of phytoplankton
$a_w(\lambda)$ = absorption coefficient of pure water

24

$C_\phi$ = concentration of chl $a$

$a^*_\phi(\lambda)$ = specific absorption coefficient of phytoplankton

$a_{CDOMD}(\lambda)$ = absorption coefficient for chromophoric dissolved organic matter (CDOM)

$S$ = spectral slope coefficient

Values of $a_w(\lambda)$ and $b_{bw}(\lambda)$ were prescribed from the literature (Morel 1974; Pope and Fry 1997). The backscattering ratio of TSS, $B_{pTSS}$, was set to 0.019 (Petzold, 1972). The specific scattering coefficient of TSS at the Landsat b3 wavelength was estimated using a power function (Morel & Prieur, 1977):

$$b^*_{SP}(\lambda) = b^*_{SP}(555)\left(\frac{555}{\lambda}\right)^n \qquad (15)$$

where the value $b^*_{TSS}(555)$ was set to 0.6 m$^2$ g$^{-1}$. The hyperbolic exponent $n$ was set to 0.63, equating to a value measured in Lake Taupo, New Zealand [*Belzile et al.*, 2004]. The $a^*_\phi(662)$ was 0.0136 m$^2$ mg$^{-1}$, equal to the average value measured in eight Dutch lakes (Dekker, Brando, et al., 2002). The bio-optical simulations were run by varying TSS concentration from 0.1 to 417.6 mg L$^{-1}$ in increments of 0.5 mg L$^{-1}$ while $a_{CDOMD(440)}$ was fixed to a value of 0.042 m$^{-1}$, which is the average in situ of measurement in Lakes Wairarapa and Onoke, with chl $a$ ($\mu$g L$^{-1}$) taken to increase with TSS (chl $a$= TSS/6) for chl $a$ of 0.017 to 67.6 $\mu$g L$^{-1}$ (encompassing a similar range to that measured *in situ* in Lakes Onoke and Wairarapa).

The semi-analytical relationship between TSS concentrations as a function of Landsat b3 remote sensing reflectance ($r_{rs}$b3) was approximated via exponential relationships (Fig. 14a). Two exponential relationships were used to approximate the analytical relationship. At values of $r_{rs}$b3 < 0.06 the exponential function intercept was set to zero to improve model accuracy at low reflectance (Fig. 14b).
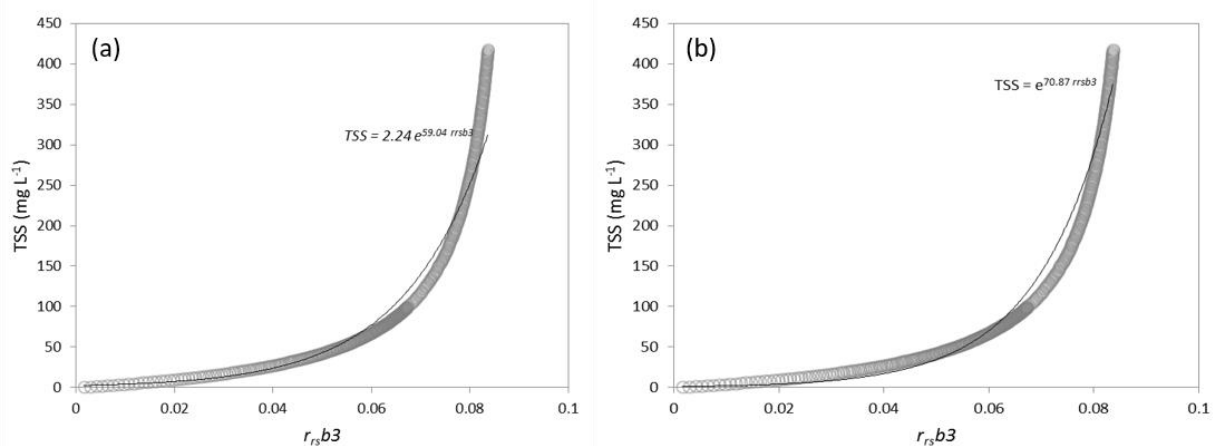


**Figure 14. (a) The analytical relationship between total suspended sediment (TSS) concentrations as a function of Landsat band 3 subsurface remote sensing reflectance ($r_{rs}$b3). The relationship is approximated using an exponential relationship. (b) For $r_{rs}$b3 < 0.06 this exponential relationship is applied using a zero intercept, which improves TSS estimations at low values of $r_{rs}$b3.**

Nine *in situ* samples captured on the same day as Landsat images (within Lakes Onoke and Wairarapa) were used to calibrate and validate the model (Fig. 15). The relationship between observed and estimated TSS produced an $r^2$ of 0.97, RMSE 16.62 mg $L^{-1}$, and 32% RMSE, over a range of *in situ* TSS from 3 - 239 mg $L^{-1}$. These results indicated that the model is suitable for the estimation of TSS.
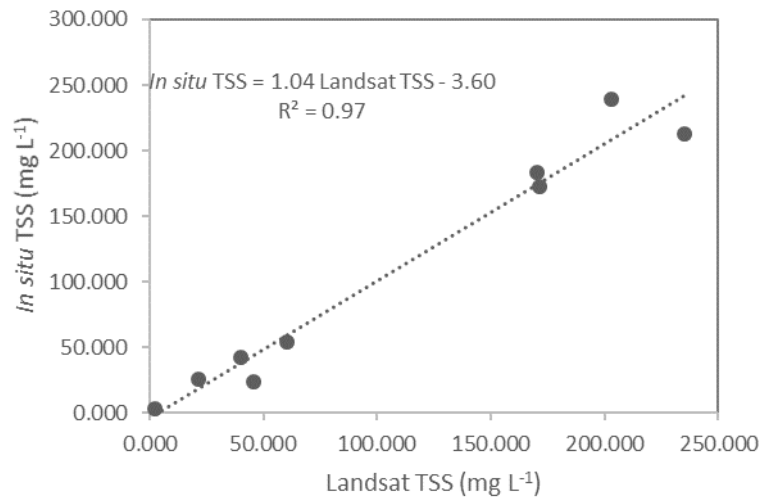


**Figure 15. Comparison of *in situ* TSS to Landsat estimated TSS (mg L⁻¹) using a semi-analytical relationship (Fig. 14).**

## Results

### *Remote Sensing of TSS*

Time series of TSS from Landsat data at Lake Wairarapa Site 1 gave TSS concentrations of similar range to those measured in situ, demonstrating the high temporal variability in TSS concentrations (Fig. 16).
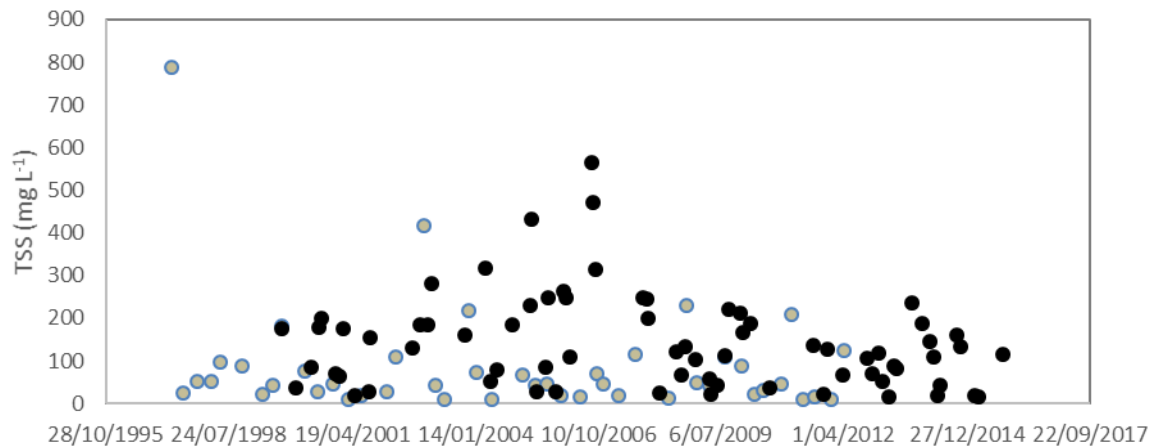


**Figure 16. Time series of total suspended solids (TSS) at Lake Wairarapa Site 1 using Landsat (black filled circles), compared to those measured *in situ* (grey filled circles). Landsat TSS explained 97% of the variation of in situ TSS (see Fig 14).**

Landsat time series of TSS within Lake Onoke also demonstrate a similar range to that observed *in situ*, and again displayed high temporal variation (Fig. 17).
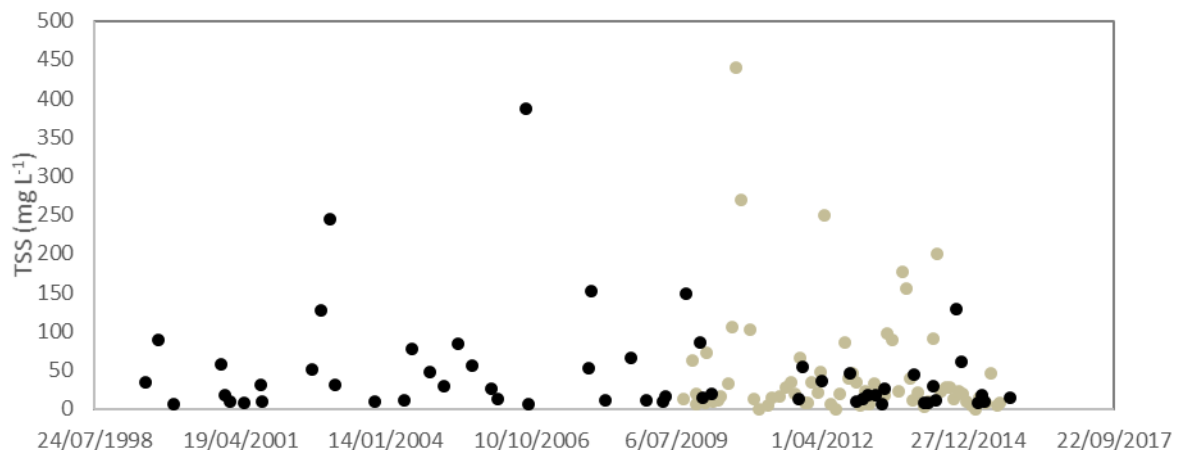


**Figure 17. Time series estimation of total suspended solids (TSS) at Lake Onoke using Landsat (black filled circles), compared to those measured *in situ* (grey filled circles). Landsat TSS explained 97% of the variation of in situ TSS (see Fig 14).**

The spatially resolved estimates of TSS clearly demonstrate the highly heterogeneous distribution within and between lakes Wairarapa and Onoke (Fig 18, digital appendix Landsat images) and the coastal zone. The TSS concentrations within the coastal ocean are generally low, however when the mouth of Lake Onoke is open, high TSS exiting has the potential to

27

elevate TSS concentrations within this zone. Within Lake Onoke TSS concentrations in the east were often dominated by concentrations of either riverine or oceanic inputs. There were periods when TSS concentrations within Onoke were clearly elevated to high concentration inflows derived from Lake Wairarapa, or high flow events derived from the Ruamāhanga river. Within Lake Wairarapa large-scale circulations (eddies) are often evident, and more obvious at high TSS concentrations. A common feature of the spatial distributions of TSS was generally higher concentrations within western regions of Lake Wairarapa. In contrast to TSS concentrations in Lake Wairarapa, concentrations within inflows which generally much lower, especially in inflowing Tauherenikau River to the north, creating zones of much lower TSS concentrations when compared to the main body of the lake. Also, there were often periods when TSS concentrations in Alsop's Bay were much lower than in the main lake basin.
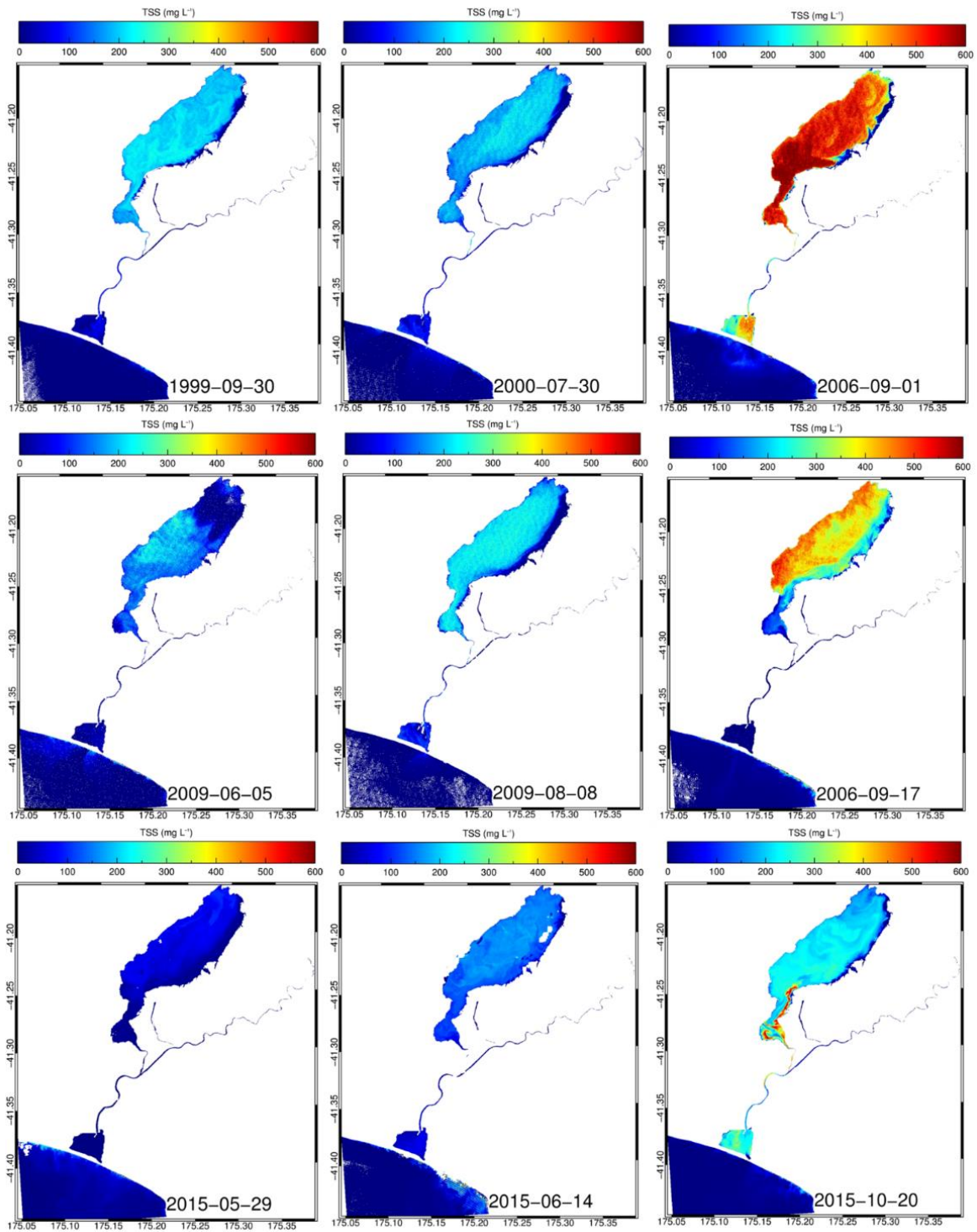
**Figure 18. Spatially resolved total suspended sediments (TSS) in Lakes Onoke and Wairarapa derived from a semi-analytical algorithm for Landsat band three subsurface remote sensing reflectance data. Images displayed here represent a subset of the 91 images generated. Displayed images were selected to represent different magnitudes and spatial variations of TSS and were cloud free images.**

29

*Calibration of 1-D ecologically coupled hydrodynamic model of Wairarapa*

The focus of achieving an acceptable calibration for Lake Wairarapa (and Onoke) was reproducing temperature, surface DO, TN, TP, TSS, and chlorophyll *a* represented as a total value for the phytoplankton community (derived parameters in appendix Table 17 and 18). Calibrations were achieved using a combination of manual and auto-calibration. Auto-calibration was applied using Monte Carlo methods, randomly varying input parameters within literature ranges of parameters using 999 model runs, using Pearson correlation as a measure of model calibration performance. The statistical comparison (Table 5) was deemed reasonable by comparison with other modelling applications, with normalised root mean squared error (NRMSE) ranging from 14% (TP) to 36% ($PO_4$). With an average estimation NRMSE error of 22%. The RMSE errors generated within the study for both Onoke and Wairarapa are comparable with similar shallow lake models (e.g. Lehmann et al. 2017), and while there is always room for model improvement, we deem these two models to be a good representation of reality when compared to *in situ* data (Fig. 19).

**Table 5. Model performance for 1-D simulation Lake Wairarapa baseline, using root mean square error (RMSE) and normalised root mean square error (NRMSE %).**

| Variable | RMSE (units of variable) | NRMSE (% fraction) |
|---|---|---|
| Chl *a* ($\mu$g L$^{-1}$) | 10.65 | 0.22 |
| TN (mg L$^{-1}$) | 0.40 | 0.27 |
| TP (mg L$^{-1}$) | 0.16 | 0.14 |
| $PO_4$-P (mg L$^{-1}$) | 0.01 | 0.36 |
| $NH_4$-N (mg L$^{-1}$) | 0.01 | 0.24 |
| $NO_3$-N (mg L$^{-1}$) | 0.19 | 0.20 |
| TSS (mg L$^{-1}$) | 71.44 | 0.20 |
| Secchi depth (m) | 0.24 | 0.20 |
| Temperature ($^O$C) | 1.71 | 0.20 |
| TLI (TLI units) | 0.73 | 0.23 |
| Salinity (psu) | 0.31 | 0.24 |

*Key characteristics based on models and observations*

Model simulations indicated no significant stratification, with water temperature not changing over depth on any day (Fig. 22). This is due to the large surface area to volume ratio and shallow depth, with associated wind mixing. The RMSE of temperature estimations is somewhat higher than that other studies (e.g. RMSE of 0.54 using DYCD on Lake Rotorua by Allan et al., 2016). This could potentially be caused by using VCN daily input data, which uses the average of daily minimum and maximum temperature, rather than mean temperature, as input. Shallow lakes will also be more susceptible to variations in air temperature.

Dissolved oxygen concentrations followed an expected seasonal pattern of higher in winter than summer, aligning with increased saturation capacity of cooler waters (Fig. 19). The model simulations generally reproduced the observations of surface DO well, but with tendency for under-prediction in summer. Simulated salinity generally followed patterns of observed salinity, with high salinity (> 0.2) reflecting backflow of brackish water entering

Lake Wairarapa through the barrage gates. Simulated lake depth also closely followed what was observed, as the water balance is forced with measured lake height.

DYRESM CAEDYM models chl *a* as a proxy for total phytoplankton biomass and also divides up the chl *a* into three groups with parameters adjusted so as to represent cyanobacteria, green algae and diatoms. Simulations with the one-dimensional model indicated that the dominant phytoplankton in Lakes Wairarapa and Onoke green algae dominated over diatoms and cyanobacteria (Fig. 19 and 21). Model simulations showed that chlorophyll *a* derived from cyanobacteria often peaked during late summer months but at moderate levels (concentrations mostly less than 20 µg L$^{-1}$). Simulated cyanobacteria chl *a* was highest during periods of settled weather which were usually associated with lower suspended sediment concentrations. Recent GWRC field data indicates that diatoms, green algae and cyanobacteria are all important constituents of the phytoplankton community at certain times, but that diatoms and green algae are dominant. There was a recorded cyanobacteria bloom on 9/5/2008 in Lake Wairarapa, however since then no blooms have been recorded (Alton Perrie, 2005). Simulations showed that green algae dominate the phytoplankton assemblage.

Total suspended sediment concentrations were not only highly spatially variable (as seen from total suspended sediment estimated from Landsat, Fig. 18), but highly temporally variable, mainly driven by resuspension from the lakebed associated with wind generated waves and currents (Fig.19). Suspended sediment concentrations were a primary driver of lake trophic status. Periods of high suspended sediment concentration were associated with lower chl *a* and higher TP. Total phosphorus was likely higher when suspended sediments were high due to bound phosphorus on suspended minerals, combined with resuspension of particulate organic matter. Simulations of phytoplankton growth limitation within Lake Wairarapa indicated that diatoms and green algae were variously limited by light, nitrogen and phosphorus (Fig. 20). Nitrogen limitation followed a regular cycle of higher limitation during summer months, associated with more algal growth during warmer months and increased algal uptake/demand of nutrients.

31
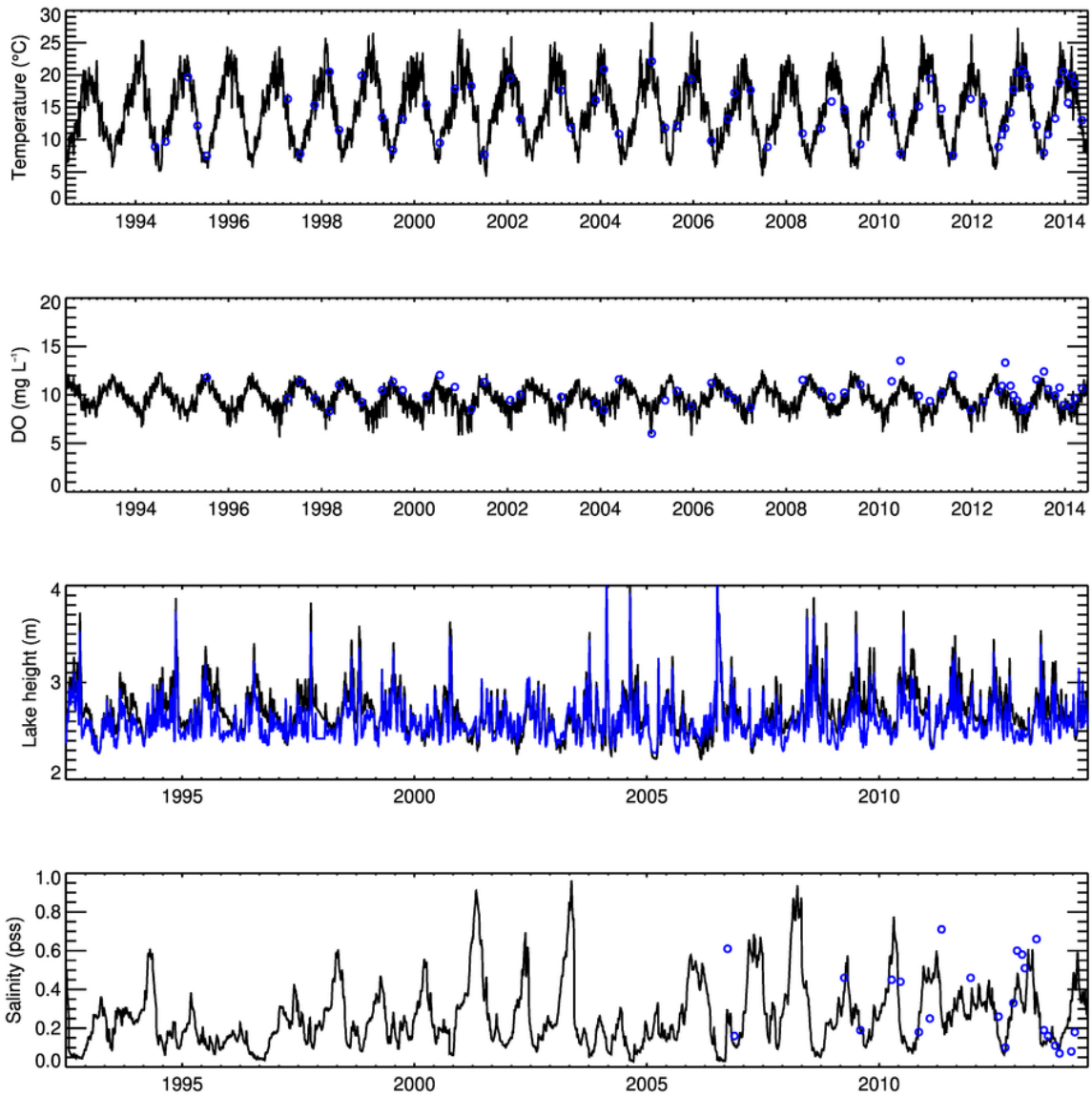
**Figure 19. Lake Wairarapa simulated (black line) versus observed (blue open circle) surface temperature (Temperature) and dissolved oxygen (DO), lake height and salinity.**
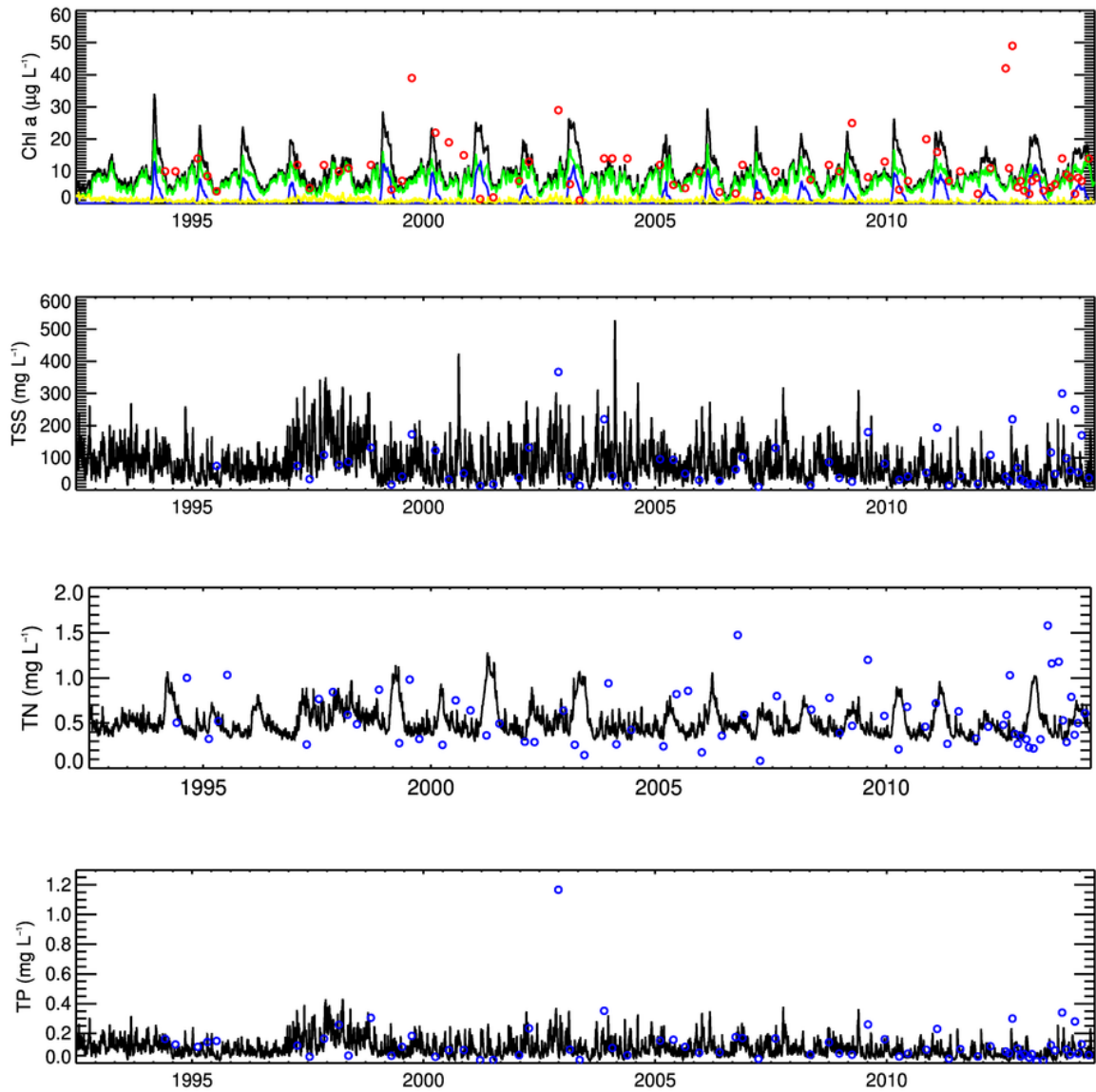
**Figure 20. Surface water quality variables for Lake Wairarapa. Black line is the simulated values, and blue open circle is observed values. Within the total chlorophyll a (Chl a) plot, green algae are represented with a green line, diatoms with a yellow line, and blue-green algae (cyanobacteria) with a blue line. Total suspended solids (TSS), total phosphorus (TP) and total nitrogen (TN) are also shown.**
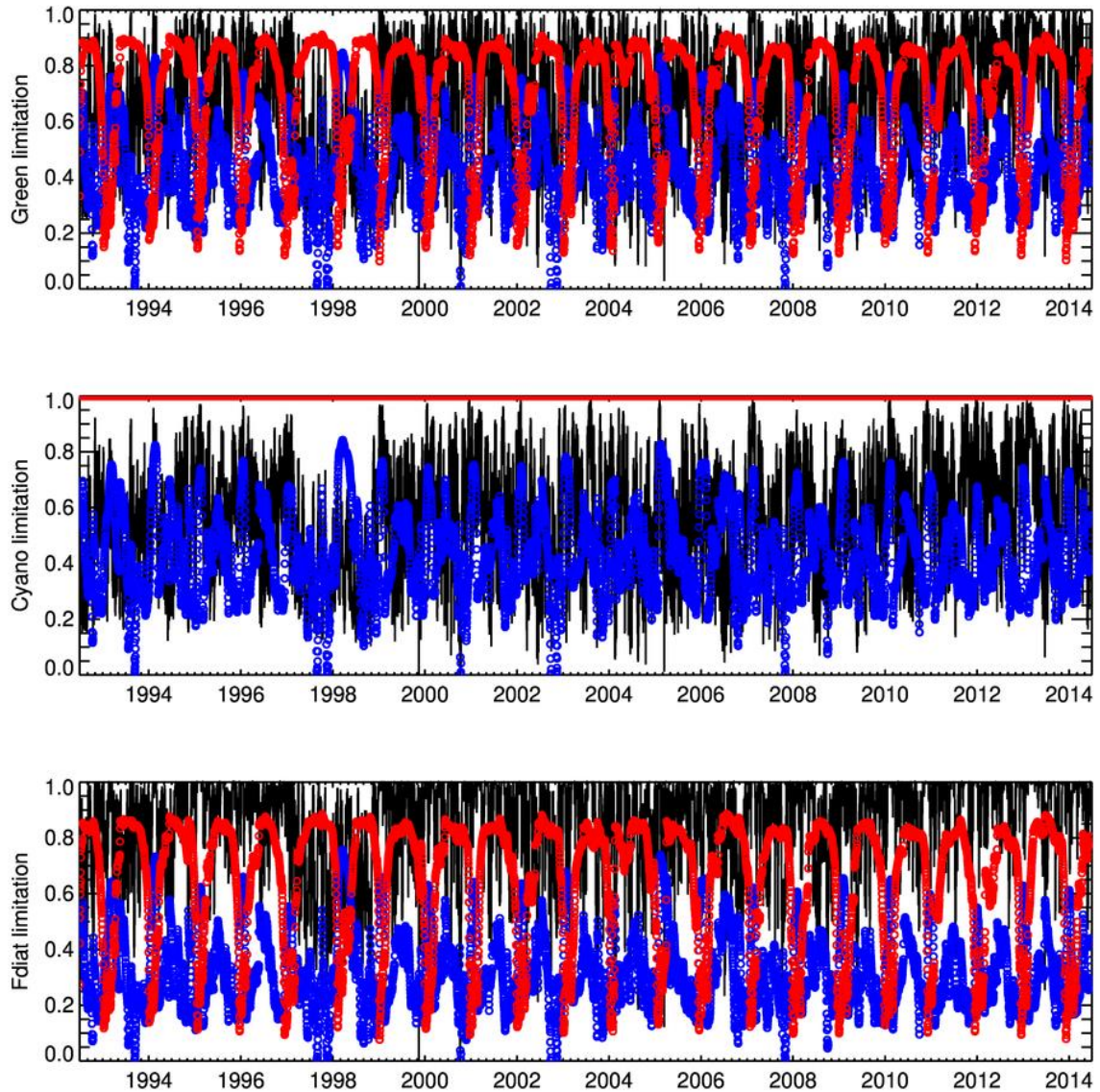
**Figure 21. Simulated nutrient limitation functions for green algae (Green), cyanobacteria (Cyano), and freshwater diatoms (Fdiat). Light limitation is plotted with a black line, phosphorus limitation with blue open circles and nitrogen limitation with red open circles. A value of 1 would represent no limitation and a value of zero would be complete limitation corresponding to no growth. Values of light are highly variable corresponding to variations between days.**

As previously mentioned the lack of persistent thermal stratification produced the water column with well mixed particles of solutes with no significant vertical gradients over the water column depth (Fig. 22). Warmer temperatures and more settled weather meant cyanobacteria were present at high concentrations during summer months (still low concentrations), and low concentrations of soluble nitrogen.
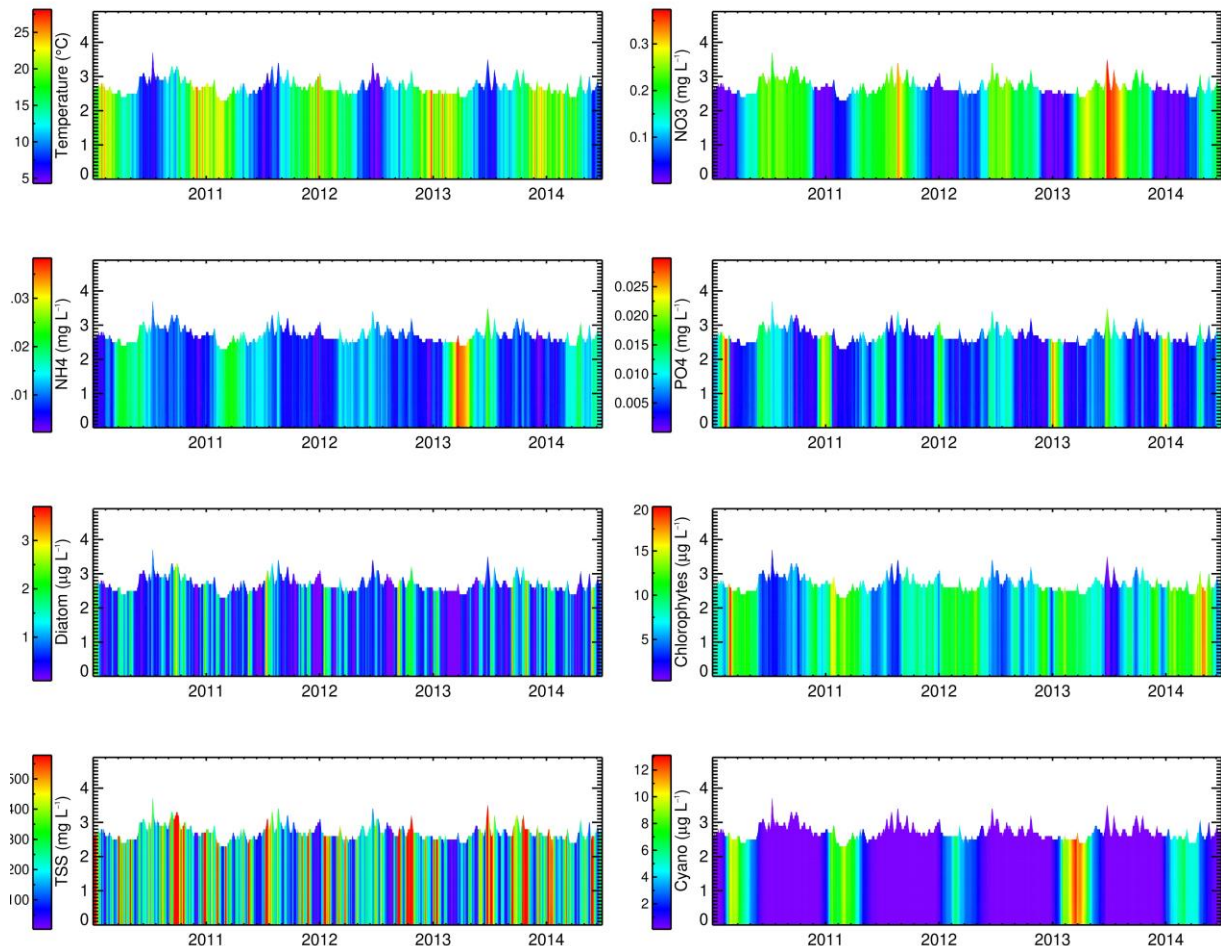


**Figure 22. Contour plot of 1-D simulated water quality variables for Lake Wairarapa. The left axis is elevation from the lake bottom (m). Nitrate is (NO3-N), Ammonia (NH4-N), Phosphate (PO4-P) and total suspended solids (TSS).**

Simulations of nitrate, phosphate and ammonium showed high temporal variability (Fig. 23). Simulated trophic status generally agreed with observed values, however there were some exceptions where low observed TLI was not represented within the model (Fig. 24). Simulated *E. coli* concentrations were highly temporally variable reflecting pulses of high *E. coli* concentration within inflows. These pulse events are also displayed in *in situ* data.
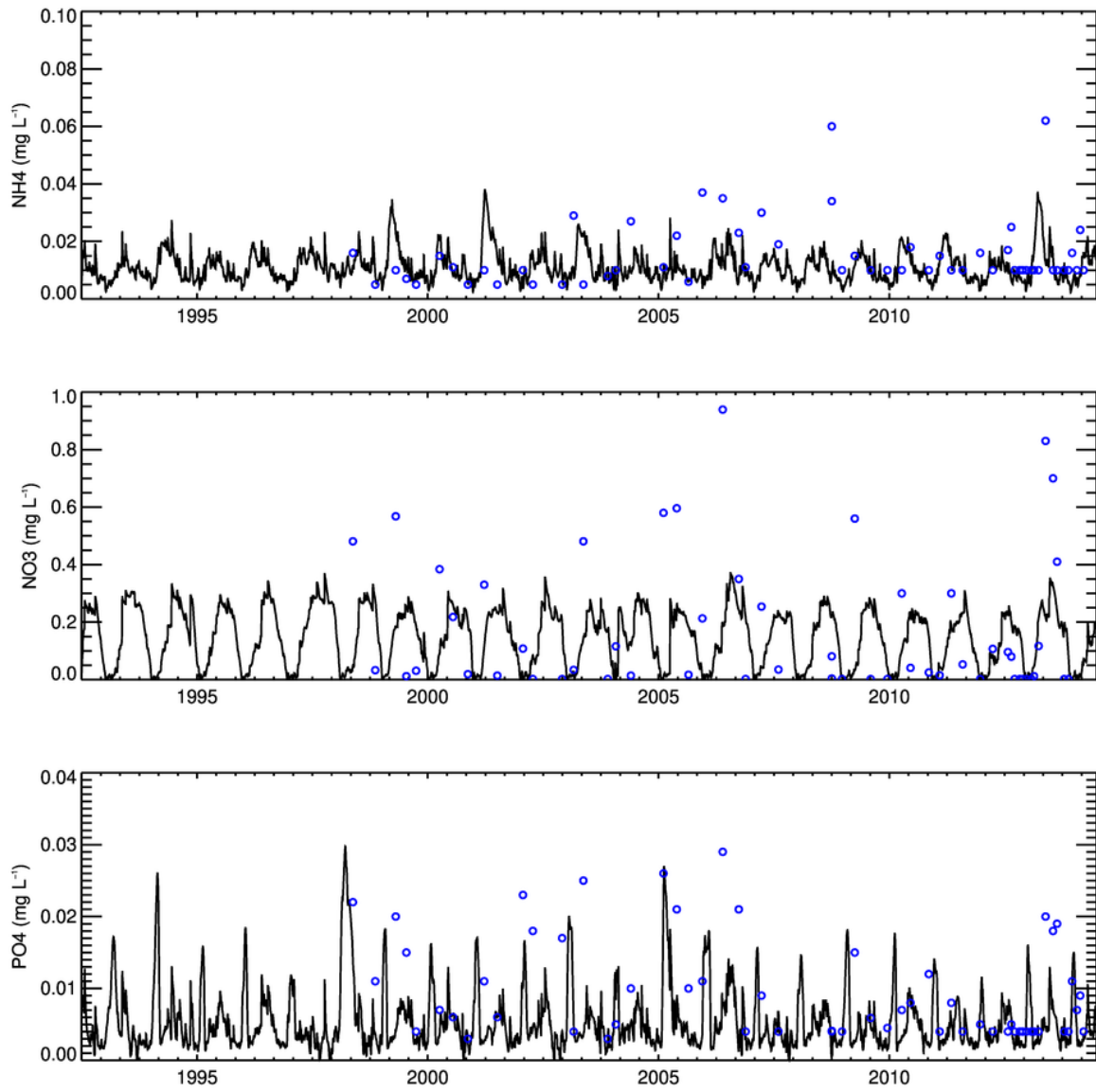
**Figure 23. Simulated 1-D surface water quality variables for Lake Wairarapa. Black line is the simulated values, and blue line is observed values.**
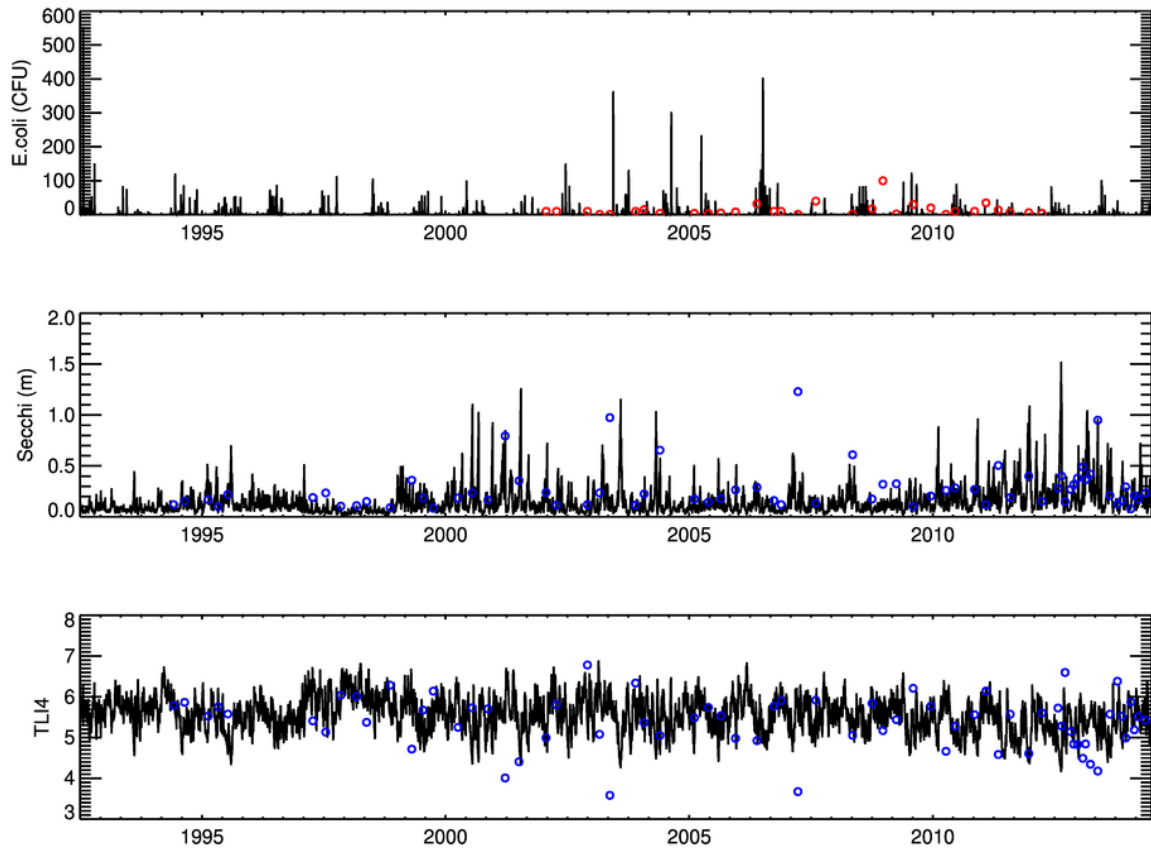
**Figure 24. Simulated 1-D surface water quality variables for Lake Wairarapa. Black line is the simulated values, and blue open circles are observed values.**

## *Calibration of 1-D ecologically coupled hydrodynamic model of Onoke*

The focus of achieving an acceptable calibration for Lake Onoke was on reproducing observed temperature, surface DO, TN, TP, TSS, and chl *a* represented as a total value. The statistical comparison (Table 6) was deemed reasonable by comparison with other modelling applications, with NRMSE ranging from 13% (temperature) to 39% (nitrate).

**Table 6. Model performance for 1-D simulation Lake Onoke baseline, using root mean square error (RMSE) and normalised root mean square error (NRMSE %).**

| Variable | RMSE (units of variable) | NRMSE (% fraction) |
|---|---|---|
| Chl $a$ ($\mu$g L$^{-1}$) | 5.23 | 0.33 |
| TN (mg L$^{-1}$) | 0.40 | 0.29 |
| TP (mg L$^{-1}$) | 0.07 | 0.20 |
| PO$_4$-P (mg L$^{-1}$) | 0.01 | 0.37 |
| NH$_4$-N (mg L$^{-1}$) | 0.01 | 0.31 |
| NO$_3$-N (mg L$^{-1}$) | 0.36 | 0.39 |
| TSS (mg L$^{-1}$) | 89.07 | 0.20 |
| Secchi depth (m) | 0.30 | 0.26 |
| Temperature ($^{O}$C) | 2.18 | 0.13 |
| TLI (TLI units) | 0.59 | 0.27 |
| Salinity (psu) | 2.02 | 0.23 |

### *Key characteristics based on models and observations*

Model simulations indicated no significant stratification with water temperature not varying with depth as noted above for the observations (Fig. 25). This is due to the shallow depth, high flow-through/low residence time and associated wind mixing. The RMSE of temperature simulations from observed values (2.18 $^{o}$C) is somewhat higher than other studies (e.g. RMSE of 0.54 $^{o}$C using DYCD on Lake Rotorua by Allan et al., 2016). As discussed above this could potentially be caused by using VCN daily input meteorological data, which uses the average of daily min and max temperature as input, instead of the mean daily temperature generally used. In addition, the accuracy of input stream and ocean flows may influence errors.
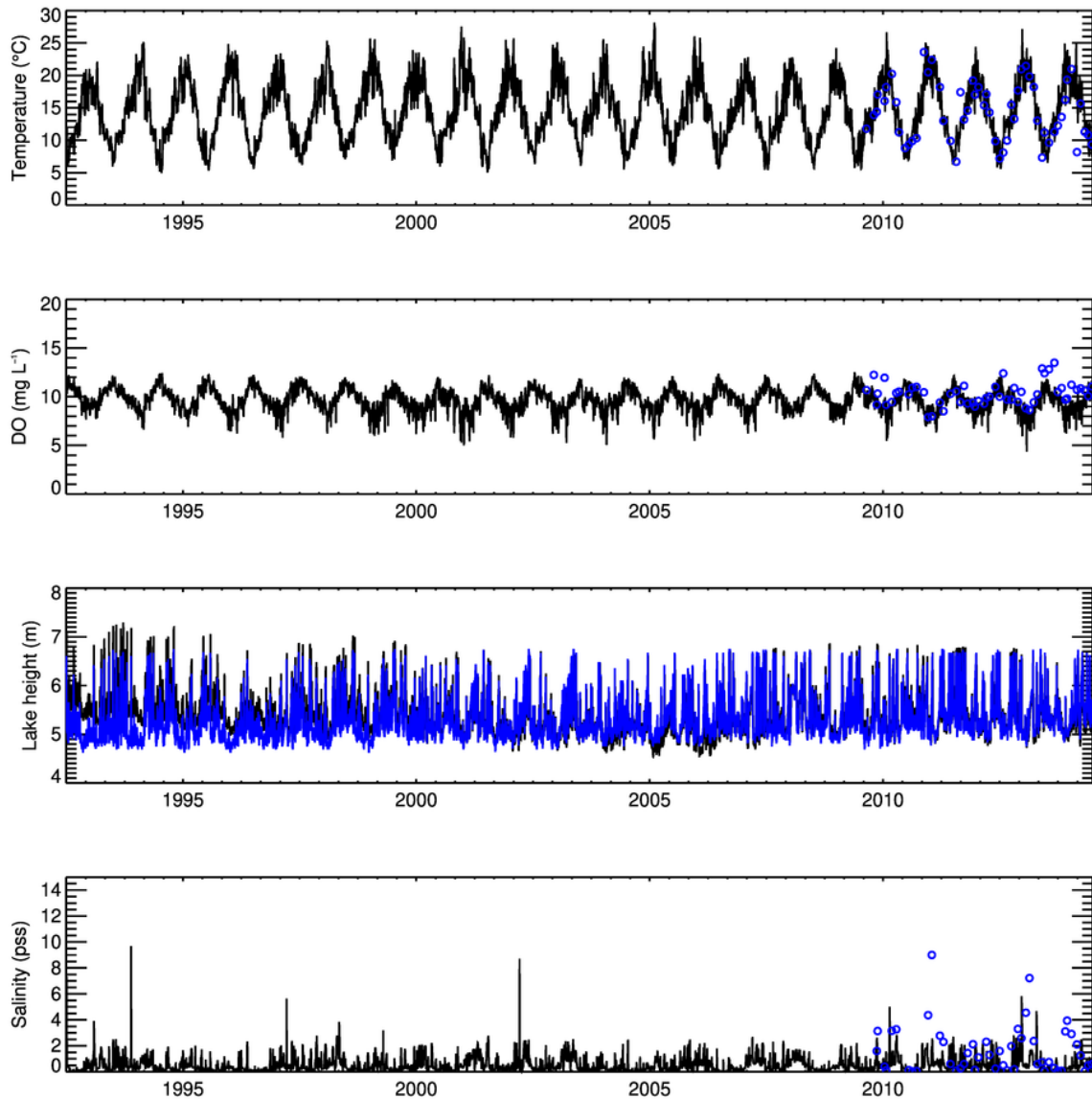
**Figure 25. Simulated 1-D surface water physical variables for Lake Onoke. Black line is the simulated values, and blue open circles are observed values. Surface temperature (Temperature) and dissolved oxygen (DO), lake height and salinity.**

Dissolved oxygen concentrations followed an expected seasonal pattern of higher in winter than summer, aligning with increased saturation capacity of cooler waters. The model simulations generally reproduced the observations of surface DO well but with a tendency for under-prediction in summer, particularly in 2013/2014. Simulated salinity was generally within the range of observations. However, in 2010 and 2013 high salinity events were not simulated within the model. This could be due to a number of factors, but storm related wave overtopping could contribute to high salinity events and are not simulated by the model.

Simulated chl *a* concentrations generally peaked in December and were dominated by green algae (Fig.s 26 and 30). Total suspended sediment concentrations were highly temporally and spatially variable, driven by resuspension from the lakebed associated with wind generated waves and currents, alongside lake circulation caused by currents generated by Ruamāhanga

39

inflows, marine intrusion and outflows (Fig. 26). While inflows derived from Lake Wairarapa comprised 20 % of total inflow, 44 % of TP entered Lake Onoke via this flow, much of it associated with resuspension in Lake Wairarapa. Nutrient has the potential to limit phytoplankton growth in Lake Onoke more than in Lake Wairarapa, as the water is clearer and there is less light limitation (Fig. 27). However, the very short residence time (less than one day) results in water quality in Lake Onoke being dominated inflows, with nutrient concentrations largely reflecting inflow concentrations. Even though nutrient concentrations are generally higher in Lake Onoke than in Lake Wairarapa, chl *a* concentrations are lower in association with the short residence time and increased levels of ocean flushing, which does not allow the build-up of phytoplankton.

Simulations of phytoplankton growth limitation within Lake Wairarapa indicated that diatoms and green algae were variously limited by light, nitrogen and phosphorus (Fig. 27). As in Lake Wairarapa nitrogen limitation followed a regular cycle of higher limitation during summer months, associated with higher algal growth rates.
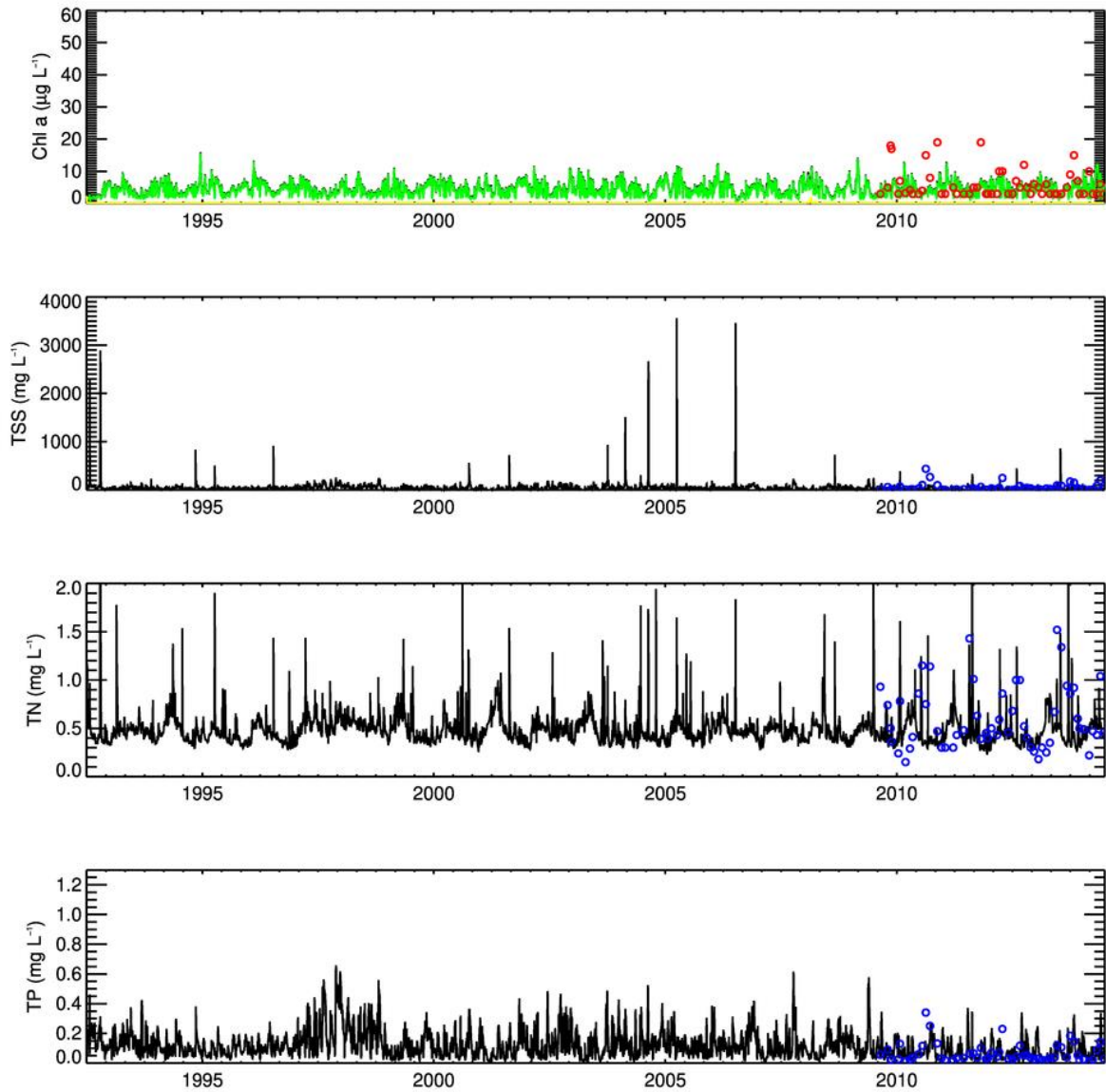
**Figure 26. Simulated 1-D surface water quality for Lake Onoke. Black line is the simulated values, and blue open circle is the observed values. Within the total chlorophyll *a* (Chl *a*) plot, green algae are represented with a green line, diatoms with a yellow line, and blue-green algae (cyanobacteria) with a blue line. Total suspended solids (TSS), total phosphorus (TP) and total nitrogen (TN) are also shown. Simulations showed dominance by green algae. Note that field data are only available from 2009 in Lake Onoke, therefore model data after this time period are presented.**

41
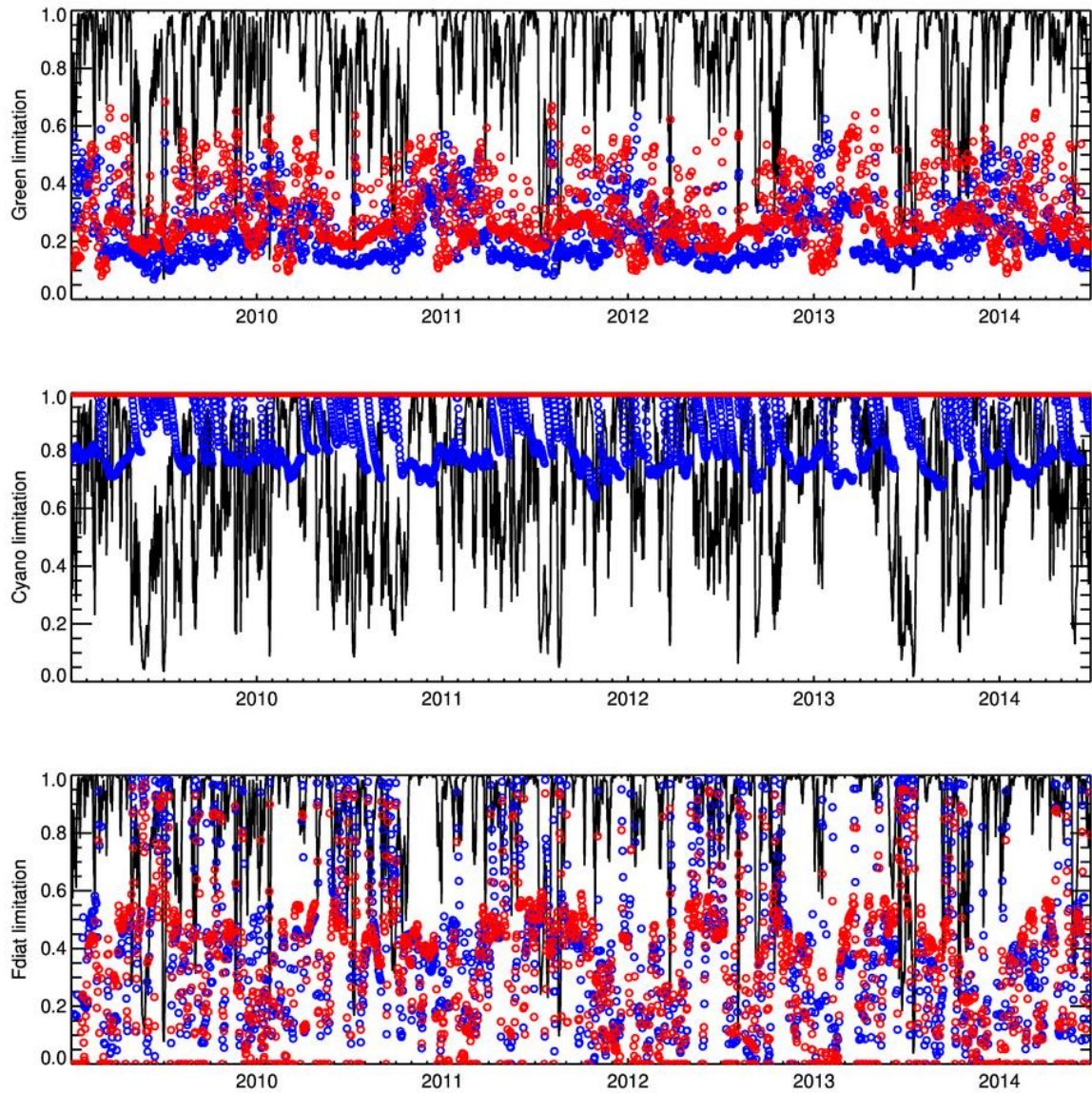
**Figure 27. Simulated nutrient limitation functions for green algae (Green), cyanobacteria (Cyano), and freshwater diatoms (Fdiat). Light limitation is plotted with a black line, phosphorus limitation with blue open circles and nitrogen limitation with red open circles.**
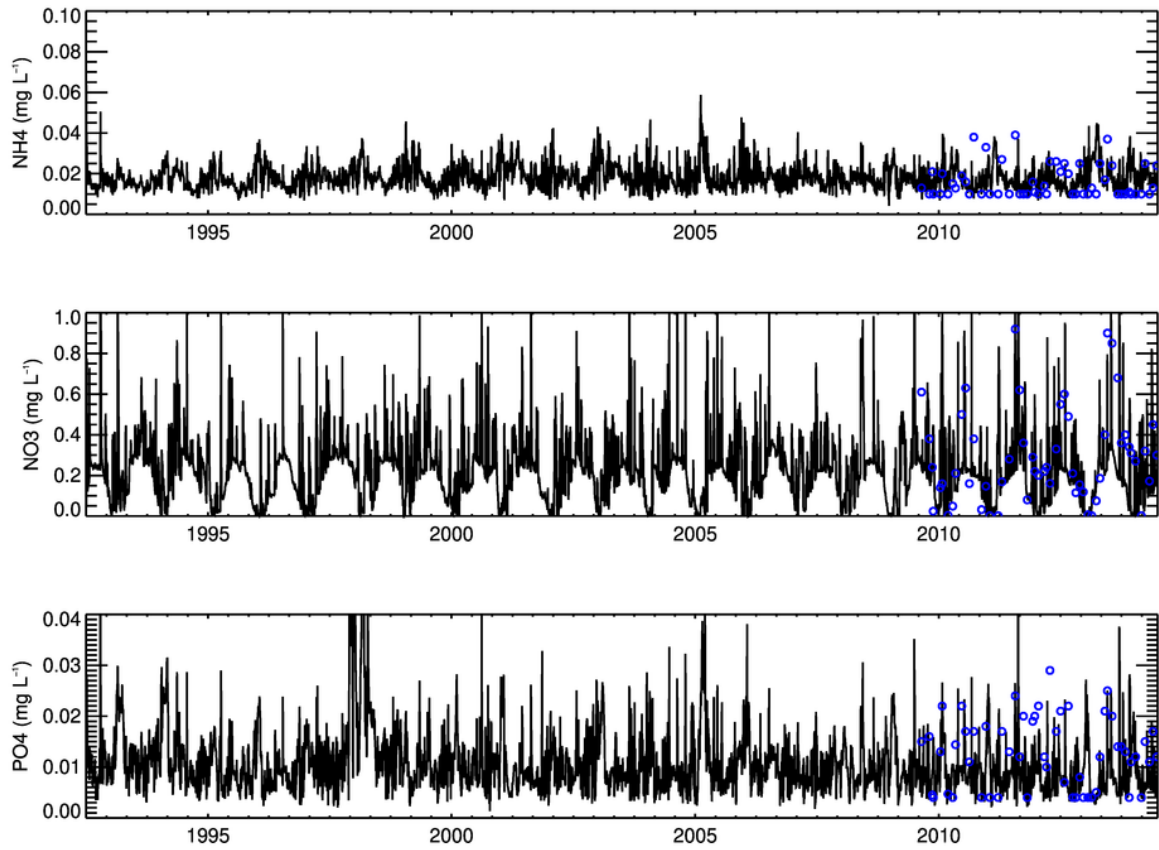
**Figure 28. Surface water quality for Lake Onoke. Black line is the simulated values, and blue open circles are observed values. Note that field data are only available from 2009 in lake Onoke.**
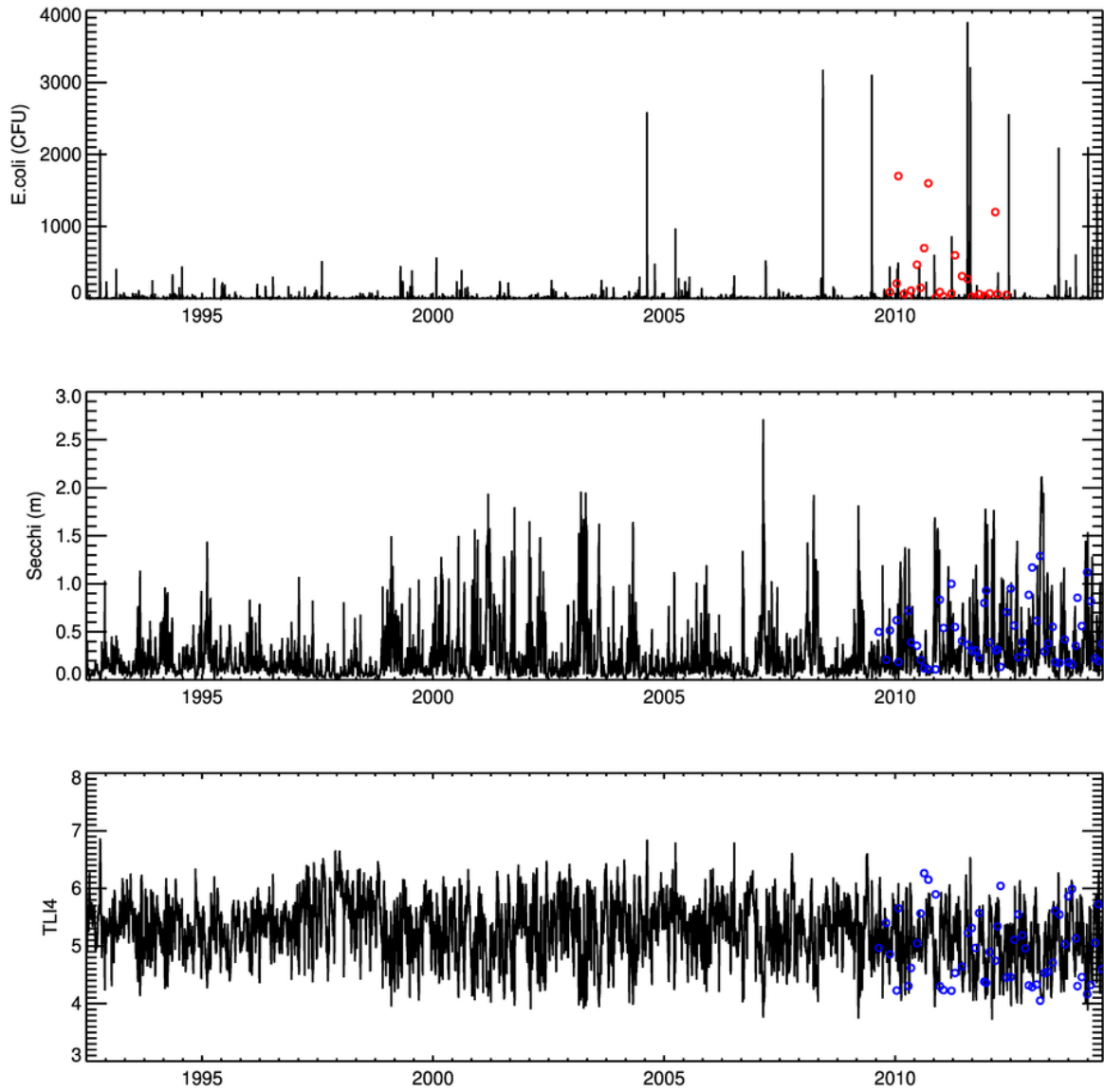
**Figure 29. Surface water quality for Lake Onoke. Black line is the simulated values, and blue open circle are observed values. Note that field data are only available from 2009 in lake Onoke.**

44
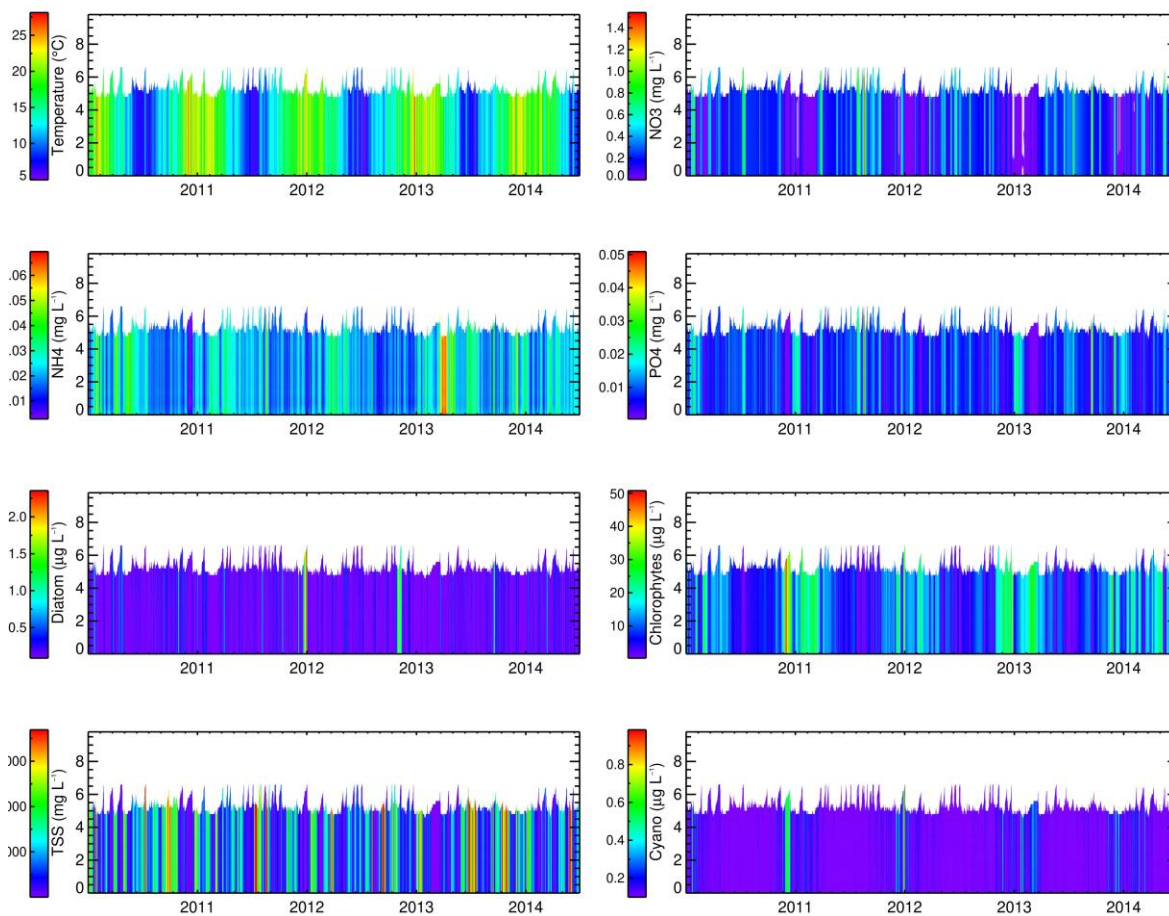
**Figure 30. Contour plot 1-D simulated water quality variables for Lake Onoke The left axis elevation from the lake bottom (m). Nitrate is (NO3-N), Ammonia (NH4-N), Phosphate (PO4-P) and total suspended solids (TSS).**

## Delft sediment transport of Lake Wairarapa

The simulation of cumulative erosion/sedimentation in Lake Wairarapa (Fig. 31) showed that there is large spatial variation in erosion and sedimentation processes. There is higher sedimentation along the western shoreline reflecting a lower energy environment with less influence of waves and currents. Along the eastern shoreline the lower sedimentation reflects a higher energy environment, likely responsible for the larger particle size (sand) found here. A higher energy environment is also simulated near the lake outlet, due to high current velocity.

45
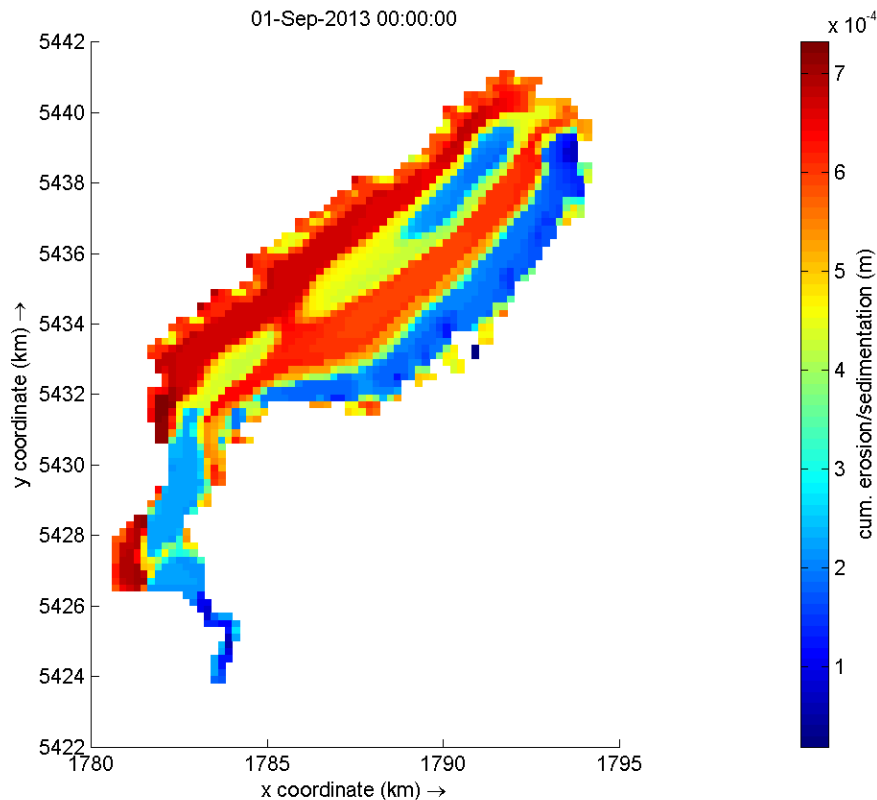
**Figure 31. Delft3D-FLOW simulation of cumulative erosion/sedimentation from 1 September 2011 until 1 September 2013. The model was set up with initial conditions of zero available sediment on the lake bottom.**

## *1-D and 3-D lake scenario results water E.coli*

Three-dimensional (AEM3D) ecologically coupled hydrodynamic models were applied for the scenarios using only 2080 inflows. For lake-specific scenarios including diversions, flow manipulations and lake level changes, 3-D models used SILVER2080 inflows (see Table 4).

Within 1-D modelling simulations relatively small reductions in the external loading (from inflow) of *E. coli* were amplified within Lakes Wairarapa (Fig. 32, Appendix Table 14). The *E. coli* concentrations in the major Lake Wairarapa inflow (Tauherenikau) are generally low, and flows are in the excellent band for NPS swimmability. Catchment mitigation scenarios resulted in comparatively small reductions in *E. coli* inflow loads (e.g. 0.8% for GOLD2080). This was reflected in simulated within-lake concentrations producing 'Excellent' band of the NOF swimmability for Lake Wairarapa scenarios. Note that while there were large simulated percentage reductions in *E. coli* in Lake Wairarapa under SILVER and GOLD scenarios (e.g. -40% under GOLD2080), and the simulated median concentrations within the lake were correspondingly low with median concentrations less than 1 colony forming unit (CFU) for all simulated scenarios including Ruamāhanga diversions. Therefore, the reductions under different catchment management scenarios are negligible in terms of changes in swimmability for Lake Wairarapa.

The Ruamāhanga River was simulated as having 'Good' NPS swimmability (Blyth 2018). However, there were some very high concentrations recorded during major flow events (e.g.

46

maximum *E. coli* concentration of 9,060 CFU). All diversion scenarios of all Ruamāhanga water into Lake Wairarapa meant large percentage increases in lake concentrations of *E. coli* (321 % increase). However, due to the rapid dilution and decay of *E. coli* this did not change the Excellent swimmability at any monitored site in both the 1-D and 3-D simulations. However, there may be localized areas within lakes with a lower swimmability (e.g. Fig. 35), as is the case for simulated swimmabilty from 3-D simulations in Lake Onoke (Table 7). Also, within the vicinity of the historical Ruamāhanga inflow location, Ruamāhanga diversion scenarios increased *E. coli* concentrations, especially "downstream" in the prevailing flow path to the south (Fig. 34).

One dimensional simulations of *E. coli* in Lake Onoke all indicated an Excellent category of swimmability, but this was not the case for site specific swimmability simulated with 3-D models. A lower swimmability category was evident in 3-D simulations of *E. coli* (Table 7). Under baseline and SILVER2080 scenarios, swimmability was simulated as 'Good' at Onoke Site 1/Middle, and 'Fair' at the Deep Site, in contrast to 'Excellent' simulated under all 1-D simulations.
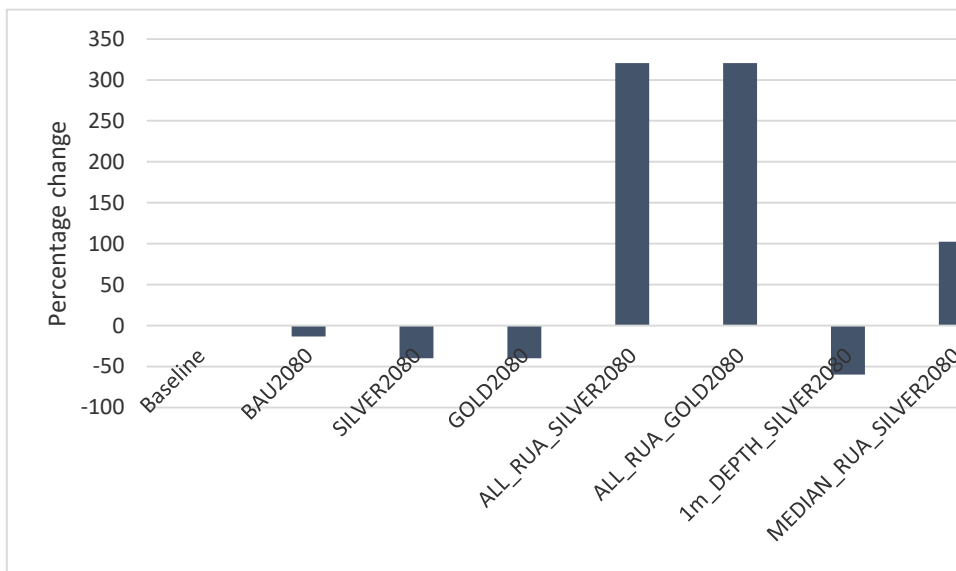


**Figure 32. The 1-D simulated percentage change in *E.coli* concentrations (y axis) in Lake Wairarapa comparing Baseline to 2080 scenarios (x axis).**
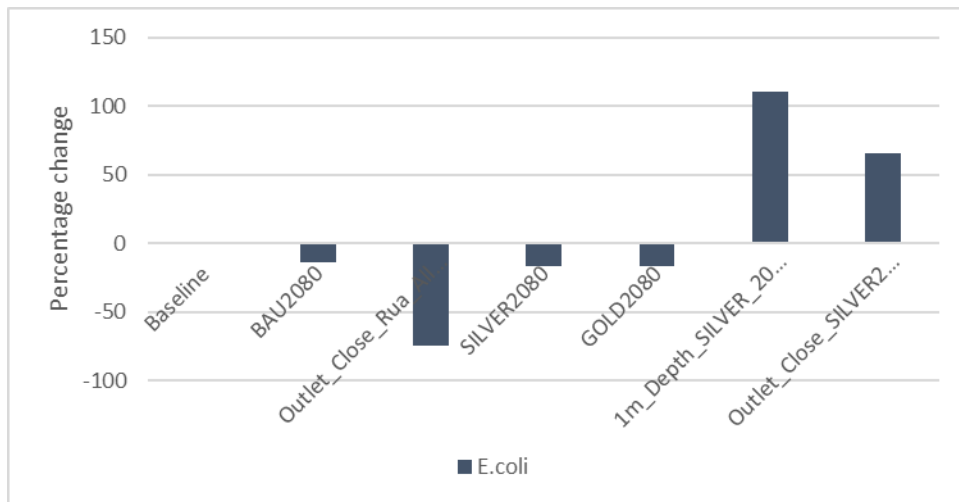
**Figure 33. The 1-D simulated percentage change in *E. coli* concentrations in Lake Onoke comparing Baseline to 2080 scenarios.**

Reductions in the external loading of *E.coli* to Onoke (19 % reduction for Silver and GOLD 2080) did not change swimmability in 1-D or 3-D scenarios. It is important to note that while lake level and flow manipulation scenarios in Lake Onoke sometimes increased *E.coli* concentrations in both 1-D and 3-D cases, changes in median lake averaged concentration (represented by 1-D simulations) were small and less than 1 CFU. These changes result primarily from changes in hydrodynamics and residence times and less flushing under the outlet closed scenario and the 1 m increase scenario. Under 3-D simulations these changes resulted in changes to swimmability criteria (Table 7). For example, under the SILVER2080 a 1 m depth increase scenario, swimmmability changed from 'Good' to 'Intermittent' for Onoke Middle and from 'Fair' to 'Good' for Site 1. This is influenced by changes in hydrodynamics, and the resulting dispersion/flush rate of *E.coli* which affects the water residence time and *E. coli* settling rate.
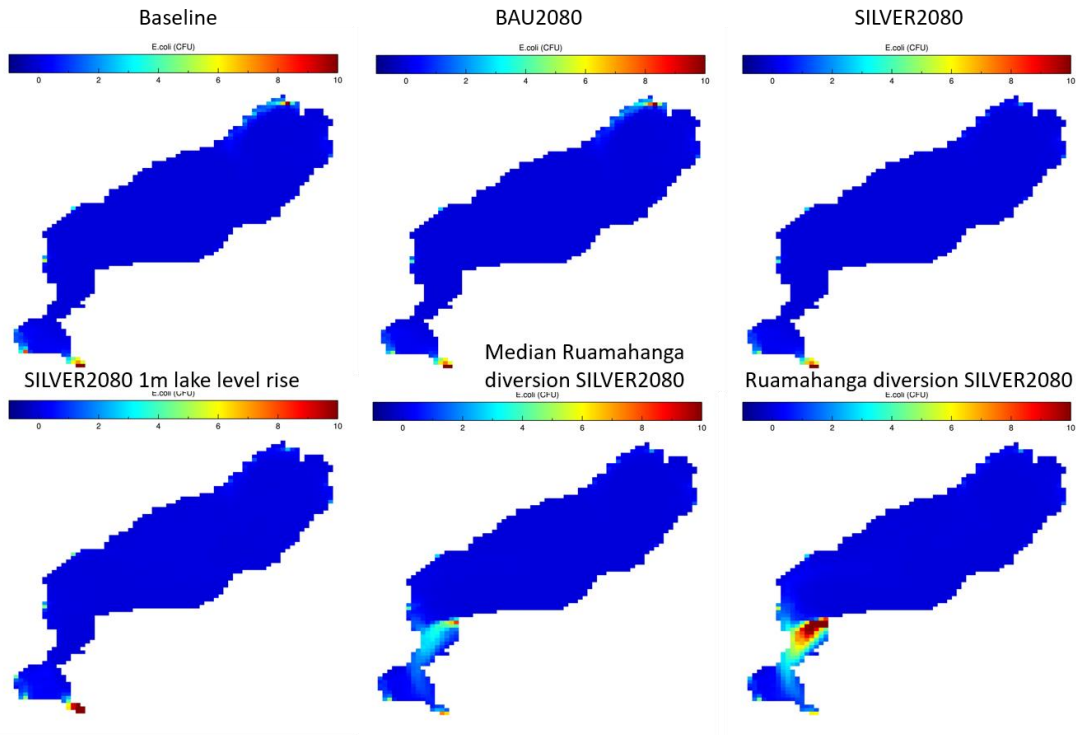
**Figure 34. Median 3-D simulated _E. coli_ concentration in Lake Wairarapa over a 91 day period beginning 1 Jan 2012 at 12 pm. The scale is from 0 to 10 CFU.**
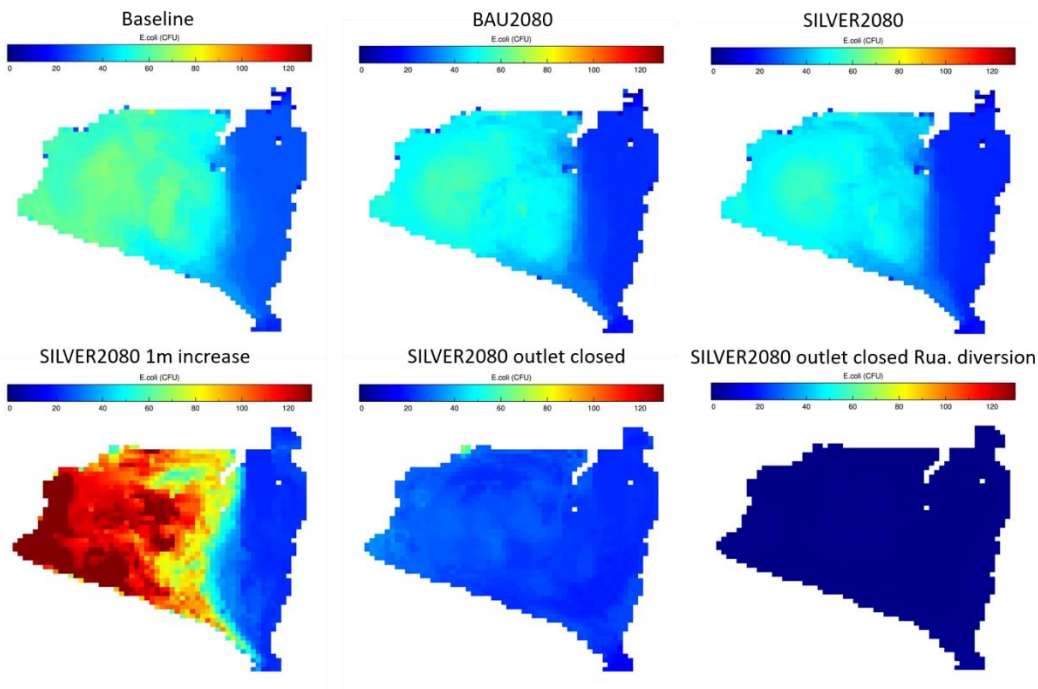


**Figure 35. Median 3-D simulated _E.coli_ concentration in Lake Onoke over a 91 day period beginning 1 Jan 2012 at 12pm. The scale runs from 0 to 130 CFU, with median 130 CFU being the swimmability boundary between excellent and intermittent.**

49

**Table 7. Site-specific results of 3-D ecologically coupled hydrodynamic modelling of E.coli swimmability (NPS) for scenarios (see Appendix Table 15).**

| Site | Baseline | BAU2080 | SILVER2080 | GOLD2080 | 1m depth increase_SILVER2080 | Outlet_close _SILVER2080 | Outlet_close _RUA_SILVER2080 | ALL_RUA_SILVER2080 | MEDIAN_RUA_SILVER2080 |
|---|---|---|---|---|---|---|---|---|---|
| Onoke S1 | B | B | B | B | B | B | A | | |
| Onoke Middle | B | B | B | B | D | B | A | | |
| Onoke Deep | C | C | C | C | B | B | A | | |
| Wai S2 | A | A | A | A | A | | | A | A |
| Wai Middle | A | A | A | A | A | | | A | A |
| Wai Alsops | A | A | A | A | A | | | A | A |
| Wai Outlet | A | A | A | A | A | | | A | A |

## Catchment load of TN and TP under BAU, GOLD and SIVER

Under the catchment land-use mitigation scenarios for GOLD and SILVER 2080, external load (from the catchment) for total nitrogen (TN) was reduced by c. 10% for Lake Onoke and c. 5% for Lake Wairarapa. External loads of total phosphorus (TP) were reduced by c. 42% for Lakes Wairarapa and Onoke (Fig.s 37 & 38).



**Figure 36. Reductions in catchment total nitrogen and total phosphorus load for Lake Wairarapa.**



**Figure 37. Percent reductions in catchment total nitrogen and total phosphorus load for Lake Onoke.**

## 1-D scenario results

Twenty-two scenarios were run for Lake Wairarapa (Appendix table 16) resulting in water quality variable changes from baseline of between 60.4% reduction (chl *a* under the MEDIAN_RUA_SILVER_2080 scenario) and 330% increase (*E. coli* under the ALL_RUA_SILVER2025 scenario).

The lake catchment scenarios GOLD and SILVER resulted in improved water quality. However, for SILVER and GOLD scenarios, increases in nitrate concentrations ranged from 0.6% (SILVER2025) to 17.2% (SILVER2080), primarily driven by lower phytoplankton nitrate uptake associated with greater phosphorus limitation (Table 8). However, under these two scenarios TN was still reduced by 13%. Simulated changes in median concentrations are presented in Table 8 and 9, with associated NOF bands presented in Table 10 and 11.

### 1-D Catchment scenario lakes results

The BAU scenarios only marginally improved water quality. For example, BAU2080 resulted in a 1.8% reduction in TP concentrations and a 2.0 % reduction in TN concentrations within Lake Wairarapa (Fig. 39). However, the SILVER and GOLD scenarios both had a significant influence on water quality, and as expected the largest improvement in water quality occurred for the 2080 scenarios. The GOLD2080 and SILVER2080 scenarios simulated very similar reductions in nutrient concentrations in both Onoke and Wairarapa and increases in water clarity (Fig.s 39 and 40). For example, in Wairarapa, for SILVER2080 there was a simulated 13.3 % reduction in total phosphorus whereas in GOLD2080 there was a 13.5% reduction. Generally, the largest changes in water quality parameters were seen in chl *a* concentrations, for example GOLD2080 resulted in a 41.0% reduction in chl *a* concentrations.

### 3-D and 1-D and lake scenario results water quality

The diversion of the Ruamāhanga River into Lake Wairarapa, combined with changes in catchment scenarios discussed above, brought about the greatest changes in water quality, both positive and negative. While this scenario generally improved water quality in Lake Wairarapa, scenarios where the entire flow was diverted increased *E. coli* concentrations by 321%, due to high concentrations in the Ruamāhanga River. In addition, residence time reduced to 9.1 days compared to 38.1 days under baseline.

The diversion of Ruamāhanga River flows below median (SILVER2080 flows) resulted in the greatest simulated improvement in water quality in Lake Wairarapa of all 1-D scenarios. This is due to increased flushing, and lower inflow nutrient and total suspended solid concentrations (even though total loads increased), leading to shorter residence times (23.5 days compared to 38.1 days under baseline), reducing the impact of high internal loading and sediment resuspension. However, 3-D models showed an increase chl *a* concentration (due to less light limitation) under the Ruamāhanga diversion scenarios. For any simulation that changes the hydrodynamics including an increase in lake depth, diversion, or the closure of lake mouth, the 3-D simulation results must be considered as a more robust representation of the system (see conclusions).

Note that while large percentage increases in Secchi depth (m), representing better water clarity, median Secchi depth only increased to 0.15 m in Lake Wairarapa (1 m depth increase SILVER) and 0.2 m in Onoke (1 m depth increase SILVER). This still represents very low water clarity and turbid conditions.

52

**Table 8. Lake Wairarapa 1-D simulated median values for 2080. B is Baseline, S is Silver, G is Gold, 1m_Inc is a 1 m increase in lake depth.**

| | B | BAU | S | G | ALL_RUA_G | ALL_RUA_S | MEDIAN_RUA_S | 1m_DEPTH_S |
|---|---|---|---|---|---|---|---|---|
| TLI4 | 5.57 | 5.54 | 5.30 | 5.30 | 5.23 | 5.24 | 5.12 | 5.22 |
| PO4 (mg/L) | 0.00 | 0.00 | 0.00 | 0.00 | 0.00 | 0.00 | 0.00 | 0.00 |
| NO3 (mg/L) | 0.16 | 0.16 | 0.20 | 0.20 | 0.37 | 0.37 | 0.28 | 0.18 |
| NH4 (mg/L) | 0.01 | 0.01 | 0.01 | 0.01 | 0.01 | 0.01 | 0.01 | 0.01 |
| TP (mg/L) | 0.09 | 0.08 | 0.08 | 0.08 | 0.06 | 0.06 | 0.06 | 0.06 |
| TN (mg/L) | 0.48 | 0.47 | 0.41 | 0.41 | 0.52 | 0.52 | 0.42 | 0.44 |
| Chl *a* (µg/L) | 8.55 | 8.22 | 5.07 | 5.05 | 4.13 | 4.20 | 3.39 | 5.89 |
| Cyano (µg/L) | 0.12 | 0.11 | 0.10 | 0.10 | 0.10 | 0.10 | 0.10 | 0.10 |
| DO (mg/L) | 9.64 | 9.64 | 9.61 | 9.61 | 9.62 | 9.63 | 9.63 | 9.69 |
| Secchi (m) | 0.11 | 0.11 | 0.11 | 0.11 | 0.12 | 0.12 | 0.12 | 0.15 |
| TSS (mg/L) | 65.37 | 63.81 | 63.16 | 63.16 | 60.39 | 60.41 | 57.58 | 46.40 |
| Salinity (psu) | 0.22 | 0.22 | 0.22 | 0.22 | 0.07 | 0.07 | 0.12 | 0.24 |
| *E.coli* (CFU/100 ml) | 0.07 | 0.06 | 0.04 | 0.04 | 0.29 | 0.29 | 0.14 | 0.03 |
| Temperature (ºC) | 14.45 | 14.45 | 14.44 | 14.44 | 14.47 | 14.47 | 14.44 | 14.52 |

**Table 9. Lake Onoke 1-D simulated median values for 2080. B is Baseline, S is Silver, G is Gold, 1m_Inc is a 1 m increase in lake depth.**

| | B | BAU | S | G | Outlet_Close_S | Outlet_Close_Rua_All_s | 1m_inc_S |
|---|---|---|---|---|---|---|---|
| TLI4 | 5.42 | 5.21 | 4.99 | 4.99 | 4.82 | 5.03 | 4.95 |
| PO4 (mg/L) | 0.008 | 0.004 | 0.003 | 0.003 | 0.002 | 0.003 | 0.003 |
| NO3 (mg/L) | 0.22 | 0.21 | 0.23 | 0.23 | 0.23 | 0.34 | 0.21 |
| NH4 (mg/L) | 0.02 | 0.02 | 0.02 | 0.02 | 0.01 | 0.01 | 0.01 |
| TP (mg/L) | 0.10 | 0.06 | 0.05 | 0.05 | 0.04 | 0.05 | 0.04 |
| TN (mg/L) | 0.46 | 0.44 | 0.39 | 0.39 | 0.37 | 0.46 | 0.38 |
| Chl $a$ (µg/L) | 6.36 | 5.75 | 3.28 | 3.27 | 3.34 | 3.72 | 4.63 |
| Cyano (µg/L) | 0.10 | 0.10 | 0.10 | 0.10 | 0.10 | 0.10 | 0.10 |
| DO (mg/L) | 9.73 | 9.71 | 9.71 | 9.71 | 9.73 | 9.60 | 9.72 |
| Secchi (m) | 0.14 | 0.15 | 0.15 | 0.15 | 0.21 | 0.14 | 0.20 |
| TSS (mg/L) | 32.1 | 31.3 | 30.4 | 30.4 | 22.0 | 33.2 | 23.0 |
| Salinity (psu) | 0.32 | 0.32 | 0.32 | 0.32 | 0.34 | 0.07 | 0.38 |
| *E.coli* (CFU/100 ml) | 0.41 | 0.35 | 0.34 | 0.34 | 0.68 | 0.10 | 0.86 |
| Temperature (ºC) | 14.2 | 14.2 | 14.2 | 14.2 | 14.3 | 14.7 | 14.3 |
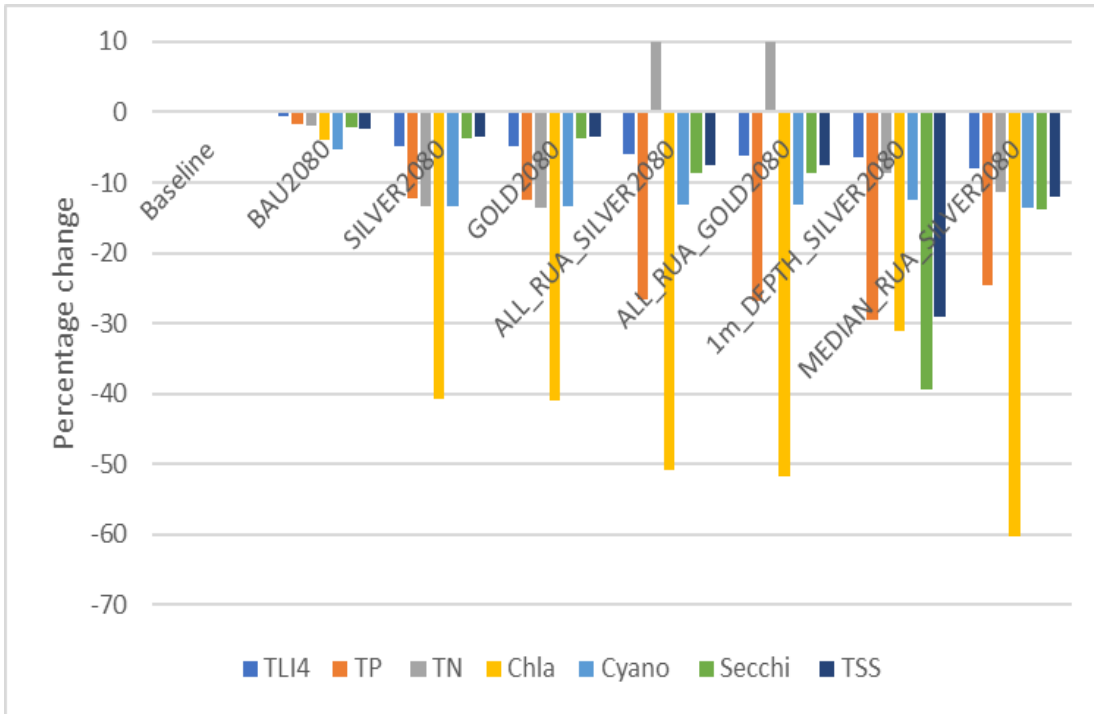
**Figure 38. Lake Wairarapa 1-D simulation summary percentage change for 2080 (positive is increase, negative is decrease). Note for Secchi depth (measure of lake clarity), negative values represent an increase in Secchi depth corresponding to water with higher clarity.**
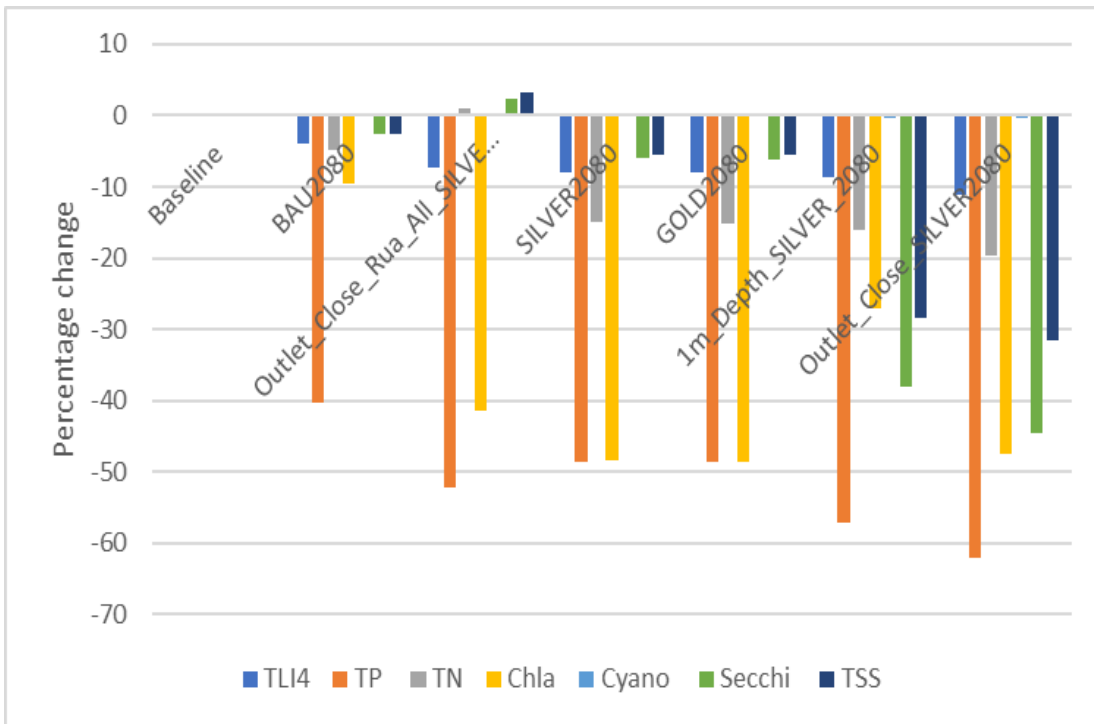


**Figure 39. Lake Onoke 1-D simulation summary percentage change for 2080 (positive is increase, negative is decrease). Note for Secchi depth (measure of lake clarity), negative values represent an increase in Secchi depth corresponding to water with higher clarity.**

55

### *Total phosphorus 1-D simulation results*

The reductions in catchment TP loads were reflected to differing extents within lakes Onoke and Wairarapa. The 42% reduction in external TP load resulted in a 12 and 49% reduction for GOLD and SILVER 2080 within Wairarapa and Onoke, respectively. The lower reduction in TP concentrations within Lake Wairarapa is likely related to the higher internal loading from the lake sediments, due to diffusion of phosphate and resuspension of suspended particles with bound phosphorus.

### *Total nitrogen 1-D simulation results*

The reductions in catchment TN loads were reflected to similar extents within lakes Onoke and Wairarapa. Catchment derived TN was reduced by 5% for Lake Wairarapa and 10% for Lake Onoke, which resulted in a 13% and 15% reduction for GOLD and SILVER 2080 within Wairarapa and Onoke, respectively. Nitrogen internal loading from lake sediments is generally much less (as a proportion of total load from catchment and sediments) due to the fact that nitrogen does not bind strongly to sediments.

### *Phytoplankton – 1-D and 3-D simulation results*

Lake Wairarapa Chlorophyll *a*

For catchment nutrient mitigation scenarios, 1-D simulations all produced simulations of reductions in phytoplankton concentration, caused mainly by a reduction in available nutrients, particularly when there was more phosphorus limitation. Reductions under catchment scenarios were greatest under SILVER and GOLD 2080 with a 40% reduction in chl *a*. The greatest reduction in phytoplankton was simulated under the Ruamāhanga below median flow diversion scenario (60% reduction). However, 3-D simulations showed a slight increase in chl *a* concentration under the same scenario, likely owing to less light limitation (Fig. 41).

The scenarios with a 1 m depth increase resulted in reduced median phytoplankton concentrations in 1-D simulations (compared to Baseline). However, 3-D modelling showed significant increases in median phytoplankton concentrations. Again, less light limitation due to less suspended sediment is likely to be the driving factor. The 1 m depth increase scenarios (SILVER2080 flows) showed an increase in median chl *a* concentration compared with the SILVER2080 scenario. Therefore, under the same flow and nutrient conditions the 1 m depth increase within the 1-D model gave simulated increases in chl *a* concentrations. Therefore, when the effect of inflow is controlled for, both the 1-D and 3-D models simulated an increase in chl *a* concentrations. However, this is not the case for the Ruamāhanga diversion scenarios, where the 1-D modelling produced decreased chl *a* concentrations and the 3-D model produced increased concentrations compared to SILVER2080 and baseline.

56

All 3-D scenarios indicate higher chl *a* concentration in the south of the lake, particularly western areas of Alsop's Bay. This is potentially due to less suspended sediment resuspension in this area, and more light available for phytoplankton growth.
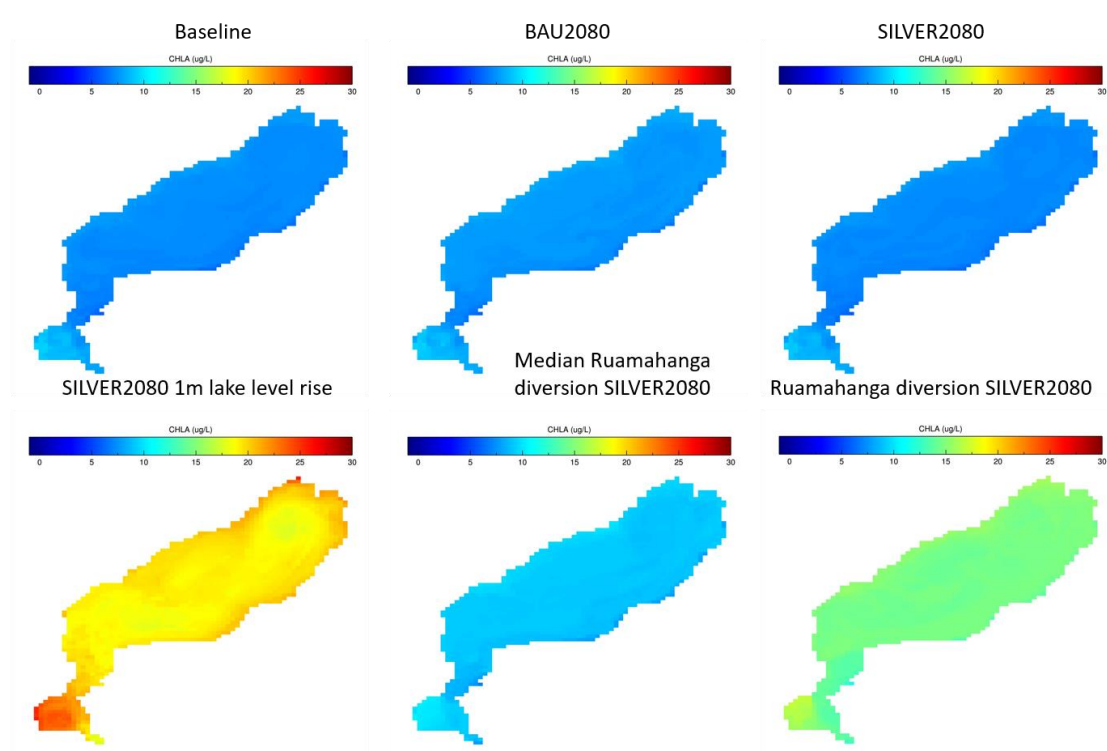


**Figure 40. Simulated total chlorophyll *a* concentrations in Lake Wairarapa using three-dimensional models (AEM3D). BAU is business as usual.**

## Lake Onoke chlorophyll *a*

For the 1-D model, reductions under different catchment scenarios were greatest for SILVER and GOLD 2080, with a 49% reduction in phytoplankton concentration. A 1 m increase in lake level (1m_Inc_SILVER2025) resulted in a 27% decrease in chl *a* concentrations. Under a 1m increase scenario, it is important to note that the deeper depth reduces the impact of waves and currents on suspended sediment resuspension. This lower reduction (as compared to 49% reduction under SILVER2080) is likely due to enhanced algal growth related to light availability associated with less sediment resuspension. Under a 1 m lake level increase, 3-D models also indicated the possibility of higher algal growth in western Lake Onoke. Aligned with 1-D modelling, 3-D modelling also showed a reduction in chl *a* concentrations at all sites under the outlet closed scenario (Fig. 42). Within Lake Onoke the outlet closed scenario produced simulations with higher TSS concentrations, which likely limited algal growth due to increased light limitation. However, when the scenario is combined with the Ruamāhanga diversion through Lake Wairarapa there was a simulated increase in the chl *a* concentration near Ruamāhanga inlet, likely due to high chl *a* concentrations in Lake Wairarapa being entrained into Lake Onoke.

57
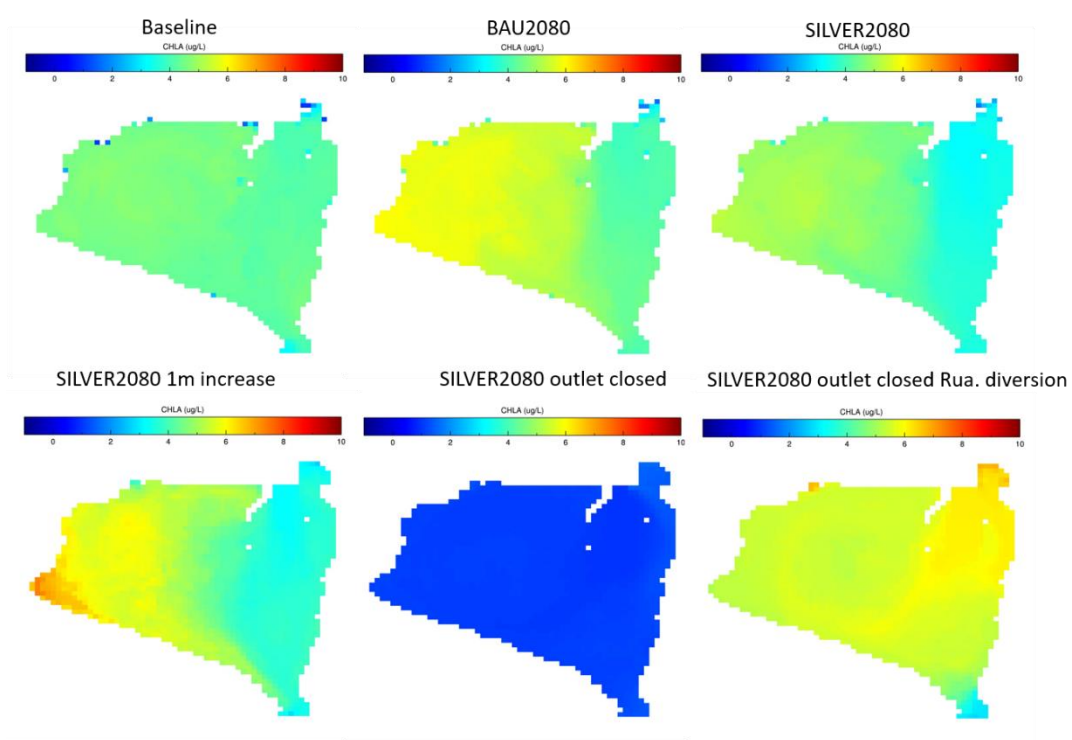
**Figure 41. Simulated total chlorophyll *a* concentrations in Lake Onoke using three-dimensional modeling (AEM3D). BAU is business as usual.**

### *Total suspended sediments 1-D and 3-D simulation results*

While the external load of sediments reaching Lake Wairarapa was reduced by 29% under SILVER and GOLD, this only resulted in a 3% reduction in median total suspended solids (TSS) within the lake. This is due to the dominant influence of sediment resuspension from currents and waves. A 43% reduction in TSS entering Lake Onoke under GOLD and SILVER 2080 resulted in a 5% reduction in median TSS concentrations within the lake. Again, this is due to the dominant influence of sediment resuspension, combined with continuing TSS entering from Lake Wairarapa. In addition, most suspended sediment entering lakes is quickly deposited, especially silt and sand fractions.

Three-dimensional simulation outputs of TSS concentrations in Lake Wairarapa all show spatial variations across the lake, with high concentrations associated with eastern areas of the lake and lower concentrations in Alsop's Bay (Fig 43). The most obvious changes in TSS concentration were from the 1 m lake level increase. This is due to the greater depth leading to less turbulence acting on the lake bottom from wind and waves, and less sediment resuspension. When all flows were diverted from the Ruamāhanga River there was an increased in simulated TSS in Alsop's Bay, likely derived from pulses of inflows with high concentrations of suspended sediment.

In the 3-D simulation outputs of TSS in Lake Onoke showed higher concentrations in western areas of the lake under different catchment scenarios, which was likely linked to the clockwise lake circulation patterns in the simulations. However, scenarios with the lake outlet closed generally had higher TSS concentrations, especially near the

58

Ruamāhanga inflow location (Fig. 44). This is most likely associated with less flushing under the scenarios, however when the Ruamāhanga was first diverted through Lake Wairarapa, the large increase in TSS is most likely derived from higher TSS from sediments arising from resuspension in Lake Wairarapa. Under the outlet closed scenario with no Ruamāhanga diversion, there is lower flushing and therefore limited removal of TSS. One-dimensional modelling also showed higher TSS concentrations in Lake Onoke under the outlet closed scenario with the Ruamāhanga diverted. The no-diversion simulations showed reduction TSS concentrations (in contrast to the 3-D model which showed an increase).
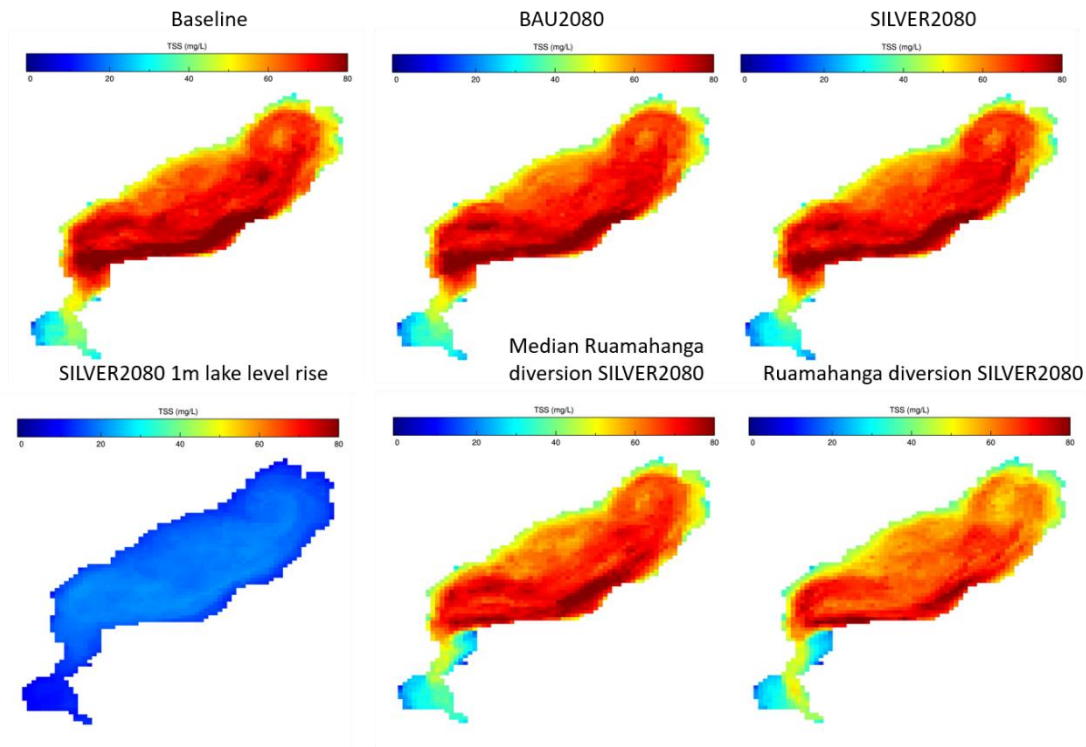


**Figure 42. Simulated total suspended solids concentrations in Lake Wairarapa using three-dimensional models (AEM3D). BAU is business as usual.**
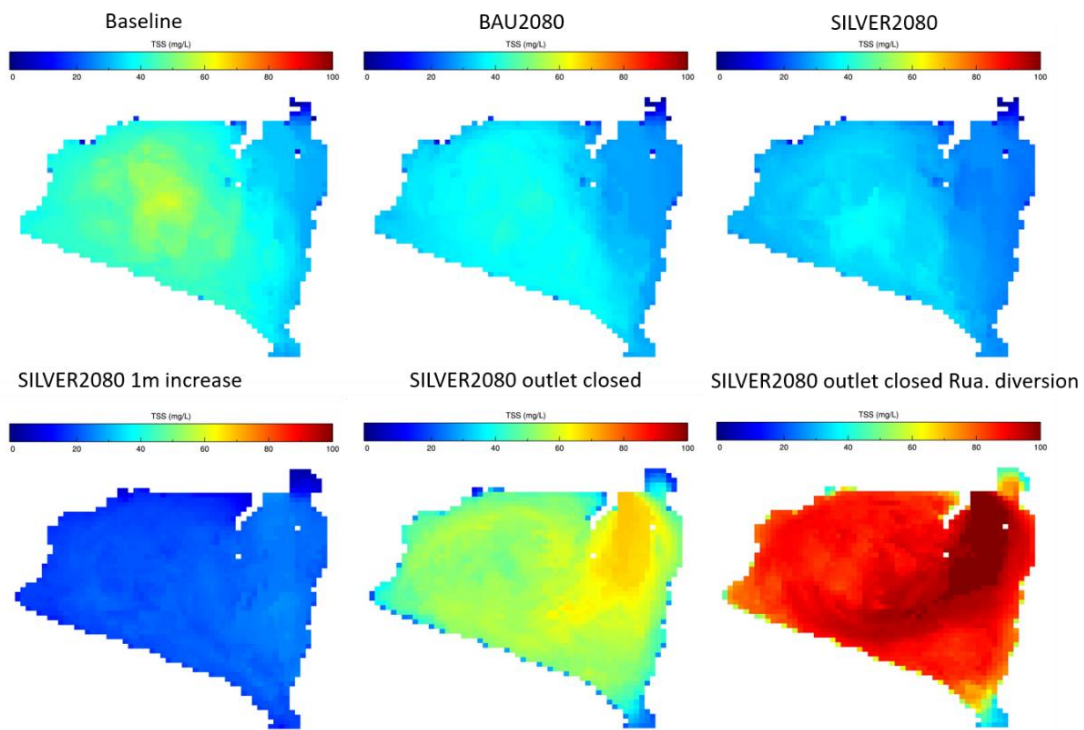
**Figure 43. Simulated total suspended solids concentration in Lake Onoke using three-dimensional models (AEM3D). BAU is business as usual.**

**Table 10. Summary of one-dimensional simulation results for water quality variables in Onoke and Wairarapa, colour-coded for NOF bands.**

| Lake Wairarapa | Modelling data No NOF band | Modelling data NOF band | BAU | SILVER | GOLD | SILVER + 1 m deth | Silver + Onoke outlet closed | Silver + Onoke outlet closed + all flows of Ruamāhanga into Lake | Silver + all flows of Ruamāhanga into Lake Wairarapa | Silver + non-flood flows of Ruamāhanga into Lake Wairarapa |
|---|---|---|---|---|---|---|---|---|---|---|
| *E. coli* | | | | | | | | | | |
| Phytoplankton | | C | C | B | B | C | | | B | B |
| Total nitrogen | | B | B | B | B | B | | | C | B |
| Total phosphorus | | D | D | D | D | D | | | D | D |
| Trophic Level Index -TLI | 5.6 | | 5.5 | 5.3 | 5.3 | 5.2 | | | 5.2 | 5.1 |
| Total suspended sediment | 65 | | 64 | 63 | 63 | 46 | | | 60 | 58 |
| Ammonia toxicity | | A | A | A | A | A | | | A | A |
| Cyanobacteria (planktonic) | A | | A | A | A | A | | | A | A |
| Macrophytes (% cover) | 0.027 | | 3.93E-08 | 11 | 11 | 44 | | | 17 | 1.40E-05 |
| | | | | | | | | | | |
| **Lake Onoke** | | | | | | | | | | |
| *E. coli* | | | | | | | | | | |
| Phytoplankton | | C | C | B | B | C | B | B | | |
| Total nitrogen | | B | B | B | B | B | B | B | | |
| Total phosphorus | | D | D | C | C | C | C | C | | |
| TLI | 5.4 | | 5.2 | 5.0 | 5.0 | 4.9 | 4.8 | 5.0 | | |
| Total suspended sediment | 32 | | 31 | 30 | 30 | 23 | 22 | 33 | | |
| Ammonia toxicity | | A | A | A | A | A | A | A | | |
| Cyanobacteria (planktonic) | A | | A | A | A | A | A | A | | |
| Macrophytes (% cover) | 0.030 | | 0.0321501 | 0.0321057 | 0.032106 | 0.0373972 | 0.00646906 | 0.0128636 | | |

**Table 11. Summary of three-dimensional simulation results for water quality variables in Onoke and Wairarapa, colour-coded for NOF bands.**

| Attribute | Modelling data | | BAU | | Silver | | Gold | | Silver + 1m additional depth | | Silver + Onoke outlet closed | | Silver + Onoke outlet closed + all flows of Ruamāhanga into | | Silver + all flows of Ruamāhanga into Lake Wairarapa | | Silver + non-flood flows of Ruamāhanga into Lake Wairarapa | |
|---|---|---|---|---|---|---|---|---|---|---|---|---|---|---|---|---|---|---|
| | No NOF band | NOF band | | | | | | | | | | | | | | | | |
| **Lake Wairarapa Middle** | | | | | | | | | | | | | | | | | | |
| Phytoplankton | | C | – | C | – | C | – | C | ↓ | D | | | | | ↓ | D | – | C |
| Total nitrogen | | B | – | B | – | B | – | B | – | B | | | | | – | B | – | B |
| Total phosphorus | | D | – | D | – | D | – | D | ↑ | C | | | | | – | D | ↑ | C |
| Trophic Level Index -TLI | 5.49 | | – | 5.49 | – | 5.31 | – | 5.32 | – | 5.17 | | | | | – | 5.56 | – | 5.24 |
| Total suspended sediment | 71 | | 1418 | 70 | 1417 | 70 | 1429 | 71 | 344 | 21 | | | | | 1357 | 68 | 1481 | 73 |
| Ammonia toxicity | | A | – | A | – | A | – | A | – | A | | | | | – | A | – | A |
| **Lake Onoke Middle** | | | | | | | | | | | | | | | | | | |
| Phytoplankton | | B | ↓ | C | – | B | – | B | ↓ | C | ↑ | A | ↓ | C | | | | |
| Total nitrogen | | C | ↑ | B | ↑ | B | ↑ | B | ↑ | B | ↑ | B | – | C | | | | |
| Total phosphorus | | B | – | B | – | B | – | B | – | B | ↑ | A | – | B | | | | |
| TLI | 4.64 | | – | 4.63 | – | 4.45 | – | 4.45 | – | 4.51 | ↑ | 3.98 | – | 5.00 | | | | |
| Total suspended sediment | 59 | | -30 | 41 | -36 | 37 | -36 | 38 | -65 | 21 | -9 | 53 | 56 | 92 | | | | |
| Ammonia toxicity | | A | – | A | – | A | – | A | – | A | – | A | – | A | | | | |

### *Macrophytes 1-D*

For Lake Wairarapa, 1-D modelling simulations indicated that under the 1 m depth increase scenario, macrophytes could re-establish within the lake to greater than 40% coverage, dramatically increasing the water quality within the lake, and reducing TLI to 4.4 (Table 12). This represents a regime shift in the lake to a desirable alternative stable state, which none of the other scenarios showed the potential to achieve. This was the only scenario that shifted NOF bands for TP out of the D category.

The SILVER and GOLD 2080 scenarios simulated that macrophytes could recover to 11% coverage.

One-dimensional modelling simulated that under the current conditions macrophytes cannot re-establish in Lake Onoke, therefore results are not presented. The model indicated that light was the major limiting function for macrophyte growth in Lake Onoke. However, we must note here that the macrophyte model has not been calibrated for Lake Wairarapa or Lake Onoke due to lack of available *in situ* data. Therefore, this creates more uncertainty in the derived outputs.

**Table 12. Lake Wairarapa macrophyte 1-D modelling results.**

| | Monitoring data | Modelling data | | BAU | Silver | Gold | Silver + 1m additional depth | Silver + all flows of Ruamāhanga into Lake Wairarapa | Silver + non-flood flows of Ruamāhanga into Lake Wairarapa |
| --- | --- | --- | --- | --- | --- | --- | --- | --- | --- |
| | | No NOF band | NOF band | | | | | | |
| **Lake Wairarapa Middle** | | | | | | | | | |
| Phytoplankton (chlorophyll *a*) | D | | C | C | C | C | C | D | B |
| Total nitrogen | C | | C | C | B | B | B | B | C |
| Total phosphorus | D | | D | D | D | D | B | C | D |
| Trophic Level Index -TLI | 5.1 (from LAWA) | 5.74 | | 5.99 | 5.21 | 5.20 | 4.41 | 4.87 | 6.05 |
| Total suspended sediment (mg/L) | | 90.97 | | 116.00 | 70.39 | 70.95 | 20.62 | 67.59 | 73.37 |
| Macrophyte coverage (%) | | 0.02 | | 0.00 | 10.60 | 10.80 | 44.30 | 16.60 | 0.00 |

*Lake Wairarapa uncertainty analysis*
Biogeochemical model parameter uncertainty analysis was compiled over a period of four years from July 1997 to July 2001. A total of 1460 models with randomly selected parameter values were simulated. Eighty-five key biogeochemical parameters were selected, and parameter perturbation was made within plus or minus 5% from the calibrated values (i.e. 10% parameter perturbation). The results were used to produce timeseries of state variables with indication of parameter uncertainty, and to rank the parameter by their sensitivity using variance-based approach (Saltelli et al., 2008), while Lehmann et al. (2017) and Muraoka et al., (in prep) methods were used for these outcomes.

The probability density plots show the uncertainty of water quality results generated (Fig. 45). The simulated (surface) TN, TP, TSS, and chl *a* generally encompass the range of observed variables. Chlorophyll *a* and TN concentrations were more uncertain during summer, suggesting importance of internal dynamics during these periods. In contrast, TSS results contained very small parameter uncertainty, suggesting the importance of TSS from forcing variables, such as water level fluctuation, inflow / outflow, weather and wind events.

Sensitivity of the 85 parameters were ranked in order of decreasing sensitivity (Table 13). The most sensitive parameters related to particle organic matter (POM) resuspension and settling rate, with POM density the most sensitive parameter determining TP, TN and chl *a*. Parameters with the most influence on TSS concentrations were unsurprisingly particle diameter and resuspension rate of inorganic suspended solids.

Chlorophyll *a* concentration was sensitive to parameters that included the temperature multiplier for phytoplankton respiration/growth, and density and diameter of suspended solid particles. Phosphate release rate was the sixth most sensitive parameter, indicating that internal loading has a minor influence on phytoplankton growth and ultimately lake trophic status.

The sensitivity analysis reveals the most fundamental biogeochemical processes influencing the trophic status of Wairarapapa. These are resuspension (of both organic and inorganic particles), and light limitation (due to suspended particle scattering). Resuspension of organic material then influences nutrient concentrations and availability within the water column, due to mineralisation and decay processes that make organic matter derived nutrients available for phytoplankton growth.
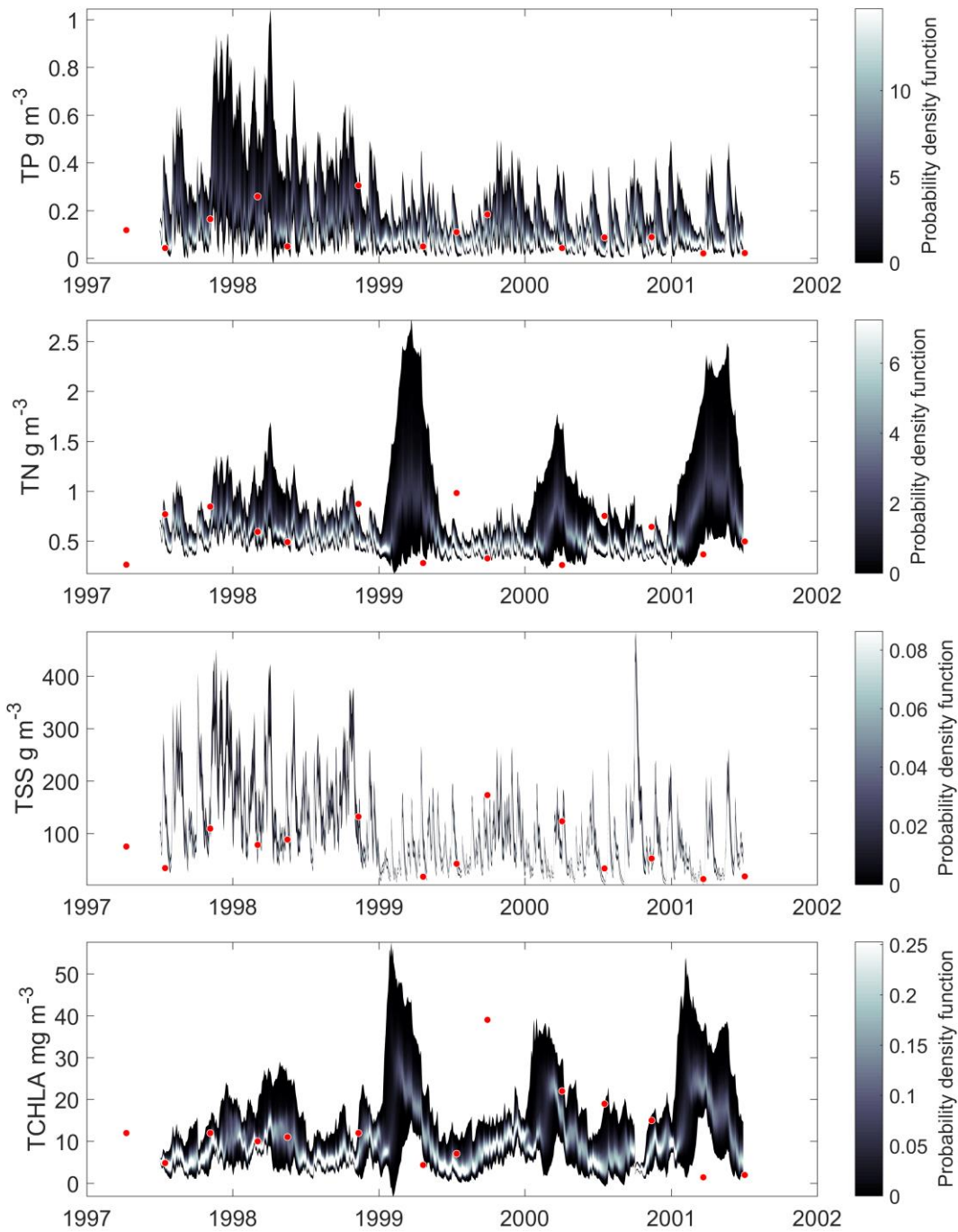
**Figure 44. Probability density plots show the range of water quality related outputs generated from plus or minus 5% if sensitive parameters. Measured *in situ* data is plotted with a red closed circle. TCHLA is total chlorophyll a,TSS is total suspended sediment, TP is total phosphorous and TN is total nitrogen.**

**Table 13. Model parameters ranked in order of decreasing sensitivity for the 1-D Wairarapa model**

| Sensitivity rank | Chl *a* | TSS | TN | TP |
|---|---|---|---|---|
| 1 | Density of POM particles (labile) | Diameter of suspended solid particles | Density of POM particles (labile) | Density of POM particles (labile) |
| 2 | Temperature multiplier for phytoplankton respiration | Composite resuspension rate | Diameter of POM particles (labile) | Diameter of POM particles (labile) |
| 3 | Density of suspended solid particles | Density of suspended solid particles | Temperature multiplier for phytoplankton growth | Half saturation constant for nitrogen |
| 4 | Diameter of suspended solid particles | Diameter of suspended solid particles | Density of suspended solid particles | Respiration rate coefficient |
| 5 | Temperature multiplier for phytoplankton growth | Density of suspended solid particles | Diameter of suspended solid particles | Max transfer of POCL-DOCL |
| 6 | Release rate of PO4 | Critical shear stress of suspended solids | Maximum growth rate | Respiration rate coefficient |
| 7 | Diameter of POM particles (labile) | Maximum temperature | Fraction of metabolic loss rate that goes to DOM | Fraction of respiration relative to total metabolic loss rate |
| 8 | Temperature multiplier of sediment fluxes | Half sat constant for DO sediment flux | Respiration rate coefficient | Composite resuspension rate |
| 9 | Diameter of suspended solid particles | Constant settling velocity | Half saturation constant for phosphorus | Optimum temperature |
| 10 | Density of suspended solid particles | Maximum growth rate | Standard temperature | Parameter for initial slope of P/I curve |

## Summary and conclusions

Within Lake Wairarapa, catchment mitigation-based scenarios showed considerable potential for the improvement of water quality. These mitigations simulated that the trophic state of the lake could reduce from the current supertrophic category, to the top of the eutrophic category, which still indicates poor water quality and high turbidity/low water clarity. In addition, these catchment mitigations did not move the lake from a NOF D category for TP. While not detailed in this report, the lake model was run again for larger reductions in TP (60%). These simulations indicated that within the last five years of the simulation, 60% reduction in TP (with SILVER2080 mitigations of other nutrients) could achieve a NOF C category for TP. However, simulations that included the re-establishment of macrophytes also indicated NOF C category for TP, under SILVER2080, but only under a 1 m depth increase scenario, or Ruamāhanga diversion scenario. The simulations indicated that the trophic status could reduce to the mid-eutrophic category, however this is still indicative of poor water quality.


Within Lake Wairarapa there were conflicting results between 1-D and 3-D models for Ruamāhanga diversion scenarios and 1 m depth increase scenarios. One dimensional models indicated an increase in water quality and lower chl *a*, however 3-D models simulated increased chl *a* concentrations. Considering these scenarios change spatial distributions of water quality, 3-D modelling provides more robust estimations of scenarios. However, these models were only run for short time periods. For the Ruamāhanga below median diversion scenario increase in chl *a* concentration was small, and within model error terms, so potentially insignificant. If under this scenario macrophytes re-establish, this small increase in chl *a* would be negated. Therefore, Ruamāhanga below median diversion SILVER2080 likely has the greatest potential for water quality improvement in lake Wairarapa, however scenarios would need to be tested that could isolate potential downstream implications (e.g. higher TSS/nutrients) in Lake Onoke.


3-D models also simulated that 1 m depth increase under SILVER2080 increase chl *a* concentrations. This was caused by less light limitation of phytoplankton, due to reduced sediment resuspension from the lake bottom (greater depth decreases the influence of surface waves on resuspension of sediment). The net effect was increased water clarity and the potential for macrophyte re-establishment. While 3-D modelling showed the Ruamāhanga diversion has the potential to increase chlorophyll *a* in Lake Wairarapa, this would likely be negated if macrophytes could re-establish within the lake. However, each simulation result is associated with a level of error – large swings can be predicted with confidence, subtle changes could be directionally different.


For Lake Wairarapa to be restored to a clear water stable state, the effects of hysteresis must be considered. For a shallow, turbid lakes, hysteresis is caused by a system of interacting ecological and physical processes which act to stabilise the current turbid state (Janse et al., 2008). For example, the high resuspension from the lake bottom decreases light available, limiting the potential for macrophyte reestablishment. High sediment resuspension from the bottom sediments in Lake Wairarapa results in continued low clarity under all scenarios (except macrophyte re-establishment under a 1 m increase scenario). However for significant macrophyte reestablishment the general rule of thumb is that Secchi depth would need to be

at least 0.5 m (Jeppesen et al., 1997). The 3-D modelling showed potential for this to be achieved with lake level manipulation. Once macrophytes become established, they would have the potential to maintain the clear water state and potentially inhibit cyanobacterial blooms, due to stabilisation of sediment, binding nutrients, and potentially absorbing nutrients from the water column. In addition, submerged macrophytes can play an ecological structuring role within lakes, providing habitat for zooplankton to avoid predation, thereby enhancing zooplankton populations and predation on phytoplankton (Jeppesen et al., 1997).

Macrophytes could re-establish within the lake to greater than 40% coverage, dramatically increasing the water quality within the lake, reducing TLI to 4.4 in Lake Wairarapa (under the 1 m depth increase scenario). This represents a regime shift in the lake to an alternative stable state, which none of the other scenarios showed the potential to achieve. However, the macrophyte simulations have limited capacity to simulate some of the complex factors that might also interactively lead to their re-establishment. For example, model simulations do not include macrophyte uprooting due to wave action and erosion. Therefore, it is possible that the 1 m depth level increase is not the only scenario that would allow potential macrophyte re-establishment. We also note here that the macrophyte model applied in the present study was not calibrated for Lake Wairarapa and Onoke. The SILVER and GOLD 2080 scenarios simulated that macrophytes could recover to about 10% coverage. One potential management option would be to temporarily increase the lake depth, allowing for macrophyte reestablishment and a regime shift within the lake. The macrophyte scenarios clearly show that if external load is reduced and water levels increased, macrophyte re-establishment is possible, and could be associated with substantial water quality improvement in Lake Wairarapa.

Internal loading of phosphorus from sediments in Lake Wairarapa results in reduction of effectiveness of mitigations compared to Lake Onoke. However, the magnitude of this internal loading is much lower compared to some other lowland degraded lakes. For example, the internal load (phosphate) is estimated as approximately 1/3 of the total load (catchment plus internal load). While significant, this is not as high as what has been found in some other shallow lakes, where external load can be of a similar magnitude external load (Søndergaard et al., 1999). For example, simulated maximum potential release rate of phosphate was approximately one third of that set for Lake Ellesmere Te Waihora in the same DYRESM-CAEDYM setup.

Catchment scenarios had a greater influence on Lake Onoke trophic status compared to Wairarapa, due to the shorter residence time and lower internal load (from the sediments) relative to external load, which was negligible. In effect the composition of Onoke aligns closely with that of its inflows. Internal loading must be considered in any restoration efforts within Wairarapa, and the length of recovery period following external phosphorus load reduction is determined by the loading history and the amount of phosphorus bound within sediment. The recovery can take decades, depending on the residence time (Martin Søndergaard et al., 2003), however within Lake Wairarapa the short residence time would likely mean that this recovery is in the order of years not decades.

69

Water quality in Lake Onoke is susceptible to changes in water quality in Lake Wairarapa, particularly in relation to chl *a* and TSS. High lake bed sediment resuspension events in Lake Wairarapa transport increased levels of suspended sediment to Lake Onoke. Modelling shows chl *a* in Onoke is partially derived from Lake Wairarapa (when chl *a* is not routed from Lake Wairarapa within the model, simulated chl *a* in Onoke is lower than observed values). The very low residence time in Onoke (0.5 days) does not allow adequate time for significant phytoplankton growth within the lake. However, 3-D simulations show higher phytoplankton concentrations at times in the western lake, relating to flushing and transport effects.

The Ruamāhanga diversion scenarios present an innovative management option. When wind speeds are high, high sediment resuspension occurs in Lake Wairarapa. Under these conditions, the lake could be flushed with Ruamāhanga flows, thereby exporting suspended sediment, and any bound phosphorus and suspended organic matter. This would be an effective strategy to potentially reduce internal nutrient and sediment loading from the lake bed and mitigate the very high sedimentation rate. However, under this scenario there would be high TSS transport into Lake Onoke. Provided the mouth is open much of this flow would be exported to the ocean. Considerations may, however, need to be given to benthic communities of the coastal ocean environment before undertaking such an option.

The greatest improvement in simulated water quality in Onoke resulted from the summer outlet closed scenario. However, it also indicated an increased risk of cyanobacterial blooms, and the 1-D simulated TLI under SILVER2080 was almost identical to outlet closed SILVER2080. As long as the residence time remains under 20 days, cyanobacterial bloom risk would be very low (Maberly et al., 2002; Soballe & Kimmel, 1987). However, under drought conditions and low-flow, the residence time could increase, along with risk of bloom formation. Under the scenario of a summer outlet closing, when Ruamāhanga waters were diverted through Lake Wairarapa, there was a 63.2% reduction in *E. coli* within Onoke, owing to higher mortality and settling within Lake Wairarapa, which provided sufficient residence time in Wairarapa for attenuation of *E. coli*. The 3-D modelling indicated that lack of flushing under this scenario increased TSS concentrations, thereby limiting phytoplankton growth. Under low-flow conditions and at times when TSS input from Lake Wairarapa is low, conditions would favour more algal growth. While the outlet closed scenario was simulated to bring the greatest water quality gains (using 3-D modelling), an increase in TSS concentrations, and phytoplankton light limitation, is not an effective mitigation technique long-term. In addition to this *in situ* monitoring has indicated that under outlet closed conditions the lake is more susceptible to eutrophication (Robertson & Stevens, 2007) and there is indication that chl *a* is higher when the lake is blocked and TSS is lower when the lake is blocked (Perrie & Milne, 2012). We also note here the 3-D models were run for only a short time period, therefore for more robust conclusion we recommend 3-D models to be applied over a longer time period. We also note that during the3-D simulation time period there was a large rainfall event. This could potentially skew any derived results as periods when Onoke mouth is blocked usually correspond to low-flow and settled weather.

For Lake Onoke, there were also conflicting results between 1-D and 3-D models for 1 m depth increase scenarios, with the 3-D model showing potential small increases in chl *a* concentrations in Western lake areas. However, 1-D modelling simulated a small (and within error terms) reduction of median chl *a* (c. 1 µg L). Under this scenario the 3-D and 1-D model both showed an increase in overall water quality (reduction in TLI), and this scenario has the greatest potential to reduce suspended solids and increase water clarity.

The spatially resolved estimations of TSS from remote sensing images were useful for the calibration and validation of 3-D hydrodynamic models. Modelling provides the opportunity for interpretation of remotely sensed imagery through the quantification of the physical and biogeochemical fluxes that redistribute variables and lead to the spatial distributions observed in remote sensing imagery. For example, the generally lower concentrations of TSS observed in the western area of Lake Wairarapa may be due to the influence inflows entering this area which are low in TSS. The lower concentrations of TSS which were commonly observed in Alsop's Bay are likely due to a lower energy environment owing to the shorter wind fetch and associated lower levels of wave and current energy for sediment resuspension.

### *Future work*
The current study has identified that resuspension of organic and organic matter and light limitation of algal and macrophyte growth are critical processes influencing the trophic status of the lakes Wairarapa and Onoke. Therefore, we recommend more *in situ* and lab-based investigation of parameters such as mineral and organic sediment settling rates, critical shear stress, and specific attenuation coefficients of phytoplankton and suspended sediment. Quantification of these parameters would decrease uncertainty in any model simulations.

In addition, quantification of marine intrusion flow volumes and nutrient concentrations into Lake Onoke would also decrease uncertainty in model simulations. This could include estimation of barrier seepage and potential storm overtopping inputs (in any). If marine inflows can be quantified with more certainty, the models could be run on an hourly time step for inflow and lake height, potentially increasing accuracy of simulations.

In addition, running the 3-D models for longer time periods would increase the robustness of any derived conclusions and decrease uncertainty.

We note that climate change effects were not included within this study. There is evidence that climate change could enhance eutrophication in mesotrophic and eutrophic lakes due physiochemically and biologically induced higher internal loading (Jeppesen et al., 2014).

# References

Airey, S., Puentener, R., & Rebergen, A. (2000). *Lake Wairarapa wetlands action plan*. Department of Conservation, Wellington, New Zealand.

Allan, M. G. (2014). *Remote sensing , numerical modelling and ground truthing for analysis of lake water quality and temperature*. Ph.D thesis, The University of Waikato, NZ.

Allan, M. G., Hamilton, D. P., Hicks, B., & Brabyn, L. (2015). Empirical and semi-analytical chlorophyll a algorithms for multi-temporal monitoring of New Zealand lakes using Landsat. *Environmental Monitoring and Assessment*, *187*(6). http://doi.org/10.1007/s10661-015-4585-4

Aurin, D. A., & Dierssen, H. M. (2012). Advantages and limitations of ocean color remote sensing in CDOM-dominated, mineral-rich coastal and estuarine waters. *Remote Sensing of Environment*, *125*, 181–197. http://doi.org/10.1016/j.rse.2012.07.001

Blondeau-Patissier, D., Brando, V. E., Oubelkheir, K., Dekker, A. G., Clementson, L. A., & Daniel, P. (2009). Bio-optical variability of the absorption and scattering properties of the Queensland inshore and reef waters, Australia. *Journal of Geophysical Research*, *114*(C5), C05003. http://doi.org/10.1029/2008JC005039

Blyth, J. (2018). *Ruamāhanga Whaitua Committee - Scenario Modelling*. Prepared for Greater Wellington Regional Council, New Zealand. IZ090000.

Burger, D. F., Hamilton, D. P., & Pilditch, C. A. (2008). Modelling the relative importance of internal and external nutrient loads on water column nutrient concentrations and phytoplankton biomass in a shallow polymictic lake. *Ecological Modelling*, *211*(3–4), 411–423. http://doi.org/10.1016/j.ecolmodel.2007.09.028

Burns, N., & Bryers, G. (2000). *Protocol for Monitoring Trophic Levels of New Zealand Lakes and Reservoirs Noel Burns of Lakes Consulting and*. Lakes Consulting Client Report: 99/2 March 2000.

Casulli, V., & Cheng, R. T. (1992). Semi-implicit finite difference methods for three-dimensional shallow water flow. *International Journal for Numerical Methods in Fluids*, *15*, 629–648.

Dekker, A. G., Brando, V. E., Anstee, J. M., Pinnel, N., Kutser, T., Hoogenboom, H. J., … Malthus, T. J. (2002). Imaging spectrometry of water. In F. D. van der Meer &  de J. S. M. (Eds.), *Imaging Spectrometry: Basic Principles and Prospective Applications* (pp. 307–359). Kluwer, Dordrecht, Netherlands.

Dekker, A. G., Hoogenboom, H. J., Goddijn, L. M., & Malthus, T. J. M. (1997). The relation between inherent optical properties and reflectance spectra in turbid inland waters. *Remote Sensing Reviews*, *15*(1–4), 59–74.

Dekker, A. G., Vos, R. J., & Peters, S. W. M. (2002). Analytical algorithms for lake water TSM estimation for retrospective analyses of TM and SPOT sensor data. *International Journal of Remote Sensing*, *23*(1), 15–35.

Dekker, A. G., Zamurović-Nenad, Ž., Hoogenboom, H. J., & Peters, S. W. M. (1996). Remote sensing, ecological water quality modelling and in situ measurements: a case study in shallow lakes. *Hydrological Sciences Journal*, *41*(4), 531–547. http://doi.org/10.1080/02626669609491524

Deltares systems. (2014). *Simulation of multi-dimensional hydrodynamics flows and transport phenonmena, including sediments. User manual version 3.15*. Deltares, Delft, The Neterlands.

Drake, D. C., Kelly, D., & Schallenberg, M. (2010). Shallow coastal lakes in New Zealand:

current conditions, catchment-scale human disturbance, and determination of ecological integrity. *Hydrobiologia*, *658*(1), 87–101. http://doi.org/10.1007/s10750-010-0452-z

Fischer, J. (1979). Modelling of water quality processes in lakes and reservoirs. *Hydrological Sciences*, (24), 157–160.

Gallegos, C. (2001). Calculating optical water quality targets to restore and protect submersed aquatic vegetation: overcoming problems in partitioning the diffuse attenuation coefficient for photosynthetically active radiation. *Estuaries*, *24*(3), 381–397.

Gluckman, P., Cooper, B., Howard-Williams, C., Larned, S., Quinn, J., Bardsley, A., … Wratt, D. (2017). *New Zealand's fresh waters: values, state, trends and human impacts. Office of the Prime Minister'S Chief Science Advisor.* Office of the Prime Minister's Chief Science Advisor, 2017.

Gordon, H. R., Brown, J. W., Brown, O. B., Evans, R. H., & Smith, R. C. (1988). A semianalytic radiance model of ocean color. *Journal of Geophysical Research*, *93*(D9), 10909–10924.

Gyopari, M. C., & McAlister, D. (2010). *Wairarapa Valley groundwater resource investigation: Lower Valley catchment hydrogeology and modelling.* Greater Wellington Regional Council, New Zealand.

Hamilton, D. P., Collier, K. J., & Howard-Williams, C. (2016). Lake Restoration in New Zealand. *Ecological Management and Restoration*, *17*(3), 191–199. http://doi.org/10.1111/emr.12226

Hamilton, D. P., & Schladow, S. G. (1997). Prediction of water quality in lakes and reservoirs . Part I - Model description. *Ecological Modelling*, *96*, 91–110.

Havens, K. E., James, R. T., East, T. L., & Smith, V. H. (2003). N : P ratios , light limitation , and cyanobacterial dominance in a subtropical lake impacted by non-point source nutrient pollution, *122*, 379–390.

Hodges, B., & Dallimore, C. (2016). *Aquatic Ecosystem Model: AEM3D v1.0 User Manual.* Hydronumerics, Victoria, Australia.

Holmes, R. W. (1970). The Secchi disk in turbid coastal waters. *Limnology and Oceanography*, *15*(2), 688–694. http://doi.org/10.4319/lo.1970.15.5.0688

Hu, K., Ding, P., Wang, Z., & Yang, S. (2009). A 2D/3D hydrodynamic and sediment transport model for the Yangtze Estuary, China. *Journal of Marine Systems*, *77*(1–2), 114–136. http://doi.org/10.1016/j.jmarsys.2008.11.014

Imerito, A. (2007). *Dynamic Reservoir Simulation Model DYRESM v4.0 Science Manual. Centre for Water Research, University of Western Australia. Exchange Organizational Behavior Teaching Journal.* Centre for Water Research, University of Western Australia.

Janse, J. H., De Senerpont Domis, L. N., Scheffer, M., Lijklema, L., Van Liere, L., Klinge, M., & Mooij, W. M. (2008). Critical phosphorus loading of different types of shallow lakes and the consequences for management estimated with the ecosystem model PCLake. *Limnologica*, *38*(3–4), 203–219. http://doi.org/10.1016/j.limno.2008.06.001

Jeppesen, E., Meerhoff, M., Davidson, T. A., Trolle, D., Søndergaard, M., Lauridsen, T. L., … Nielsen, A. (2014). Climate change impacts on lakes: An integrated ecological perspective based on a multi-faceted approach, with special focus on shallow lakes. *Journal of Limnology*, *73*(1 SUPPL), 88–111. http://doi.org/10.4081/jlimnol.2014.844

Jeppesen, E., Søndergaard, M., Jensen, J. P., Havens, K. E., Anneville, O., Carvalho, L., … Winder, M. (2005). Lake responses to reduced nutrient loading - An analysis of contemporary long-term data from 35 case studies. *Freshwater Biology*, *50*(10), 1747–1771. http://doi.org/10.1111/j.1365-2427.2005.01415.x

Jeppesen, E., Søndergaard, M., Søndergaard, M., & Christoffersen, K. (1997). *The structuring role of submerged macrophytes in lakes*. (E. J. Morten Søndergaard, Kirsten Christofferson, Ed.) (Vol. 131). Springer New York. http://doi.org/10.1007/978-1-4612-0695-8

Jones, H. F. E., Özkundakci, D., McBride, C. G., Pilditch, C. A., Allan, M. G., & Hamilton, D. P. (2018). Modelling interactive effects of multiple disturbances on a coastal lake ecosystem: Implications for management. *Journal of Environmental Management*, *207*, 444–455. http://doi.org/10.1016/j.jenvman.2017.11.063

Kloiber, S. M., Brezonik, P. L., & Bauer, M. E. (2002). Application of Landsat imagery to regional-scale assessments of lake clarity. *Water Research*, *36*, 4330–4340.

Kotchenova, S. Y., Vermote, E. F., Levy, R., & Lyapustin, A. (2008). Radiative transfer codes for atmospheric correction and aerosol retrieval: intercomparison study. *Applied Optics*, *47*(13), 2215–2226.

Leach, B. F., & Anderson, a. (1974). The transformation of an estuarine to a lacustrine environment in the lower Wairarapa. *Journal of the Royal Society of New Zealand*, *4*(November), 267–275. http://doi.org/10.1080/03036758.1974.10419394

Leonard, B. P. (1991). The ULTIMATE conservative difference scheme applied to unsteady one-dimensional advection. *Computer Methods in Applied Mechanics and Engineering*, *88*, 17–74.

Lesser, G. R., Roelvink, J. A., van Kester, J. A. T. M., & Stelling, G. S. (2004). Development and validation of a three-dimensional morphological model. *Coastal Engineering*, *51*(8–9), 883–915. http://doi.org/10.1016/j.coastaleng.2004.07.014

Li, L., Li, L., Song, K., Li, Y., Tedesco, L. P., Shi, K., & Li, Z. (2013). An inversion model for deriving inherent optical properties of inland waters: Establishment, validation and application. *Remote Sensing of Environment*, *135*, 150–166. http://doi.org/10.1016/j.rse.2013.03.031

Lill, A. W. T., Schallenberg, M., Lal, A., Savage, C., & Closs, G. P. (2013). Isolation and connectivity: Relationships between periodic connection to the ocean and environmental variables in intermittently closed estuaries. *Estuarine, Coastal and Shelf Science*, *128*, 76–83. http://doi.org/10.1016/j.ecss.2013.05.011

Maberly, S. C., King, L., Dent, M. M., Jones, R. I., & Gibson, C. E. (2002). Nutrient limitation of phytoplankton and periphyton growth in upland lakes. *Freshwater Biology*, *47*(11), 2136–2152. http://doi.org/10.1046/j.1365-2427.2002.00962.x

Matthews, M. (2011). A current review of empirical procedures of remote sensing in inland and near-coastal transitional waters. *International Journal of Remote Sensing*, *32*, 6855–6899.

Mcewan, A. (2009). *Lake Wairarapa Fish Survey 2009*. Prepared for Greater Wellington Regional Council by Institute of Natural Resources Massey University.

Menneer, J. C., Ledgard, S. F., & Gillingham, A. G. (2004). *Land use imaacts on Nitrogen and Phosphorus loass and management options for intervention*. Client Report Prepared for Environment Bay of Plenty.

MFE. (2017a). *National policy statement for Freshwater Management 2014 (amended 2017)*. Wellington: Ministry for the Environment.

MFE. (2017b). *Swimming categories for E . coli in the Clean Water package A summary of the categories and their relationship to human health risk from swimming*. Wellington: Ministry for the Environment.

Mitchell, A. G. (1989). *Late Quaternary deposits of the eastern shore of Lake Wairarapa, North Island, New Zealand*. Ph.D thesis, Massey University.

Moore, C., Gyopari, M., Toews, M., & Mzila, D. (2017). *Ruamāhanga Catchment Groundwater Modelling*. GNS Science Consultancy Report 2016/162. 189 p.

Morel, A., & Prieur, L. (1977). Analysis of variations in ocean color. *Limonology And Oceanography*, *22*(4), 709–722. http://doi.org/10.4319/lo.1977.22.4.0709

Moritz K. Lehmann, David P. Hamilton, Kohji Muraoka, G. W. T., Collier, K. J., & Hicks, B. (2017). *Waikato Shallow Lakes Modelling*. ERI Report 94. Environmental Research Institute, University of Waikato, Hamilton, New Zealand. 1xx pp.

Muirhead, R., Monaghan, R., Smith, C., & Stantiall, J. (2016). *Modelling Farm-scale Mitigation Options for the Ruamahanga Whaitua Collaborative Modelling Project June 2016 Modelling Farm-scale Mitigation Options for the Ruamahanga Whaitua Collaborative Modelling Project*. Report prepared for Ministry for Primary Industries. Agresearch. RE500/2016/059. NIWA.

Muraoka, K. M., Hamilton, D. P., Lehmann, M., Özkundakci, D., Verburg, P., Luo, L., & Hartland, A. (n.d.). Generating uncertainty output from a deterministic lake ecological model using parameter perturbations. *(In Prep)*.

Oliver, M. D., & Milne, J. R. (2012). *Recreational water quality in the Wellington region State and trends Recreational water quality in the Wellington region*. Greater Wellington Regional Council, New Zealand GW/EMI-T-12/144.

Özkundakci, D., Hamilton, D., & Trolle, D. (2011). Modelling the response of a highly eutrophic lake to reductions in external and internal nutrient loading. *New Zealand Journal of Marine and Freshwater Research*, *45*(2), 165–185. http://doi.org/10.1080/00288330.2010.548072

Parkyn, S. M., Davies-colley, R. J., Halliday, N. J., Costley, K. J., & Croker, G. F. (2000). Planted riparian buffer zones in New Zealand : do they live up to expectations ? *Restoration Ecology*, *11*(4), 1–13.

PCE. (2012). *Water quality in New Zealand: Understanding the science*. ParliaParliamentary Commission for the Environment, Wellington.

PCE. (2013). *Water quality in New Zealand: Land use and nutrient pollution*. Parliamentary Commission for the Environment, Wellington.

Perrie, A. (2005). *Lake Wairarapa water quality monitoring technical report*. Greater Wellington Regional Council.

Perrie, A., & Milne, J. R. (2012). *Lake water quality and ecology in the Wellington region*. Greater Wellington Regional Council.

Petzold, T. (1972). *Volume Scattering Functions for Selected Ocean Waters*. Scripps Institution of Oceanography, San Diego.

Robertson, B., & Stevens, L. (2007). *Lake Onoke 2007 vulnerability assessment and monitoring recommendations*. Prepared for the Greater Wellington regional Council by Wriggle LTD, Nelson.

Roy, P. S., Williams, R. J., Jones, A. R., Yassini, I., Gibbs, P. J., Coates, B., … Nichol, S. (2001). Structure and Function of South-east Australian Estuaries. *Estuarine, Coastal and Shelf Science*, *53*(2001), 351–384. http://doi.org/10.1006/ecss.2001.0796

Saltelli, A., Ratto, M., Andres, T., Campolongo, F., Cariboni, J., Gatelli, D., … Tarantola, S. (2008). *Global Sensitivity Analysis. The Primer. Global Sensitivity Analysis. The Primer*. http://doi.org/10.1002/9780470725184

Sands, M. (2018). *Water quality modelling of the Ruamahanga Catchment*. Prepared for Greater Wellington Regional Council by Jacobs.

Schladow, S. G., & Hamilton, D. P. (1997). Prediction of water quality in lakes and reservoirs : Part II - Model calibration , sensitivity analysis and application. *Ecological*

*Modelling*, *96*, 111–123.

Soballe, D. M., & Kimmel, B. L. (1987). A large-scale comparison of factors influencing phytoplankton abundance in rivers, lakes, and impoundments. *Ecology*, *68*(6), 1943–1954. http://doi.org/10.2307/1939885

Søndergaard, M., Jensen, J. . P., & Jeppesen, E. (1999). Internal phosphorus loading in shallow Danish lakes, 145–152.

Søndergaard, M., Jensen, J. P., & Jeppesen, E. (2003). Role of sediment and internal loading of phosphorus in shallow lakes. *Hydrobiologia*, *506–509*(1–3), 135–145. http://doi.org/10.1023/B:HYDR.0000008611.12704.dd

Thompson, M., & Mzila, D. (2015). *Lake Wairarapa water balance investigation*. Greater Wellington Regional Council.

Trodahl, M. I. (2010). *Late Holocene Sediment Deposition in Lake Wairarapa*. Ph.D thesis. Victoria University of Wellington.

Trolle, D., Hamilton, D. P., Pilditch, C. A., Duggan, I. C., & Jeppesen, E. (2011). Predicting the effects of climate change on trophic status of three morphologically varying lakes: Implications for lake restoration and management. *Environmental Modelling & Software*, *26*(4), 354–370.

Vidot, J., & Santer, R. (2005). Atmospheric correction for inland waters—application to SeaWiFS. *International Journal of Remote Sensing*, *26*(17), 3663–3682. http://doi.org/10.1080/01431160500034029

Zarzuelo, C., Díez-Minguito, M., Ortega-Sánchez, M., López-Ruiz, A., & Losada, M. T. (2015). Hydrodynamics response to planned human interventions in a highly altered embayment: The example of the Bay of Cádiz (Spain). *Estuarine, Coastal and Shelf Science*, *167*, 75–85. http://doi.org/10.1016/j.ecss.2015.07.010

# Appendix

**Table 14. Lake Wairarapa flow and nutrient load summary.**

| Flow | Associated stream/river | TN (t yr⁻¹) | TP (t yr⁻¹) | TSS (t yr⁻¹) | *E. coli* (cells yr⁻¹) | Flow (m³ yr⁻¹) | TN (%) | TP (%) | TSS (%) | *E. coli* (%) | Flow (%) |
|---|---|---|---|---|---|---|---|---|---|---|---|
| **DSflow_link_SC042.dat** | Abbots Ck. | **38.22** | **3.78** | **5671.12** | 9.13E+14 | 8.88E+07 | 7.8 | 0.08 | 6.1 | 14.7 | 8.2 |
| **DSflow_link_SC043.dat** | | **9.39** | 0.56 | 1538.03 | 1.24E+14 | 2.46E+07 | 1.9 | 0.01 | 1.7 | 2.0 | 2.3 |
| **DSflow_link_SC045.dat** | | **14.85** | 1.00 | 4135.28 | 1.26E+14 | 2.30E+07 | 3.0 | 0.02 | 4.5 | 2.0 | 2.1 |
| **DSflow_link_SC046.dat** | | **7.98** | 0.80 | 555.17 | 1.02E+14 | 7.55E+06 | 1.6 | 0.02 | 0.6 | 1.6 | 0.7 |
| **DSflow_link_SC047.dat** | Cross Ck. | **8.42** | 0.82 | 3677.25 | 4.36E+14 | 5.05E+07 | 1.7 | 0.02 | 4.0 | 7.0 | 4.6 |
| **DSflow_link_SC048.dat** | | **22.68** | 1.35 | 3753.96 | 6.48E+13 | 3.82E+07 | 4.7 | 0.03 | 4.0 | 1.0 | 3.5 |
| **DSflow_link_SC051.dat** | Otukura Str. | **65.18** | 1.90 | 2728.87 | 6.64E+14 | 4.56E+07 | 13.4 | 0.04 | 2.9 | 10.7 | 4.2 |
| **DSflow_link_SC052.dat** | Mangatete Str. | **7.91** | 0.48 | 171.27 | 1.68E+14 | 8.53E+06 | 1.6 | 0.01 | 0.2 | 2.7 | 0.8 |
| **DSflow_link_SC053.dat** | | **5.96** | 0.22 | 336.69 | 7.32E+13 | 2.18E+06 | 1.2 | 0.00 | 0.4 | 1.2 | 0.2 |
| **DSflow_link_SC057.dat** | Te Miara str. Ororua Spillway | **23.14** | 1.28 | 1624.82 | 1.64E+15 | 5.57E+07 | 4.8 | 0.03 | 1.8 | 26.5 | 5.1 |
| **DSflow_link_SC062.dat** | | **0.78** | 0.04 | 239.89 | 8.55E+12 | 3.73E+06 | 0.2 | 0.00 | 0.3 | 0.1 | 0.3 |
| **DSflow_link_SC065.dat** | | **0.77** | 0.05 | 189.22 | 5.15E+12 | 3.87E+05 | 0.2 | 0.00 | 0.2 | 0.1 | 0.0 |
| **DSflow_link_SC067.dat** | Waiorongomai | **11.55** | 0.97 | 7436.50 | 2.44E+14 | 7.50E+07 | 2.4 | 0.02 | 8.0 | 3.9 | 6.9 |
| **DSflow_link_SC078.dat** | | **11.81** | 1.01 | 493.54 | 1.74E+14 | 1.55E+07 | 2.4 | 0.02 | 0.5 | 2.8 | 1.4 |
| **DSflow_link_SC089.dat** | Tauherenikau R. | **53.12** | 7.33 | 46476.42 | 5.12E+14 | 3.15E+08 | 10.9 | 0.15 | 50.1 | 8.2 | 29.0 |
| **DSflow_link_SC195.dat** | | **0.02** | 0.00 | 57.43 | 0.00E+00 | 1.08E+05 | 0.0 | 0.00 | 0.1 | 0.0 | 0.0 |
| **DSflow_link_SC196.dat** | | **0.64** | 0.05 | 89.97 | 6.93E+12 | 2.06E+05 | 0.1 | 0.00 | 0.1 | 0.1 | 0.0 |
| **DSflow_link_SC197.dat** | | **40.41** | 2.37 | 3899.52 | 1.28E+14 | 4.83E+07 | 8.3 | 0.05 | 4.2 | 2.1 | 4.4 |
| **DSflow_link_SC199.dat** | Manganui | **33.73** | 3.22 | 2965.58 | 4.45E+14 | 4.82E+07 | 6.9 | 0.07 | 3.2 | 7.2 | 4.4 |
| **DSflow_link_SC204.dat** | Ruamāhanga Cutoff | **2.97** | 0.14 | 282.96 | 3.97E+13 | 1.07E+07 | 0.6 | 0.00 | 0.3 | 0.6 | 1.0 |
| **DSflow_link_SC219.dat** | | **25.35** | 1.52 | 859.94 | 1.66E+14 | 2.84E+07 | 5.2 | 0.03 | 0.9 | 2.7 | 2.6 |
| **Residual inflow** | | **5.43** | 0.69 | 2329.79 | 2.30E+13 | 3.77E+07 | 1.1 | 0.01 | 2.5 | 0.4 | 3.5 |
| **Rainfall** | | **10.31** | 0.49 | 0.00 | 0.00E+00 | 9.72E+07 | 2.1 | 0.01 | 0.0 | 0.0 | 8.9 |
| **Groundwater** | | **8.53** | 0.00 | 0.00 | 0.00E+00 | 1.09E+07 | 1.8 | 0.00 | 0.0 | 0.0 | 1.0 |

| | | | | | | | | | | |
|---|---|---|---|---|---|---|---|---|---|---|
| **Barrage inflow** | | **31.56** | 1.50 | 3306.56 | 1.39E+14 | 5.20E+07 | 6.5 | 0.03 | 3.6 | 2.2 | 4.8 |
| **Internal load** | | 46.33 | **16.56** | | | | 9.5 | 0.34 | | | |
| **Sum** | | 487.07 | **48.11** | **92819.77** | **6.21E+15** | **1.09E+09** | **100** | **100** | **100** | **100** | **100** |

**Table 15. Lake Onoke flow and load summary.**

| Flow | Associated stream/river | TN (t yr$^{-1}$) | TP (t yr$^{-1}$) | TSS (t yr$^{-1}$) | _E.coli_ (cells yr$^{-1}$) | Flow (m$^3$ yr$^{-1}$) | TN (%) | TP (%) | TSS (%) | E.coli (%) | Flow (%) |
|---|---|---|---|---|---|---|---|---|---|---|---|
| **DSflow_link_SC179.dat** | Pounui Str. | 36.98 | 1.99 | 3186.63 | 9.47E+11 | 4.74E+07 | 1.0 | 0.5 | 0.3 | 0.7 | 0.9 |
| **DSflow_link_SC189.dat** | Boundary Ck. | 26.01 | 2.32 | 1376.52 | 4.46E+11 | 2.23E+07 | 0.7 | 0.6 | 0.1 | 0.3 | 0.4 |
| **DSflow_link_SC198.dat** | Turanganui R. | 40.73 | 2.55 | 12119.49 | 1.29E+12 | 6.44E+07 | 1.1 | 0.6 | 1.2 | 0.9 | 1.2 |
| **DSflow_link_SC200.dat** | Ruamāhanga R. | 3033.03 | 200.61 | 856151.18 | 6.95E+13 | 3.47E+09 | 82.5 | 50.0 | 87.6 | 49.3 | 67.2 |
| **DSflow_link_SC202.dat** | | 32.62 | 2.43 | 4721.41 | 6.04E+11 | 3.02E+07 | 0.9 | 0.6 | 0.5 | 0.4 | 0.6 |
| **DSflow_link_SC203.dat** | | 5.66 | 0.42 | 5135.23 | 4.86E+11 | 2.43E+07 | 0.2 | 0.1 | 0.5 | 0.3 | 0.5 |
| **DSflow_link_SC217.dat** | | 1.02 | 0.02 | 112.80 | 1.72E+10 | 8.62E+05 | 0.0 | 0.0 | 0.0 | 0.0 | 0.0 |
| **DSflow_link_SC218.dat** | | 3.48 | 0.20 | 0.00 | 5.12E+10 | 2.56E+06 | 0.1 | 0.0 | 0.0 | 0.0 | 0.0 |
| **Wairarapa** | | 464.76 | 176.31 | 92646.12 | 6.30E+13 | 1.04E+09 | 12.6 | 43.9 | 9.5 | 44.7 | 20.0 |
| **Residual from water balance** | 0 | 0 | 0.00 | 0.00 | 0.00E+00 | 0.00E+00 | 0.0 | 0.0 | 0.0 | 0.0 | 0.0 |
| **Rainfall** | | 0.92 | 0.04 | 0.00 | 1.73E+11 | 8.65E+06 | 0.0 | 0.0 | 0.0 | 0.1 | 0.2 |
| **Groundwater** | | 6.26 | 0.00 | 0.00 | 0.00E+00 | 3.68E+06 | 0.2 | 0.0 | 0.0 | 0.0 | 0.1 |
| **Ocean** | | 18.29 | 13.72 | 2423.51 | 4.57E+12 | 4.57E+08 | 0.5 | 3.4 | 0.2 | 3.2 | 8.8 |
| **Internal load** | | 5.48 | 0.79 | | | | 0.1 | 0.2 | | | |
| **Sum** | | 3675.23 | 401.39 | 977872.99 | 1.41E+14 | 5.17E+09 | 100 | 100 | 100 | 100 | 100 |

**Table 16. Scenarios and assumptions for lakes Wairarapa and Onoke**

| Management option | Modelling inputs | Notes | Shorthand associated naming conventions |
|---|---|---|---|
| **BASELINE** | **Calibrated catchment model.** Existing management practices between 1992 and 2014. | **All flows and concentrations based off a 22 year flow simulation from 1/7/1992 to 30/6/2014 (applies to all scenarios)** | **BASELINE** |
| *BAU (business as usual)* | Steep slope retirement/planting, stock exclusion from waterways, wastewater discharging partially to land, Minimum flows and allocation amounts based on limits set in Proposed Natural Resources Plan (PNRP), Tier 1 immediately. | | **BAU2025/2040/2080** |
| *SILVER* | Steep slope retirement/planting, stock exclusion from waterways, riparian planting, wastewater discharging only to land, Minimum flows and allocation amounts based on limits set in Proposed Natural Resources Plan (PNRP), Tier 1 immediately. Tier 2 mitigations by 2040. Tier 3 mitigations by 2080. | | **SILVER2025/2040/2080** |
| *GOLD* | Steep slope retirement/planting, stock exclusion from waterways, riparian planting, wastewater discharging only to land, Minimum flows and allocation amounts based on limits set in Proposed Natural Resources Plan (PNRP), Tier 1 mitigations immediately (as BAU), Tier 2 mitigations by 2025, Tier 3 mitigations by 2040. | | **GOLD2025/2040/2080** |
| *All flows of the Ruamāhanga* | Gold scenario inflows (river flows and | | **ALL_RUA_GOLD2025/2040/2080** |

| | | | |
|---|---|---|---|
| *River entering Lake Wairarapa. No flow by-passing via the diversion.* | concentrations) | | |
| *All flows of the Ruamāhanga River entering Lake Wairarapa. No flow by-passing via the diversion.* | Silver scenario inflows (river flows and concentrations) | | **ALL_RUA_SILVER2025/2040/2080** |
| *Flows below median flow go into Lake Wairarapa, and flows above median flow are by-passed.* | Silver scenario contaminant concentrations inflows | Flows below median of 78.10 $m^3\ s^{-1}$ | **MEDIAN_RUA_SILVER2025/2040/2080** |
| *Lake Onoke outlet closed January to March every year.* | Silver scenario contaminant concentrations inflows. | This includes a separate sub-scenario with the Ruamāhanga River diverted back into Lake Wairarapa, Water balance with no ocean inflow Jan-March and high water level (95 percentile). | **Outlet_Close_SILVER2025/2040/2080**<br>**Outlet_Close_Rua_All_SILVER2025/2040/2080** |
| *Deepening both lakes by 1 m.* | Extra depth created by operating at a higher level. Silver scenario inputs | Operate at 1 m higher level | **1m_Inc_SILVER2025/2040/2080** |
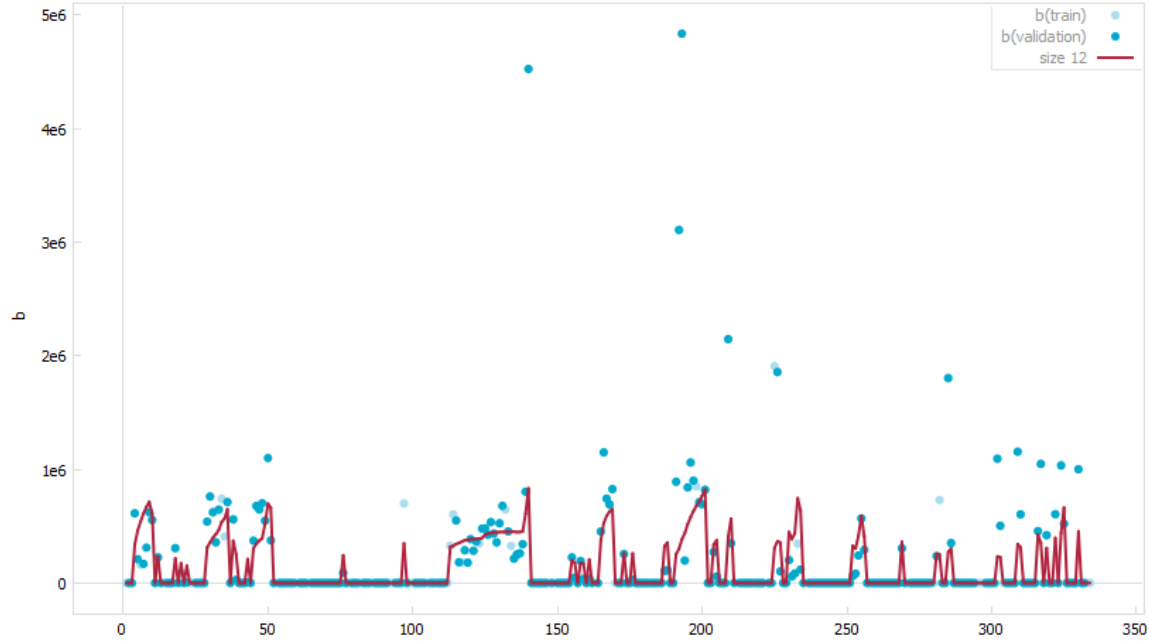
**Appendix Figure 1. Barrage inflow estimations (redline) compared to in situ measurements (blue dots). Correlation Coefficient = 0.58, mean absolute error=122125.75 m3/day.**

**Table 17. DYRESM-CAEDYM physical parameter values.**

| Parameter | Unit | Calibrated value Wairarapa | Calibrated value Onoke |
|---|---|---|---|
| Light extinction coefficient | $m^{-1}$ | **0.33** | **0.33** |
| Min. layer thickness | m | **0.2** | **0.2** |
| Max layer thickness | m | **0.5** | **0.5** |
| Critical wind speed | $m\ s^{-1}$ | 3 | 3 |
| Emissivity of water surface | - | 0.96 | 0.96 |
| Mean albedo of water | - | 0.09 | 0.09 |
| Potential energy mixing efficiency | - | 0.2 | 0.2 |
| Shear production efficiency | - | 0.08 | 0.08 |
| Vertical mixing coefficient | - | 200 | 200 |
| Wind stirring efficiency | - | 0.4 | 0.4 |
| Effective surface area coefficient | $m^{-2}$ | 1.00E+07 | 1.00E+07 |

**Table 18. DYRESM-CAEDYM biological, chemical and sediment parameter values.**

| Parameter | Unit | Calibrated value Wairarapa | Calibrated value Onoke |
|---|---|---|---|
| *Sediment parameters* | | | |
| **Sediment oxygen demand** | g m$^{-2}$ d$^{-1}$ | 1.65 | 1.65 |
| **Half-saturation coefficient for sediment oxygen demand** | mg L$^{-1}$ | 0.25 | 0.25 |
| **Maximum potential PO$_4$-P release rate** | g m$^{-2}$ d$^{-1}$ | 0.007 | 0.002 |
| **Oxygen and nitrate half-saturation for release of phosphate from bottom sediments** | g m$^{-3}$ | 1.5 | 3.5 |
| **Maximum potential NH$_4$-N release rate** | g m$^{-2}$ d$^{-1}$ | 0.01 | 0.03 |
| **Oxygen half-saturation constant for release of ammonium from bottom sediments** | g m$^{-3}$ | 1.5 | 3 |
| **Maximum potential NO$_3$ release rate** | g m$^{-2}$ d$^{-1}$ | -0.03 | -0.04 |
| **Oxygen half-saturation constant for release of nitrate from bottom sediments** | g m$^{-3}$ | 2.5 | 8.5 |
| **Temperature multiplier for nutrient release** | - | 1.06 | 1.06 |
| **Nutrient parameters** | | | |
| **Max transfer of POPL to DOPL** | d$^{-1}$ | 0.005 | 0.005 |
| **Mineralisation rate of DOPL to PO$_4$-P** | d$^{-1}$ | 0.05 | 0.05 |
| **Max transfer of PONL to DONL** | d$^{-1}$ | 0.004 | 0.004 |
| **Mineralisation rate of DONL to NH$_4$-N** | d$^{-1}$ | 0.005 | 0.005 |
| **Denitrification rate coefficient** | d$^{-1}$ | 0.08 | 0.08 |
| **Oxygen half-saturation constant for denitrification** | mg L$^{-1}$ | 0.5 | 0.5 |
| **Temperature multiplier for denitrification** | - | 1.07 | 1.07 |
| **Nitrification rate coefficient** | d$^{-1}$ | 0.1 | 0.1 |
| **Nitrification half-saturation constant for oxygen** | mg L$^{-1}$ | 0.5 | 0.5 |
| **Temperature multiplier for nitrification** | - | 1.07 | 1.07 |
| *Phytoplankton parameters* | | | |
| | | *Cyanophytes, Greens, Diatoms* | *Cyanophytes, Greens, Diatoms* |

| Parameter | Units | Value set 1 | Value set 2 |
|---|---|---|---|
| **Maximum potential growth rate at 20°C** | $d^{-1}$ | 0.51,0.99,1.40 | 0.6,1.5,1.6 |
| **Irradiance parameter non-photoinhibited growth** | $\mu mol\ m^{-2}\ s^{-1}$ | 189.48, 83.78,17.98 | 150,30,20 |
| **Half saturation constant for phosphorus uptake** | $mg\ L^{-1}$ | 5.57E-003,5.39E-003, 9.51E-003 | 0.003, 0.0031,0.004 |
| **Half saturation constant for nitrogen uptake** | $mg\ L^{-1}$ | 3.30E-002,3.84E-002, 5.08E-002 | 0.017, 0.06, 0.065 |
| **Minimum internal nitrogen concentration** | $mg\ N\ (mg\ chl\ a)^{-1}$ | 2.86,1.95,3.04 | 3.5, 3.1, 3.4 |
| **Maximum internal nitrogen concentration** | $mg\ N\ (mg\ chl\ a)^{-1}$ | 5.01,3.47,3.47 | 9.5, 11.5, 10.2 |
| **Maximum rate of nitrogen uptake** | $mg\ N\ (mg\ chl\ a)^{-1}\ d^{-1}$ | 1.81, 1.58, 1.43 | 2.75, 3.8, 3.3 |
| **Minimum internal phosphorus concentration** | $mg\ P\ (mg\ chl\ a)^{-1}$ | 0.49, 1.81, 0.35 | 0.22, 0.21, 0.22 |
| **Maximum internal phosphorus concentration** | $mg\ P\ (mg\ chl\ a)^{-1}$ | 0.97,2.23, 1.07 | 2,2.1,2 |
| **Maximum rate of phosphorus uptake** | $mg\ P\ (mg\ chl\ a)^{-1}\ d^{-1}$ | 0.39, 0.15, 0.25 | 0.3, 0.22, 0.24 |
| **Temperature multiplier for growth limitation** | - | 1.09, 1.06, 1.05 | 1.08, 1.08, 1.06 |
| **Standard temperature for growth** | °C | 20.0, 20.0, 17.92 | 20,20,20 |
| **Optimum temperature for growth** | °C | 27.45, 25.73, 22.7 | 34, 30, 29 |
| **Maximum temperature for growth** | °C | 40.72, 33.76, 32.39 | 39, 33, 34 |
| **Respiration rate coefficient** | $d^{-1}$ | 0.078, 0.11, 0.08 | 0.09, 0.13, 0.16 |
| **Temperature multiplier for respiration** | - | 1.03, 1.07, 1.06 | 1.06, 1.06, 1.10 |
| **Fraction of respiration relative to total metabolic loss rate** | - | 0.78, 0.64, 0.79 | 0.1, 0.7, 7 |
| **Fraction of metabolic loss rate that goes to DOM** | - | 0.57, 0.83, 74 | 0.10, 0.33, 0.30 |
| **Constant settling velocity** | $m\ s^{-1}$ | 1.5, -7.65E-006, -1.50E-006 | 0.0, 0.0, -0.23E-07 |